

ผลของภาวะพร่องซีโรโตนินและการอักเสบบริเวณใบหน้าที่ถูกกระตุ้นด้วยสารเคมี
ต่อการทำงานของสมองใหญ่และการแสดงออกของ vanilloid receptor subtype 1
ในระบบไตรเจมินัลของหนูขาว



นาย วีระ สุพรรณิษฐ์ชัย

สถาบันวิทยบริการ
วิทยานิพนธ์นี้เป็นส่วนหนึ่งของการศึกษาตามหลักสูตรปริญญาวิทยาศาสตรมหาบัณฑิต
จุฬาลงกรณ์มหาวิทยาลัย
สาขาวิชาสรีรวิทยา (สหสาขาวิชา)

บัณฑิตวิทยาลัย จุฬาลงกรณ์มหาวิทยาลัย

ปีการศึกษา 2547

ISBN 974-17-6733-1

ลิขสิทธิ์ของจุฬาลงกรณ์มหาวิทยาลัย

EFFECT OF SEROTONIN DEPLETION AND CHEMICALLY INDUCED FACIAL
INFLAMMATION ON CEREBRAL CORTICAL ACTIVITY AND EXPRESSION
OF VANILLOID RECEPTOR SUBTYPE 1 IN RAT TRIGEMINAL SYSTEM



Mr. Weera Suprongsinchai

สถาบันวิทยบริการ
จุฬาลงกรณ์มหาวิทยาลัย

A Thesis Submitted in Partial Fulfillment of the Requirements
for the Degree of master of Science in Physiology (Inter-department)
Graduate school
Chulalongkorn University
Academic year 2004
ISBN 974-17-6733-1

Thesis Title Effect of serotonin depletion and chemically-induced facial
 inflammation on cerebral cortical activity and expression of
 vanilloid receptor subtype 1 in rat trigeminal system
By Mr. Weera Suprongsinchai
Field of Study Physiology
Thesis Advisor Professor Anan Srikiatkachorn, M.D.
Thesis Co-advisor Assistant Professor Sompol Sanguanrungrsirikul, M.D.

Accepted by the Graduated School, Chulalongkorn University in Partial
Fulfillment of the Requirements for the Master's Degree

.....Dean of the Graduated School
(Assistant Professor M.R.Kalaya Tingsabadh, Ph.D.)

THESIS COMMITTEE

.....Chairman
(Associate Professor Prasong Siriviriyakul, M.D.)

.....Thesis Advisor
(Professor Anan Srikiatkachorn, M.D.)

.....Thesis Co-advisor
(Assistant Professor Sompol Sanguanrungrsirikul, M.D.)

.....Member
(Associate Professor Yupin Sanvarinda, Ph.D.)

.....Member
(Sarinee Kalandakanond, Ph.D.)

วีระ สุพรศิลป์ชัย; ผลของภาวะพร่องซีโรโตนินและการอักเสบบริเวณใบหน้าที่ถูกกระตุ้นด้วยสารเคมี ต่อการทำงานของสมองใหญ่และการแสดงออกของ vanilloid receptor subtype1 ในระบบไตรเจมินัลของหนูขาว (EFFECT OF SEROTONIN DEPLETION AND CHEMICALLY-INDUCED FACIAL INFLAMMATION ON CEREBRAL CORTICAL ACTIVITY AND EXPRESSION OF VANILLOID RECEPTOR SUBTYPE 1 IN RAT TRIGEMINAL SYSTEM) อ. ที่ปรึกษา; ศ.นพ อนันต์ ศรีเกียรติขจร; อ. ที่ปรึกษาร่วม: ผศ. นพ. สมพล สงวรงค์ศิริกุล; 124 หน้า ISBN 974-17-6733-1

การศึกษาครั้งนี้มีจุดประสงค์เพื่อศึกษาผลของภาวะพร่องซีโรโตนินและ/หรือการอักเสบของใบหน้า ต่อการเปลี่ยนแปลงของปรากฏการณ์คอร์ติคัล สเปรดดิ้ง ดีเพรสชัน (Cortical spreading depression; CSD) และระบบรับรู้ความรู้สึกไตรเจมินัล โดยแบ่งหนูพันธุ์วิสตาเพศผู้ ออกเป็น 4 กลุ่ม ประกอบด้วย กลุ่มที่ได้รับ Complete Freund's Adjuvant (CFA) กลุ่มที่ได้รับ para-chlorophenylalanine (PCPA) กลุ่มที่ได้รับทั้ง CFA และ PCPA และกลุ่มควบคุม การอักเสบของใบหน้าทำโดยการฉีด CFA ได้ชั้นผิวหนังบริเวณใบหน้า ภาวะพร่องซีโรโตนินทำโดยการยับยั้งการทำงานของเอนไซม์ tryptophan ด้วยการฉีด PCPA 100 มิลลิกรัม/กิโลกรัมของน้ำหนักตัว ทางช่องท้อง การกระตุ้นให้เกิดปรากฏการณ์คอร์ติคัล สเปรดดิ้ง ดีเพรสชัน ทำโดยการวางผลึกโพแทสเซียมคลอไรด์ขนาด 3 มิลลิกรัม ลงบนผิวสมอง การบันทึกการทำงานของสมองใหญ่ทำการใส่ขั้วบันทึกขนาดเล็กลงในแกวลงบริเวณสมองส่วนหน้าข้างเดียวกับที่วางโพแทสเซียมคลอไรด์ ส่วนผลกระทบต่อระบบรับรู้ความรู้สึกไตรเจมินัลจะศึกษาการแสดงออกของ vanilloid receptor subtype 1 (VR1) ในปมประสาทไตรเจมินัลและโปรตีน Fos ในกลุ่มเซลล์ประสาทไตรเจมินัลคอโคคาลิส ผลการศึกษาพบว่า การวางโพแทสเซียมคลอไรด์ลงบนผิวสมอง สามารถกระตุ้นทำให้เกิด depolarization shift ซึ่งเป็นลักษณะของปรากฏการณ์คอร์ติคัล สเปรดดิ้ง ดีเพรสชันได้ โดยพบการเปลี่ยนแปลงของคลื่นคอร์ติคัล สเปรดดิ้ง ดีเพรสชันมากขึ้นทั้งในกลุ่มที่ให้ PCPA และ CFA แต่ไม่พบผลส่งเสริมกันเมื่อให้สารทั้งสองชนิดร่วมกัน โดยการเปลี่ยนแปลงนั้นพบการเพิ่มขึ้นของพื้นที่ได้กราฟของแต่ละปรากฏการณ์คอร์ติคัล สเปรดดิ้ง ดีเพรสชัน และระยะเวลาระหว่างการเกิดปรากฏการณ์คอร์ติคัล สเปรดดิ้ง ดีเพรสชัน สั้นลงรวมทั้งมีความถี่ของคลื่นสูงขึ้น แต่ไม่พบความแตกต่างของความสูงและระยะเวลาการเกิดปรากฏการณ์คอร์ติคัล สเปรดดิ้ง ดีเพรสชันในแต่ละครั้ง การศึกษาอิมมูโนฮิสโตเคมีสตรี้ของ โปรตีน Fos และ VR1 ให้ผลในลักษณะเดียวกันกล่าวคือมีจำนวนเซลล์ประสาทที่ย้อมติด Fos ในกลุ่มเซลล์ประสาทไตรเจมินัลคอโคคาลิสและ VR1 ในปมประสาทไตรเจมินัลเพิ่มขึ้นทั้งในกลุ่มที่ให้ PCPA และ CFA แต่ไม่พบผลส่งเสริมกันเมื่อให้สารทั้งสองชนิดร่วมกัน

จากการศึกษานี้แสดงถึงลักษณะการตอบสนองของระบบรับรู้ความรู้สึกไตรเจมินัล ทั้งนี้ปัจจัยต่างๆ อาทิ การอักเสบของเนื้อเยื่อบริเวณใบหน้าและภาวะพร่องซีโรโตนิน สามารถเพิ่มการทำงานของระบบนี้โดยเพิ่มการตอบสนองของสมองใหญ่ร่วมกับเพิ่มความไวของระบบไตรเจมินัล

สาขาวิชา.....สรีรวิทยา.....ลายมือชื่อนิสิต.....
ปีการศึกษา.....2547.....ลายมือชื่ออาจารย์ที่ปรึกษา.....
ลายมือชื่ออาจารย์ที่ปรึกษาร่วม.....

4589156620: MAJOR PHYSIOLOGY

KEYWORD VANILLOID RECEPTOR SUBTYPE1/INFLAMMATION/
SEROTONIN DEPLETION/TRIGEMINAL GANGLIA/
/DEPOLARIZATION SHIFT

WEERA SUPRONSINCHAI: EFFECT OF SEROTONIN DEPLETION
AND CHEMICALLY-INDUCED FACIAL INFLAMMATION ON
CEREBRAL CORTICAL ACTIVITY AND EXPRESSION OF
VANILLOID RECEPTOR SUBTYPE 1 IN RAT TRIGEMINAL
SYSTEM. THESIS ADVISOR: PROF. ANAN SRIKIATKHACHORN,
M.D. THESIS CO-ADVISOR: ASSIST.PROF. SOMPOL
SANGUANRUNGSIRIKUL, MD 124 pp. ISBN 974-17-6733-1

The objectives of the present study were to determine the effect of serotonin (5-HT) depletion and/or facial inflammation on the development of cortical spreading depression (CSD) and trigeminal nociception. Adult male Wistar rats were divided into four groups, including those receiving complete Freund's adjuvant (CFA), receiving para-chlorophenylalanine (PCPA), receiving both CFA and PCPA and control groups. Facial inflammation was induced by subcutaneous injection with CFA in the forehead area. 5-HT was depleted by administration of PCPA (100 mg/kg BW, intraperitoneally), a tryptophan hydroxylase inhibitor. CSD was induced by application of 3 mg of potassium chloride crystal on parietal cortex. Cortical activity was monitored using glass microelectrode inserted into frontal cortex ipsilateral to the potassium chloride application. Impact on trigeminal nociceptive system was studied using the expression of vanilloid receptor (VR1) in trigeminal ganglia as well as the expression of a transcription factor Fos in trigeminal nucleus caudalis as indicators. The results showed that application of potassium chloride resulted in a series of depolarization activity characteristic for CSD. The development of these CSD waves was enhanced in both PCPA-treated and CFA-treated groups. No additional effect was evident when both interventions were combined. Such enhancement was characterized by increased area under the curve of each CSD wave, shortened interpeak latency as well as an increase in frequency of CSD waves. No significant change was observed regarding the peak amplitude and duration. Results from the Fos- and VR1-immunohistochemical studies revealed the similar pattern. Greater numbers of Fos in trigeminal nucleus caudalis and VR1 in trigeminal ganglia were observed in both PCPA- and CFA-treated groups. Again, no addition effect was evidenced. The present study demonstrated the plasticity of trigeminal nociceptive system. Several factors, including facial tissue inflammation and 5-HT depletion as shown in the present study, can enhance this system by increasing the cortical response as well as facilitating the trigeminal nociception in general.

Field of study.....PhysiologyStudent's signature.....

Academic year.....2004.....Advisor's signature.....

Co-advisor's signature.....

ACKNOWLEDGEMENTS

I wish to express my gratitude and appreciation to my kind advisor, Professor DR. Anan Srikiatkhachorn MD, for his excellent instruction, guidance, encouragement and support during the long working process, which enable me to carry out this study. His kindness will be long remembered.

I would like to express my gratitude to Associate Professor DR. Sompol Sanguanrungririkul for training me about the setting of Depolarization shift technique and helping me to more deeply understands my research.

I would like give a very special vote to thank to DR. Supang Maneesri for training me about immunohistochemical technique, cheerfulness and support my mind throughout this study. My special thanks are also extending to Mr. Maroot Kaewwongse, and Mr. Peter le Grand for their valuable help and cheerfulness.

I wish to express my sincere thanks to all my teachers at Department of Physiology, Faculty of Medicine, Chulalongkorn University who are not mentioned here for all their loving helps during the time I was studying.

My appreciations are also devoted to my dear father, mother for their love, kindness and support my mind throughout this study.

สถาบันวิทยบริการ
จุฬาลงกรณ์มหาวิทยาลัย

TABLE OF CONTENTS

	PAGE
ABSTRACT (THAI)	iv
ABSTRACT (ENGLISH)	v
ACKNOWLEDGEMENTS	vi
TABLE OF CONTENTS	vii
LIST OF TABLES	viii
LIST OF FIGURES	xi
LIST OF ABBREVIATIONS	xvi
CHAPTER	
I. INTRODUCTION	1
II. REVIEW OF LITERATURE	3
III. MATERIALS AND METHODS	35
IV. RESULTS	55
V. DISCUSSION	104
VI. CONCLUSION	109
REFERENCES	110
BIOGRAPHY	124

สถาบันวิทยบริการ
จุฬาลงกรณ์มหาวิทยาลัย

LIST OF TABLES

		PAGE
Table 2.1	Characteristics of vanilloid-sensitive primary sensory neurons	32
Table 2.2	Biochemical pharmacology of vanilloid receptors	33
Table 4.1	The mean value \pm SD of amplitude of DC shift obtained from control group and CFA-treated group.....	59
Table 4.2	The mean value \pm SD of duration of DC shift obtained from control group and CFA-treated group.....	60
Table 4.3	The mean value \pm SD of number of peak of DC shift obtained from control group and CFA-treated group	61
Table 4.4	The mean value \pm SD of interpeak latency of DC shift obtained from control group and CFA-treated group	62
Table 4.5	The mean value \pm SD of average AUC of DC shift in one hour obtained from control group and CFA-treated group	63
Table 4.6	The mean value \pm SD of sum AUC of DC shift in one hour obtained from control group and CFA-treated group	64
Table 4.7	Comparing the electrophysiological variables related to CSD between the control and inflammation groups.....	65
Table 4.8	The mean value \pm SD of the number of VR1-IR cells in the TG sections obtained from control group and CFA-treated group ...	67
Table 4.9	The mean value \pm SD of number of Fos-IR cells in the C1 and C2 cervical spinal cord sections obtained from control group and CFA-treated group	70
Table 4.10	The mean value \pm SD of amplitude of DC shift obtained from control group and PCPA-treated group.....	75
Table 4.11	The mean value \pm SD of duration of DC shift obtained from control group and PCPA-treated group.....	76
Table 4.12	The mean value \pm SD of number of peak of DC shift obtained from control group and PCPA-treated group.....	77
Table 4.13	The mean value \pm SD of interpeak latency of DC shift obtained from control group and PCPA-treated group.....	78

	PAGE
Table 4.14	The mean value \pm SD of average AUC of DC shift in one hour obtained from control group and PCPA-treated group79
Table 4.15	The mean value \pm SD of sum AUC of DC shift in one hour obtained from control group and PCPA-treated group80
Table 4.16	Comparing the electrophysiological variables related to CSD between the control and 5-HT depletion groups.....81
Table 4.17	The mean value \pm SD of the number of VR1-IR cells in the TG sections obtained from control group and PCPA-treated group83
Table 4.18	The mean value \pm SD of number of Fos-IR cells in the C1 and C2 cervical spinal cord sections obtained from control group and PCPA-treated group86
Table 4.19	The mean value \pm SD of amplitude of DC shift obtained from CFA-treated group and PCPA with CFA-treated group91
Table 4.20	The mean value \pm SD of duration of DC shift obtained from CFA-treated group and PCPA with CFA-treated group92
Table 4.21	The mean value \pm SD of number of peak of DC shift obtained from CFA-treated group and PCPA with CFA-treated group93
Table 4.22	The mean value \pm SD of interpeak latency of DC shift obtained from CFA-treated group and PCPA with CFA-treated group94
Table 4.23	The mean value \pm SD of average AUC of DC shift in one hour obtained from CFA-treated group and PCPA with CFA-treated group95
Table 4.24	The mean value \pm SD of sum AUC of DC shift in one hour obtained from CFA-treated group and PCPA with CFA-treated group96
Table 4.25	Comparing the electrophysiological variables related to CSD between the inflammation and 5-HT depletion with inflammation groups97
Table 4.26	The mean value \pm SD of the number of VR1-IR cells in the sections obtained from CFA-treated group and PCPA with CFA-treated group99

	PAGE
Table 4.27 The mean value \pm SD of number of Fos-IR cells in the C1 and C2 cervical spinal cord sections obtained from inflammation and 5-HT depletion with inflammation groups.....	102



สถาบันวิทยบริการ
จุฬาลงกรณ์มหาวิทยาลัย

LIST OF FIGURES

		PAGE
Figure 2.1	Structure of trigeminal nerve	3
Figure 2.2	Trigeminal pathway	4
Figure 2.3	Nociceptive afferent fibers terminate on projection neurons in the dorsal horn of the spinal cord. Projection neurons in laminar I receive direct input from myelinated (A δ) nociceptive afferent fibers via stalk cell interneurons in laminar II	7
Figure 2.4	Hypothesis of development of a migraine attack based on aspects of CSD and migraine	11
Figure 2.5	The shape of a typical DC-potential recorded following the appearance of one CSD.....	15
Figure 2.6	Electrophysiological changes accompanying cortical spreading depression in the rat brain. Interstitial ion concentrations of sodium ,potassium, calcium and hydrogen were measured by ion-selective electrodes. The extracellular potential (V _e) and the single unit activity were measured by single-barreled electrophysiological changes which were recorded in the parietal cortex	15
Figure 2.7	Simplistic scheme of autocatalytic cycle possibly Occurring during CSD	16
Figure 2.8	Original traces showing change in cortical D.C. potential (mV), rCBF LDF (laser Doppler flux units) and NO release (pA) over time (min) following application of KCl solid to the parietal cortex of a vehicle treated animal	16
Figure 2.9	Structure of vanilloid receptor subtype 1.....	24
Figure 3.1	Diagram of experimental I design.....	39
Figure 3.2	Diagram of experimental II design	41
Figure 3.3	Diagram of experimental III design.....	43
Figure 3.4	The tracing showing the effect of solid KCl 3 mg and NaCl on depolarization shift.....	45
Figure 3.5	Diagram of experimental animal groups: measurement of depolarization shift.....	47

Figure 3.6	Schematic of DC shift showed the ascending point (A) and descending point (B). Area under the curve of DC shift was measured as the area above of A-B.....	48
Figure 3.7	Schematic of DC shift showed the reference point A and defined point B and C. The amplitude of DC shift was measured as the distance between C-AB	49
Figure 3.8	Schematic of DC shift showed the start time point (A) and finish time point (B). Duration of DC shift was measured as the time of A-B	49
Figure 3.9	Schematic of DC shift showed the total number of the peak of DC shift was measured as the length of 60 minute.....	50
Figure 3.10	Schematic of DC shift showed the reference point A and point B. the interpeak interval of DC shift was measured as the length of A-B.	50
Figure 3.11	Schematic of DC shift showed the total AUC of the peak of DC shift was measured as the length of 60 minute.....	51
Figure 4.1	The tracing showing the depolarization shift changes after KCl 3 mg application in control group.....	58
Figure 4.2	The tracing showing the depolarization shift changes after KCl 3 mg application in CFA-treated group	58
Figure 4.3	Bar graphs showing the mean value \pm SD of amplitude of DC shift obtained from control and CFA-treated groups	59
Figure 4.4	Bar graphs showing the mean value \pm SD of duration of DC shift obtained from control and CFA-treated groups	60
Figure 4.5	Bar graphs showing the mean value \pm SD of number of peaks of DC shift obtained from control and CFA-treated groups	61
Figure 4.6	Bar graphs showing the mean value \pm SD of interpeak latency of DC shift obtained from control and CFA-treated groups	62
Figure 4.7	Bar graphs showing the mean value \pm SD of average AUC of DC shift in one hour obtained from control and CFA-treated groups.....	63
Figure 4.8	Bar graphs showing the mean value \pm SD of sum AUC of DC shift in one hour obtained from control and CFA-treated groups.....	64

Figure 4.9	Bar graphs showing the mean value \pm SD of the number of VR1-IR cells in the TG sections obtained from the control group and the CFA-treated group	67
Figure 4.10	The photomicrograph showing the VR1-IR cells in the TG sections (ipsilateral side to KCl application) obtained from the A) Control group, B) CFA-treated group	68
Figure 4.11	Bar graph showing the mean value \pm SD of the number of Fos-IR cells in the C1 and C2 cervical spinal cord sections obtained from the control group and the CFA-treated group	70
Figure 4.12	The photomicrograph showing the Fos-IR cells in the C1 and C2 cervical spinal cord sections (ipsilateral side to KCl application) obtained from the A) Control group, B) CFA-treated group.....	71
Figure 4.13	The tracing showing the depolarization shift changes after KCl 3 mg application in PCPA-treated group.....	74
Figure 4.14	Bar graphs showing the mean value \pm SD of amplitude of DC shift obtained from control and PCPA-treated groups.....	75
Figure 4.15	Bar graphs showing the mean value \pm SD of duration of DC shift obtained from control and PCPA-treated groups.....	76
Figure 4.16	Bar graphs showing the mean value \pm SD of number of peaks of DC shift obtained from control and PCPA-treated groups	77
Figure 4.17	Bar graphs showing the mean value \pm SD of interpeak latency of DC shift obtained from control and PCPA-treated groups	78
Figure 4.18	Bar graphs showing the mean value \pm SD of average AUC of DC shift in one hour obtained from control and PCPA-treated groups.....	79
Figure 4.19	Bar graphs showing the mean value \pm SD of sum AUC of DC shift in one hour obtained from control and PCPA-treated groups.....	80
Figure 4.20	Bar graphs showing the mean value \pm SD of the number of VR1-IR cells in the TG sections obtained from the control group and PCPA-treated group.....	83

Figure 4.21	The photomicrograph showing the VR1-IR cells in the TG sections (ipsilateral side to KCl application) obtained from the A) Control group, B) PCPA-treated group	84
Figure 4.22	Bar graph showing the mean value \pm SD of the number of Fos-IR cells in the C1 and C2 cervical spinal cord sections obtained from the control group and PCPA-treated group	86
Figure 4.23	The photomicrograph showing the Fos-IR cells in the C1 and C2 cervical spinal cord sections (ipsilateral side to KCl application) obtained from the A) Control group, B) PCPA-treated group.....	87
Figure 4.24	The tracing showing the depolarization shift changes after KCl 3 mg application in PCPA with CFA-treated group	90
Figure 4.25	Bar graphs showing the mean value \pm SD of amplitude of DC shift obtained from CFA-treated group and PCPA with CFA-treated group	91
Figure 4.26	Bar graphs showing the mean value \pm SD of duration of DC shift obtained from CFA-treated group and PCPA-treated with CFA-treated group	92
Figure 4.27	Bar graphs showing the mean value \pm SD of number of peaks of DC shift obtained from CFA-treated group and PCPA with CFA-treated groups.....	93
Figure 4.28	Bar graphs showing the mean value \pm SD of interpeak latency of DC shift obtained from CFA-treated group and PCPA with CFA-treated groups.....	94
Figure 4.29	Bar graphs showing the mean value \pm SD of average AUC of DC shift in one hour obtained from CFA-treated group and PCPA with CFA-treated group	95
Figure 4.30	Bar graphs showing the mean value \pm SD of sum AUC of DC shift in one hour obtained from CFA-treated group and PCPA with CFA-treated group	96
Figure 4.31	Bar graphs showing the mean value \pm SD of the number of VR1-IR cells in the TG sections obtained from CFA-treated group and PCPA with CFA-treated group	99

Figure 4.32	The photomicrograph showing the VR1-IR cells in the TG sections (ipsilateral side to KCl application) obtained from the A) Inflammation group, B) 5-HT depletion with inflammation group.....	100
Figure 4.33	Bar graph showing the mean value \pm SD of the number of Fos-IR cells in the C1 and C2 cervical spinal cord sections obtained from CFA-treated group and PCPA with CFA-treated group	102
Figure 4.34	The photomicrograph showing the Fos-IR cells in the C1 and C2 cervical spinal cord sections (ipsilateral side to KCl application) obtained from the A) Inflammation group, B) 5-HT depletion with inflammation group.....	103

LIST OF ABBREVIATIONS

VR1	= vanilloid receptor subtype 1
5-HT	= serotonin
5-HTP	= 5- Hydroxytryptophan
5-HIAA	= 5- Hydroxyindoleacetic acid
TG	= trigeminal ganglion
TNC	= trigeminal nucleus caudalis
CSD	= cortical spreading depression
DC shift	= depolarization shift
CFA	= Complete Freund's Adjuvant
PCPA	= para-chlorophenylalanine
CGRP	= calcitonin gene-related peptide
μm	= micrometer
Ca^{2+}	= calcium ion
Na^+	= sodium ion
H^+	= hydrogen ion
K^+	= potassium ion
KCl	= potassium chloride
kg	= kilogram
mV	= millivolt
NaCl	= sodium chloride
PBS	= phosphate buffer saline
mg	= milligram
mm	= millimeter
C1	= cervical spinal cord segment 1
C2	= cervical spinal cord segment 2
DAB	= 3,3-diaminobenzidin
BW	= body weight

CHAPTER I

INTRODUCTION

Migraine and other forms of primary headaches have recently become of major interest to neuroscientists. A prevalence of 15-18% in female and 6% in males (Lipton and Stewart, 1997) argues in favor of the syndrome being due to transiently disordered physiology rather than a disease state. Migraine is one of the most common conditions encountered both in the general neurology and special headache clinic. According to the International Headache Society criteria (2004), this condition can be classified to various subtypes depending on their clinical features. There are two main types of migraine. The first, migraine without aura (previously called common migraine), is characterized by headache attacks lasting 4-72 hours. The headache is usually severe, unilateral pulsating, and accompanied by nausea, vomiting, photophobia. In the second type, migraine with aura (previously known as classical migraine) is characterized by the presence of transient neurological deficits preceding the phase of headache. Its gradual course of progression and the distribution of neurological deficits do support the hypothesis.

In 1944, Leao reported his observation concerning a specific pattern of change of the electroencephalogram (EEG) which can be triggered by non-noxious stimulation. This electrophysiologic phenomenon is characterized by an increase in EEG activity of focal cortical areas usually occipital lobe. This excitation-depression wave gradually expands forward and normally disappears at the central sulcus. Based on the similarity in time course and pattern of spreading, Leao proposed that this electrophysiologic phenomenon, which was later termed cortical spreading depression (CSD), might be the mechanism underlying the aura phase of migraine (Leao, 1944). Though CSD correlated well with the clinical features of neurological deficits, occurring during the aura phase, the relationship between this phenomenon and the generation of headache is still inadequately explained.

Discovery of vanilloid receptor subtype1 (VR1) is considered one of the most important findings in current pain research. Its physiological properties satisfy several aspects of nociceptive mechanism. For instance, its gating mechanisms which can be controlled either by tissue acidity or heat fit well with non-selective property of nociceptors. Its expression in small-sized dorsal root ganglion (DRG) and trigeminal

ganglia (TG) neurons also reflects its involvement in nociceptive process (Millan, 1999)

Recently, it has been shown that expression of VR1 receptor can be altered in several nociceptive states. In 2003, Amaya et al. demonstrated that chemically-induced tissue inflammation can increase VR1 positive neuronal profile in rat DRG neurons. In 2002, Fukuoka et al. demonstrated an increase in VR1 receptor expression in rat DRG neurons after spinal nerve ligation. These data provide evidence that both noxious stimulation and injury in nervous system can increase VR1 expression in DRG. Such change may relate to functional alteration of pain perception and may underlie the development of chronic pain syndrome. Plasticity change of VR1 in TG has not yet been investigated.

It is widely recognized that serotonin has role in indicate of pain and headache. Substantial evidences indicate that serotonin is implicated in the pathophysiology of migraine (Raskin, 1991). Urinary excretion of 5-hydroxyindole-3-acetic acid, the metabolite of 5-HT, has been reported to increase during the headache phase (Sicuteri et al., 1961), whereas platelet 5-HT levels decrease (Anthony et al., 1969). Intravenous administration of 5-HT can alleviate migraine symptoms elicited by 5-HT depleting agents (Kimball et al., 1960). These clinical evidences indicate the relationship between low 5-HT and headache.

The following study is designed to investigate the plasticity of trigeminal nociceptive system in two conditions, namely 5-HT depletion and facial inflammation. We study expression of Fos in TNC as an indicate of trigeminal nociception. We also studied the change in VR1 expression in TG in this condition. The studies also aim at determining the effect on cortical activity evoked by non-noxious stimulation.

CHAPTER II

REVIEW OF LITERATURES

TRIGEMINAL NERVOUS SYSTEM

The trigeminal nerve is the largest cranial nerve and contains both sensory and motor fibers. It is the sensory nerve to the greater part of the head and the motor nerve to several muscles, including the muscles of mastication. The trigeminal nerve has three branches, the ophthalmic, maxillary and mandibular divisions (Fig 2.1) (Snell, 1992).

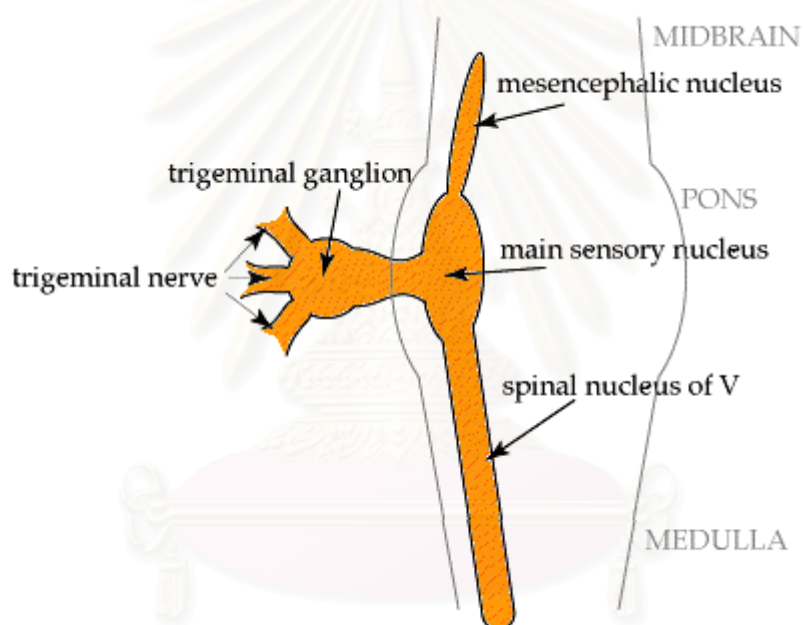


Figure 2.1 Structure of trigeminal nerve (Snell, 1992)

The tract that the descending axons travel in is called the spinal tract of nucleus of V, and the long tail of a nucleus that they finally synapse in is called the spinal nucleus of V. These names come from the fact that they actually reach as far down as the upper cervical spinal cord. The spinal nucleus of V can be divided into three regions along its length; the region closest to the mouth is called subnucleus oralis, the middle region is called subnucleus interpolaris, and the region closest to the tail is called subnucleus caudalis. The pain fibers actually synapse in subnucleus

caudalis. The secondary afferents from subnucleus caudalis cross to the opposite side, and join the spinothalamic tract on its way to the thalamus (Fig 2.2).

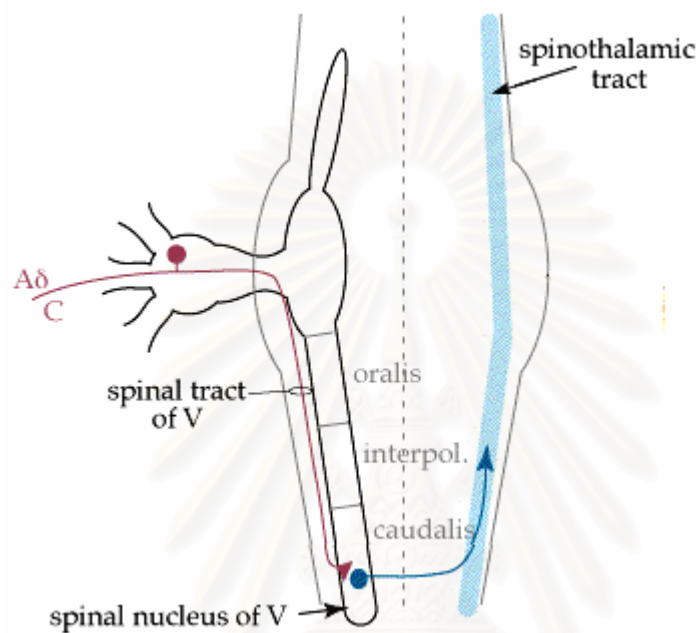


Figure 2.2 Trigeminal pathway (Snell, 1992)

THE TRIGEMINAL NUCLEUS COMPLEX:

The small diameter fibers carrying pain and temperature enter at mid pons, and turn down the brainstem. They travel down the pons and medulla until they reach the caudal medulla, which is where they finally synapse and cross (Fig 2.2).

Most of the sensory fibers enter the trigeminal ganglion, regardless of which trigeminal division they are coming from. Their cell bodies, like those of all somatosensory neurons, lie outside the CNS in the ganglion, and their proximal processes enter the brainstem in the mid-pons. From there they fan out to their different targets. Each modality will be described separately below.

The somatosensory information from the face joins that from the body and enters the thalamus with it. However, face information actually enters a different nucleus in the thalamus. Recall that information from the body enters the ventroposterior lateral nucleus (VPL). Information from the face actually enters the ventroposterior medial nucleus (VPM). The thalamocortical afferents take all of the signals, whether from VPL or VPM, to primary somatosensory cortex. Once there, it is distributed in a somatopic (body-mapped) fashion, with the legs represented medially, at the top of the head, and the face represented laterally.

TRIGEMINAL NOCICEPTIVE SYSTEM

The dura and cranial blood vessel, which are pain sensitive structures, are also supplied by trigeminal afferents, particularly from the ophthalmic and mandibular divisions (Arbab et al., 1986; Andres et al., 1987). Surrounding the large, supratentorial cerebral vessels, pial vessels, large venous sinuses, and dura mater is a plexus of nociceptive fibers, largely myelinated (A δ) fibers and unmyelinated (C) fibers, that arise from the trigeminal ganglion, while the posterior fossa innervation arises from the upper cervical dorsal roots (Goadsby, 1997). The cell bodies of most of the afferent fibers lie in the trigeminal (Semilunar or Gasserian) ganglion in the middle cranial fossa at the base of the skull (Waite and David, 1995). Trigeminal ganglion cells are pseudounipolar and can also be classified on the basis of ultrastructural and immunocytochemical differences (Kai-kai, 1989), into large, type A cells and smaller, type B cells, with subclasses of each trigeminal ganglion cells also contain amino acids and neuropeptides similar to those in spinal ganglia (Kai-Kai, 1989; Ichikawa and Helke, 1993; Liu et al., 1993). In general, dorsal root ganglion cells contain one or more peptides. Some of the peptides that have been identified in dorsal root ganglion cells by immunohistochemical staining include the following: substance P (SP), somatostatin (SOM), cholecystokinin (CCK), calcitonin gene-related peptide (CGRP), bombesin, vasoactive intestinal polypeptide (VIP), galanin, vasopressin, oxytocin, dynorphin (DYN), enkephalin (ENK), α -neoendorphin, corticotrophin releasing factor, and neurokinin A (Willis and Coggeshall, 1991). To date it unclear if the presence of a particular set of peptides can predict the function type of sensory receptor (Cameron et al., 1988). It seems likely that the peptides are neuromodulators that act in concert with fast-acting neurotransmitters, either enhancing or diminishing their action (Willis et al., 1995).

The trigeminal sensory nuclei extend from the midbrain to the upper cervical spinal cord and are divided into three main groups: the mesencephalic nucleus, the main or principal sensory nucleus, and the spinal trigeminal nucleus. Spinal trigeminal nucleus is itself subdivided into oral, interpolar and caudal parts. About half of the trigeminal fiber divides into ascending and descending branches when they enter the pons; the remainder ascend or descend without division. The ascending branches terminate in the main sensory nucleus and the descending branches terminate in the spinal nucleus. The sensation of touch and pressure are conveyed by nerve fibers that terminate in the main sensory nucleus. The sensory fibers from ophthalmic division of the trigeminal nerve terminate in the inferior part of the spinal nucleus (caudal part); fibers from the maxillary division terminate in the middle of spinal nucleus (interpolar part); and fibers from the mandibular division end in the superior part of the spinal nucleus (oral part) (Snell, 1992).

Trigeminal nucleus caudalis (TNC) extends from the level of the obex to the upper cervical dorsal horn with which it is continuous. TNC, which receive nociceptive afferent fibers from the ophthalmic division of trigeminal nerve, has functional and anatomical organization of nociceptive neurons as same as the dorsal horn of the spinal cord. Nociceptive neurons are located in the superficial dorsal horn, in the marginal layer (also called lamina I) and the substantial gelatinosa (lamina II). The majority of these neurons receive direct synaptic input from $A\delta$ and C fibers. Many of the neurons in the marginal layer (lamina I) respond exclusively to noxious stimulation (and thus are called nociceptive-specific neurons) and project to higher brain centers. Some neurons in this layer, called wide-dynamic range neurons respond in a graded fashion to both nonnoxious and noxious mechanical stimulation. The substantial gelatinosa (lamina II) is made up almost exclusively of interneurons (both excitatory and inhibitory), some of which respond only to nociceptive inputs while other respond also to nonnoxious stimuli. Lamina III and IV contain neurons that receive monosynaptic input from $A\beta$ fibers. Lamina V contains primarily wide dynamic-range neurons that project to the brain stem and to region of the thalamus. These neurons receive monosynaptic input from $A\beta$ and $A\delta$ fibers. They also receive input from C fibers, either directly on their dendrites, which extend dorsally into the superficial dorsal horn, or indirectly via excitatory interneurons that themselves receive input directly from C fibers (Figure 2.3).

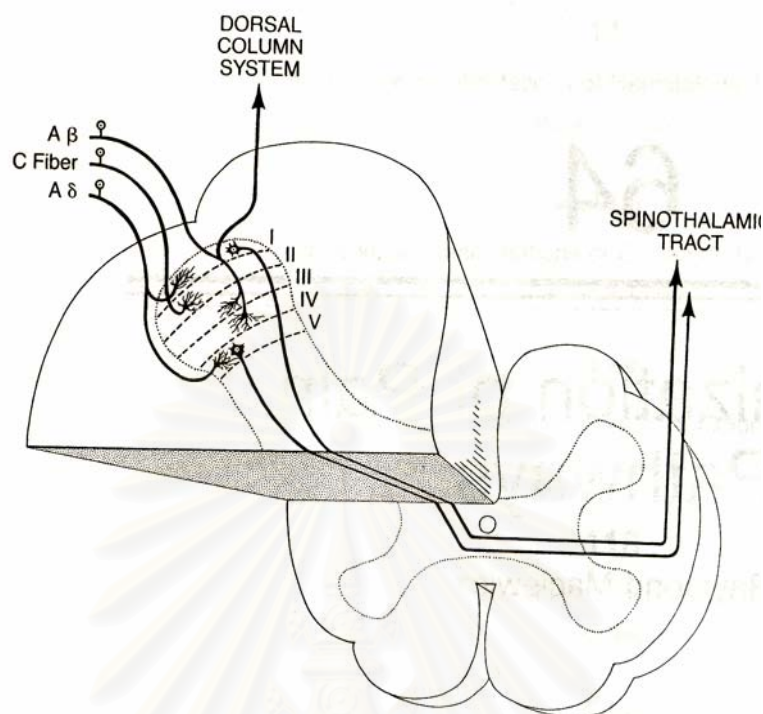


Figure 2.3 Nociceptive afferent fibers terminate on projection neurons in the dorsal horn of the spinal cord. Projection neurons in laminar I receive direct input from myelinated ($A\delta$) nociceptive afferent fibers via stalk cell interneurons in laminar II. Laminar V neurons are predominately of the wide dynamic-range type. They receive low threshold input from the large-diameter myelinated fibers ($A\beta$) of mechanoreceptors as well as both direct and indirect input from nociceptive afferent fibers ($A\delta$ and C). In this figure the laminar V neuron sends a dendrite up through laminar IV, where it is contacted by the terminal of an $A\beta$ primary afferent. A dendrite in laminar III arising from a cell in laminar V is contacted by the axon terminal of a laminar II interneuron (Basbaum and Jessel, 2000).

Cells containing GABA, glutamate or aspartate are seen in all layers (Haring et al., 1990; Magnusson et al., 1986). Colocalization of glutamate with SP and CGRP has been demonstrated in primary afferent terminal in the dorsal horn (Wiesenfeld-Hallin et al., 1984). The second order neurons that lie in the TNC and in the dorsal horn of upper cervical spinal cord at the C1 and C2 levels project their fibers via quintothalamic tract. This tract decussates before snapping on third order neurons in the thalamus (Goadsby, 1997). Traditionally TNC and its thalamic projections have been considered to be the pathway responsible for temperature sensibility and nociception from cranial inputs, analogous to the dorsal horn and spinothalamic pathway in the spinal cord.

Furthermore, second order neurons of TNC synapses in the superior salivatory nucleus, which is parasympathetic outflow (Goadsby, 1997). The parasympathetic innervation of the head arises from cell bodies in the superior salivatory nucleus, passes out with fibers of the facial and glossopharyngeal nerve; and synapses in the sphenopalatine and otic ganglia before reaching the vessels. The classical transmitters in these systems are noradrenaline and acetylcholine. During the past 25 years it has been demonstrated that some perivascular autonomic nerves contain other so called NANC (non-adrenergic non-cholinergic) transmitters or modulator substances. In the parasympathetic system, peptide histidine methionine (PHM), NO are transmitters or modulator (Thomson, 1997; Nozaki et al., 1993). Most of the neurovascular nerve fiber display neuronal nitric oxide synthase (nNOS) immunoreactivity, which produce NO, justifying the novel term “nitroxergic nerves”. Berger et al. (1994) has revealed the presence of nNOS in nerve fibers of the rat dura mater. Being a potent vasodilator, NO was proposed to participate in the pathogenesis of vascular headache by activation of nitroxergic nerves in a manner similar to CGRP (Goadsby and Edvinsson, 1993).

MIGRAINE

DEFINITION AND CLASSIFICATION

Migraine is a primary neurobiology disorder, resulting from dysfunction of the trigeminovascular system. The disorder manifests as recurring attacks, usually lasting 4-72 hours. These attacks, which can interfere with normal functioning, involve unilateral throbbing headache pain of moderate to severe intensity. They also usually

involve nausea, sometimes vomiting, and light, sound, and sensitivity to other sensory stimuli (Blau, 1992)

Migraine may occur with or without an aura that, when present, generally lasts between 5 and 60 minutes. Aura occurs in about 15-20% of patients with migraine. The most common type of aura is visual but also can be somatosensory. The typical presentation of the visual aura is the scintillating scotoma, also referred to as “fortification spectra” or “teichopsia”.

In most patients who experience aura, the aura develops before the head pain being, but on occasion an aura may appear or recur when the headache is most intense. An aura is present before every migraine attack in some individuals, but in the other patients, aura accompanies only a small proportion of attacks. The intensity of aura varies among attacks and may remain constant from attack to attack in a particular person or may vary in successive attacks in the same person. However, aura only occurs in a minority of patients with migraine.

Furthermore, premonitory symptoms, called prodrome, may precede migraine attack; these symptoms occur 24-72 hours before the onset of other symptoms. During this period, patients may experience feeling of well-being, talkativeness, surges of energy, hunger, anorexia, drowsiness, excessive yawning, depression, irritability, restlessness, or tension.

CLASSIFICATION OF MIGRAINE

Migraine headaches are classified according to their clinical features, as well as according to current concepts of pathophysiology. Patients who have migraine without aura generally have normal cerebral blood flow and do not report focal neurologic symptoms. In those who have migraine with aura, changes in regional cerebral blood flow can be demonstrated and neurologic symptoms originating in the brain or brain stem are reported (Lauritzen et al., 1984).

MIGRAINE WITHOUT AURA

Migraine without aura is an idiopathic recurring headache disorder that manifests in the form of attacks that last 4-72 hours. Typically, the headaches are unilateral, have a pulsating quality, and are moderate to severe in intensity. These headaches are aggravated by routine physical activity and are associated with nausea or vomiting, photophobia, and phonophobia.

MIGRAINE WITH AURA

Migraine with aura is also an idiopathic recurring disorder that manifests in some women as migraine without aura but is also accompanied by transient neurologic symptoms. Aura symptoms usually develop gradually, over 5-20 minutes, and last less than 60 minutes. Headache, nausea, or photophobia usually followed neurologic aura symptoms directly or after a free interval of less than 1 hour. The headache usually lasts 4-72 hour, but rarely will be completely absent (migraine aura without headache).

THE CORTICAL SPREADING DEPRESSION AND PATHOGENESIS OF MIGRAINE AURA

Cortical spreading depression (CSD) is a transient disturbance of mechanisms maintaining ionic homeostasis which spread across the brain, moving from the back (occipital region) of the cerebral cortex toward the front at about 3-5 mm/minute (Figure 2.4). These perturbations in ionic homeostasis are characterized by a negative shift of extracellular d.c. potential, suggesting a cell depolarization (Figure 2.6). This electrical phenomenon can be induced in animals with non-noxious stimuli, and is frequently referred to in the literature as the "spreading depression of Leao" (Lauritzen, 1994).

The migraine aura may be defined as any neurological disturbance that appears shortly before or during the development of a migraine headache. Seemingly similar migraine auras may have different features, suggesting that different brain regions are involved (Lauritzen, 1994). A typical migraine aura from the visual cortex is a scintillation scotoma with a characteristic distribution of fortification figures. Usually, the disturbance starts at the visual field center and propagates to the peripheral part within 10-15 min. Function returns to normal within another 10-15 min.

Migraine auras are usually visual, apparently starting in area 17, i.e. the part of the brain with the highest neuronal density. This is consistent with the observation that CSD is much easier to elicit in brains with a high neuronal density. Functioning glia cells tend to decrease the probability of successful elicitation of a CSD. Both the migraine aura and CSD propagate along the cortical surface (Figure 2.4).

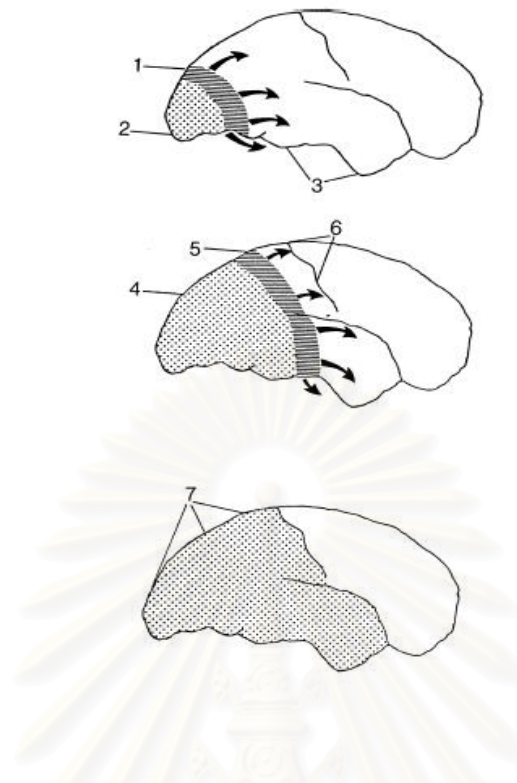


Figure 2.4 Hypothesis of development of a migraine attack based on aspects of CSD and migraine (Lauritzen, 1987). The figures represent lateral views of the human brain at different time intervals after the start of the attack, spaced by 30 min. The dotted area represents the region of reduced rCBF, the striped area represents the region of neuronal depolarization during the first minute of CSD. 1, Initially during a migraine attack a CSD is elicited at the occipital pole, spreading anteriorly at the lateral, medial, and ventral sides of the brain. At the CSD wave front, transient ionic and metabolic disequilibria trigger perturbed neuronal function, rCBF changes and neurological symptoms. 2, Following CSD, cortical rCBF decreases by 20-30% for 2-6 hours. 3, rCBF in regions not invaded by CSD remains normal until encountered by CSD. 4, The region of reduced rCBF expands as the CSD moves anteriorly. 5, Somatosensory symptoms from the extremities appear when the CSD invades the primary sensory cortex at the post-central gyrus. 6, CSD usually stop on reaching the central sulcus, but in many patients it dose not even propagate this far. The ventral spread of CSD causes activation of pain-sensitive fibers and headache. 7, Full-scale attack. The CSD has stopped and is now detectable as a persistent reduction of cortical rCBF. At this time the patient suffers from headache, but has no focal deficits (Lauritzen, 1987b).

Cortical spreading depression: basic features

The reaction was first identified in rabbit cerebral cortex using a Cambridge electrocardiograph (Leao, 1944). The basic observation was that the EEG following mild noxious stimuli would become completely extinguished for a minute or so and that the depression would propagate very slowly across a wide cortical region.

Cortical spreading depression has been induced in most grey matter region (Bures et al., 1974). It has been observed in human cortical tissue *in vitro* (Avoli et al., 1991), and in human hippocampus and striatum *in vivo* (Sramka et al., 1978). Thus, human cortical tissues do support the development of CSD, but a recording of CSD from the human neocortex *in vivo* is still missing (Gloor, 1986).

Successful elicitation of CSD in experiments depends on the susceptibility of the tissue and the trigger factor involved. Common methods of triggering CSD include local electrical and mechanical stimulation or injections of high concentrations of KCl. Potassium plays a central role for CSD and it is reasonable to assume that any disturbance of K^+ homeostasis would predispose the brain region to CSD (Grafstein, 1963). Brain K^+ clearance systems are heavily dependent on the capacity of glial-neuronal cell ratio in the primary visual cortex. Therefore, one would expect human CSD to be initiated occipitally. As is well known, visual auras are indeed very frequent in migraine (Olesen et al., 1990).

Neurons and glial cells depolarize during CSD, giving rise to an intense, but transient spike activity when the reaction enters the tissue (Sugaya et al., 1975). Neuronal silence immediately follows, lasting for a few minutes, but evoked potentials usually take a longer time to recover, 15-30 min (Bures et al., 1974). This sequence of brief excitation followed by a short-lasting depression is supposed to be the neurophysiology basis of the sensory symptoms during migraine auras (Leao and Morison, 1945; Milner, 1958; Gardner-Medwin, 1981; Lauritzen, 1987b).

The depolarization is associated with dramatic changes in the distribution of ions between the intra- and extracellular compartments: K^+ and hydrogen ions leave the cells, while Na^+ , Ca^{2+} and Cl^- enter together with water, as the size of the extracellular space decreases to approximately half of the control values. A return to normal of most ion concentrations and of the size of the extracellular space occurs spontaneously after 30-60 s, whereas Ca^{2+} and pH usually take a few more minutes to recover. There is no satisfactory explanation of the spreading mechanism of CSD, but the spread probably involves the diffusion of one or more chemical mediators, most

likely K^+ and glutamate, into the extracellular compartment (Nicholson, 1993). It has been suggested that a calcium wave in glial cells underlies CSD, but this still remains to be proven (Leibowitz, 1992).

A simplistic scheme of the mechanism of spread of CSD is given in figure 2.7. It is important to appreciate the transient nature of CSD. If the electrophysiological changes are sustained and propagation is absent, then the phenomenon is usually anoxia or hypoglycemia rather than CSD. Repeated episodes of CSD increase the immunohistochemical staining of glial fibrillary acidic protein in the rat cortex that is associated with activation of this cell type (Kraig et al., 1991) and a prolonged period (24 h) of expression of the c-fos pro-oncogene (Herrera et al., 1993) and inhibition of protein synthesis (Mies, 1993).

Cortical spreading depression phenomena occur in experimental animals in the penumbra zone, immediately adjacent to a cortical infarct, where nerve cells are viable but electrically silent (Nedergard and Astrup, 1986; Gill et al., 1992; Ijima et al., 1992). In many respects, the ionic disequilibria during CSD resemble transient ischemia, but there is usually no shortage of energy supply during CSD (Lauritzen et al., 1990). There dramatic changes of neuronal function and ion homeostasis are associated with profound changes of the local circulation (Figure 2.8).

CSD AND TRIGEMINAL ACTIVATION

CSD is the pathophysiological correlated of migraine aura. According to the spreading depression theory of migraine, a CSD-like event leads via the depolarization-induced release of vasoactive, proinflammatory neuropeptides to “neurogenic inflammation”, which excites unmyelinated sensory C-fiber of the trigeminal system, thus causing pain (Hardebo, 1991; Lauritzen, 1994). The neurogenic inflammation accounts for several phases of migraine and is supported by many lines of evidences. Several studies in animals have shown that upon stimulation of the trigeminovascular system, the complex of trigeminal sensory afferents that innervate the dura mater and the larger blood vessels of the brain, neuropeptides such as substance P (SP) and calcitonin gene related peptide (CGRP) are released at the afferent terminal site, causing neurogenic inflammation (NI) in the perivascular space of blood vessels of the meninges. Plasma protein extravasation (PPE) and vasodilatations are proven to result from neurogenic inflammation (Siberstein, 1992). Using animal models it has been shown that the classic ergot alkaloids, sumatriptan

and also the new generation, centrally active triptans inhibit dural PPE which is induced by trigeminal afferent stimulation. Also, non-steroidal-anti-inflammatory-drugs inhibit dural PPE and have been reported to be effective in the treatment of migraine.

Moskowitz has provided an elegant series of experiments whose results suggest that the pain of migraine may be a form of sterile neurogenic inflammation (Moskowitz, 1993). Neurogenic plasma extravasations can be seen during electrical stimulation of the trigeminal ganglion in the rat. Plasma extravasations can be blocked by several anti-migraine drugs (Buzzi et al., 1990; Cuter et al., 1995; Kallela et al., 1998). These experiments provided evidence that neurogenic inflammation can be prevented by blocking transmission in the nerve fibers, and they explain a peripheral mechanism of action for acute-headache medications that work by blocking nerve-fiber transmission in the trigeminal system rather than through a vascular route.



สถาบันวิทยบริการ
จุฬาลงกรณ์มหาวิทยาลัย

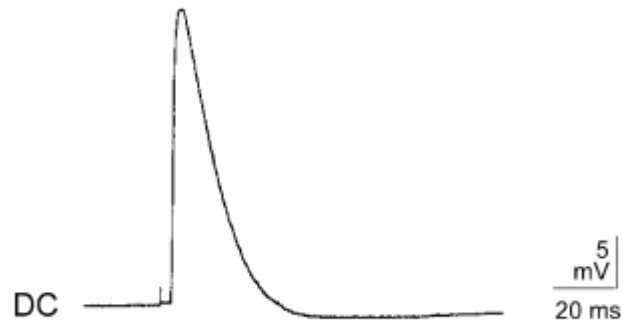


Figure 2.5 The shape of a typical DC-potential recorded following the appearance of one CSD (Gorji et al., 2004).

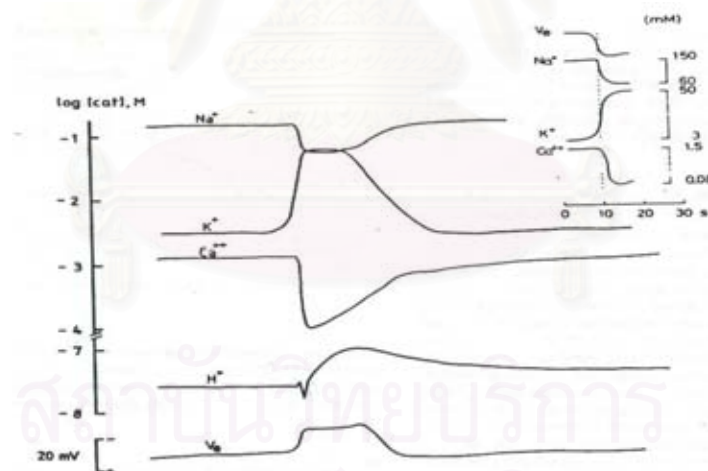


Figure 2.6 Electrophysiological changes accompanying cortical spreading depression in the rat brain. Interstitial ion concentrations of sodium, potassium, calcium and hydrogen were measured by ion-selective electrodes. The extracellular potential (V_e) and the single unit activity were measured by single-barreled electrophysiological changes which were recorded in the parietal cortex (Laurizen, 1994).

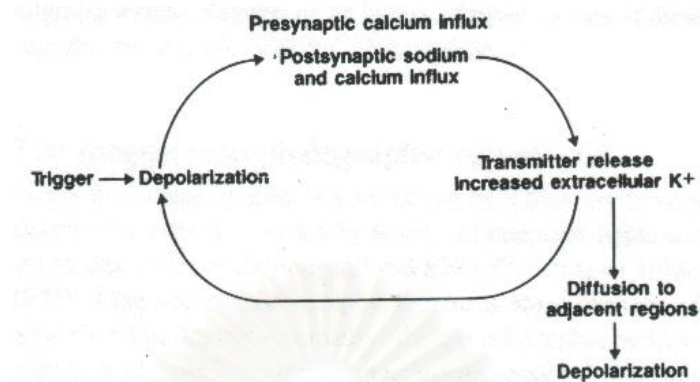


Figure 2.7 Simplistic scheme of autocatalytic cycle possibly occurring during CSD (Laurizen, 1994).

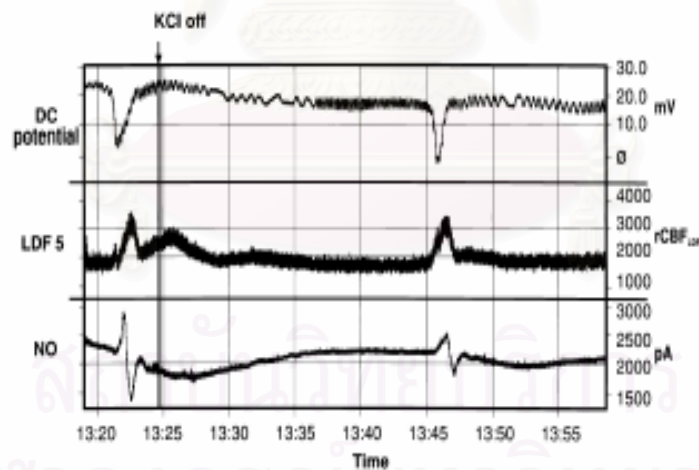


Figure 2.8 Original traces showing change in cortical D.C. potential (mV), rCBF LDF (laser Doppler flux units) and NO release (pA) over time (min) following application of KCl solid to the parietal cortex of a vehicle treated animal (Read, Smith and Benham, 1997).

TECHNIQUE FOR INDUCTION OF CSD IN ANIMALS

Several methods have been employed to initiate CSD in animal brain. These methods can be grouped into 3 major categories including local electrical, mechanical or chemical stimulation. Among these methods two techniques which are frequently used are mechanical stimulation and KCl application.

MECHANICAL STIMULATION

Blunt stabbing and pin pricking are common method to elicit CSD. Several research groups, such as Lambert et al., 1999 and Ebersberger et al., 2001 always choose the pinprick technique to evoke CSD on the animal cortex, including cats, rats and rabbits (Lambert et al., 1999; Lambert and Michalicek, 1994; Piper et al, 1991; Ebersberger et al., 2001). This method is delivered by rapid insertion of a 26-30 gauge needle, through the dipole and dura (1-2 mm depth) into cortical tissue and immediately withdrawn. The location needs avoiding the pial vessels. However, this technique has been disagreed with some research groups. They suggested that this technique may link to the noxious stimulation (Read et al., 2000).

KCl APPLICATION

As previously mentioned, potassium play a central role for CSD and it is reasonable to assume that any disturbances of K^+ homeostasis would predispose the brain region to CSD (Grafstein, 1963). The KCl application is the most popular technique that has been chosen by many research groups, such as Read et al., (1997), Smith et al., (2000), Moskowitz et al., (1993) and colonna et al., (1997). This technique can be further divided into 2 methods, including the microinjection of KCl on the cortical surface and the placement of solid KCl on the surface of cortex.

The microinjection of KCl technique

After performing craniotomy, a fused silica needle or PE-90 (a catheter tube) or glass micropipette is placed 1 mm below the dural surface. Then KCl is injected to the cortical area. The concentration of KCl vary 670 mM to 1 M. (Ingvarnsen et al., 1997; Meng et al., 1995; Moskowitz et al., 1993; Colonna et al., 1997)

The placement of solid KCl technique

After the craniotomy opening is performed, a solid KCl is placed directly to the cortical surface area. The weights of KCl vary 3 to 30 mg. depending on the size of animal (for example, rat uses 3 mg and cat uses 30 mg). (Smith et al., 2000; Read et al., 1997; Read et al., 2000)

Less popular methods of KCl application are able available, such as a remote intracortical injection, application of KCl-soaked paper on cortical surface, etc. (Wahl et al., 1994; Douen et al., 2000; Koponen et al., 1999). For the sake of comparison, application of NaCl into brain tissue is usually included as the control.

THE SEROTONIN, TRIGEMINOVASCULAR CONTROL AND MIGRAINE

Serotonin is formed by the hydroxylation and decarboxylation of tryptophan. The greatest concentration of 5-HT (90%) is found in the enterochromaffin cells of the gastrointestinal tract. Most of the remainder of the body's 5-HT is found in platelets and the CNS. The raphe caudal nucleus projects largely to the medulla and spinal cord for the regulation of pain perception. The rostral nucleus projects extensively to the limbic structures and the cerebral cortex. In the limbic system, especially, the projections are co-localized with norepinephrine receptors and the two transmitters seem to work in conjunction in the regulation of arousal.

1. ROLE IN VASCULAR TONE

5-HT is synthesized in nerve terminals innervating the cranial and cerebral vascular (Bonvento et al., 1991; Cohen et al., 1992; Lincoln, 1995). The extent of the physiologic importance of 5-HT in the control of vascular smooth muscle tone, either as a co- or neurotransmitter, is not clear. However, cranial blood vessels are particularly sensitive to 5-HT, and they can either contract or relax to 5-HT, acting on 5-HT_{2A}, 5-HT_{1B} or 5-HT₇ receptors (Martin, 1994; Saxena, 1995; Villalon et al., 1997). The affinity of 5-HT for 5-HT_{1B} and 5-HT₇ receptors is much higher than for 5-HT_{2A} receptors (Martin, 1994; Saxena, 1995; Villalon et al., 1997). Thus, as depicted 5-HT constricts large conducting arteries and arteriovenous anastomoses mainly via the 5-HT_{1B} receptor and dilates arterioles via the 5-HT₇ receptor. If either plasma or neuronal 5-HT is involved in the maintenance of vessel wall tone, a decrease in the concentration of 5-HT in the neurovascular junction can lead to

constriction of arterioles, but a dilatation of large arteries and arteriovenous anastomoses. There is some evidence of such hemodynamic changes occurring during the headache phase of migraine (Sexena, 1995; Villalon et al., 1997).

Whether or not 5-HT plays a pathologic role in migraine at the neurovascular junction, there is no denial that acutely acting antimigraine drugs (ergots and triptans) constrict cranial arteries and arteriovenous anastomoses (De Vries et al., 1998; Villalon et al., 1997). It seems clear that constriction of arteriovenous anastomoses by the triptans and, partly also the ergot alkaloids involves the 5-HT_{1B} receptor (De Vries et al., 1998). However it is surprising that the contractile effect of 5-HT itself on porcine carotid arteriovenous anastomoses is not affected much by GR 127935, a selective and potent 5-HT_{1B/1D} receptor antagonist (De Vries et al., 1998). This unexpected finding suggests that arteriovenous constriction by 5-HT in the pig involves a novel receptor subtype.

2. ROLE IN NOCICEPTIVE MODULATION

Serotonergic neurons are also involved in a well-described pain-modulating circuit that includes the amygdala, periaqueductal gray (PAG), dorsolateral pontine tegmentum (DLPT), and rostroventral medulla (RVM). According to this model, cells in the PAG project primarily to RVM cells that in turn act on the spinal dorsal horn. When activated, RVM neurons inhibit pain sensory processing, presumably by inhibiting the dorsal horn cells that are receiving pain information. Through descending projections, this circuit controls spinal pain-signaling mechanisms as well as dorsal horn pain transmission and is an endogenous mechanism of pain relief. In multiple studies in rodents, Fields and coworker, 1991 have shown that 5-HT is important neurotransmitter in this pain-modulating circuit (Fields et al., 1991). All pain is not created equal, however sharp, stabbing pain and dull aching pain involve different neural pathways. Under normal circumstances, an acute pain will be transmitted to the brain and will then be resolved in part due to the endogenous pain-modulating system. In persistent pain, however, resolution does not take place. Instead, plastic changes take place in the neural pathways involved in transmitting acute pain. Several other animal studies further support the important role of 5-HT in the process of pain modulation. Molecules that block the synthesis of 5-HT have been shown to inhibit antidepressant-mediated pain relief in mice. In related research,

depletion of central serotonergic systems has been shown to block antidepressant-mediated pain relief in mice. 5-HT is likewise important for the functioning of the endogenous pain-suppressing descending projections described originally by Fields and Basbaum (1978). Normally, as part of a negative feedback loop, the output of the pain-transmission neurons helps activate the pain-suppression system. The PAG, DLPT, and RVM are the key regions of the brain involved in this descending pain modulation. Research shows that lesions made to these areas of the brain block pain relief associated with the antidepressant clomipramine. Furthermore, within the spinal cord itself, activation of serotonergic receptors also produces pain relief.

3. ROLE IN CONTROLLING CENTRAL ACTIVITY

Numerous observations suggest diverse and modulatory roles for 5-HT in cortex. Because of the diversity of cell types and multiple receptor subtypes and action of 5-HT, it has proven difficult to determine the overall role of 5-HT in cortical function. Normal fluctuations in cortical states, mood, attention, and information processing rely on activation of neocortical 5-HT receptors (Waterhouse et al., 1986b; Jacobs et al., 1990; Reuter and Jacobs, 1996; Marek and Aghajanian, 1998). Altered serotonergic transmission is implicated in anxiety and depression, seizures, action of psychotropic hallucinogens, and schizophrenia (Statnick et al., 1996; Marek and Aghajanian, 1998). Frontoparietal cortex receives serotonergic projections from the dorsal and median raphe nuclei (Waterhouse et al., 1986a; Tork, 1990). More than one dozen 5-HT receptor types have been described (Hoyer et al., 1994), several of which are expressed in frontoparietal cortex (Bruinvels et al., 1994; Pompeiano et al., 1994; Burnet et al., 1995; Wright et al., 1995; Morales and Bloom, 1997; Vysokanov et al., 1998). With the exception of the 5-HT₃ receptor (ligand-gated ion channel), 5-HT receptors couple to G-proteins to exert their effects (Hoyer et al., 1994). These observations suggest diverse modulatory roles for 5-HT in cortex.

In vivo, firing rates of pyramidal neurons are generally decrease by iontophoresis of 5-HT (Krnjevic and Phillis, 1963; Jordan et al., 1972; Reader et al., 1979; Lakoski and Aghajanian, 1985). 5-HT also reduced the responses of somatosensory cortical neurons to afferent input (Waterhouse et al., 1986b) and altered memory fields in prefrontal cortex (Williams et al., 2002).

Previous in vitro studies of the action of 5-HT in cortex concentrated on layer V pyramidal neurons. In rat cortex, these cell were hyperpolarized or depolarized by

5-HT, with most cells exhibiting both responses (Davies et al., 1987; Araneda and Andrade, 1991; Tanaka and North, 1993; Spain, 1994; Marek and Aghajanian, 1998). The hyperpolarizations involved activation of 5-HT_{1A} receptors and increased potassium conductance (G_K). Depolarizations were reported to involve 5-HT_{2A} receptors and a decrease in G_K . 5-HT also reduced the slow afterhyperpolarization (sAHP) (Araneda and Andrade, 1991; Tanaka and North, 1993) and induced and afterdepolarization (ADP) (Araneda and Andrade, 1991). In cat sensorimotor cortex, the 5-HT response correlated with pyramidal cell firing type (Spain, 1994).

5-HT has long been involved in the pathophysiology of migraine. Shortly after its discovery, 5-HT was implicated in the pathophysiology of migraine based on the original finding by Sicuteri and colleagues (Olesen et al., 2000) of an increased urinary excretion of 5-HT's primary metabolite, 5-hydroxyindoleacetic acid (5-HIAA) during migraine attacks. A most convincing piece of evidence, in favor of migraine being a low serotonergic syndrome has been provided from physiologic studies on the evaluation of auditory evoked potentials. The amplitude of these evoked potentials has shown to be inversely related to central serotonergic neurotransmission. In migraine patients, a marked increase in amplitude was observed between attacks, in support of a low 5-HT transmission and abnormal cortical processing of sensory information. The implication of serotonergic pathways in this response has further been confirmed by the observation that 5-HT_{1B/1D} receptor agonists, which can penetrate the brain and activate cortical inhibitory prejunctional 5-HT_{1B/1D} autoreceptors, can decrease the amplitude of auditory evoked potentials in migraine sufferers. These observations all converge to support the notion that migraine is associated with a cortical hypersensitivity to stimulate the headache-free interval, which is, at least in part, due to low 5-HT transmission (Wang et al., 1996; Srikiatkachorn et al., 1998).

Such a scenario of a chronically low availability of the 5-HT could result in a sensitization of all or specific populations of 5-HT receptors in migraine sufferers. Interestingly pharmacologic and molecular evidence seems to support the original hypothesis that migraine is the consequence of an inappropriate increased sensitivity of 5-HT_{2B} receptors (Kalkman 1994). More specifically, suggested that activation of cerebrovascular endothelial 5-HT_{2B} receptors, following and increase bioavailability of 5-HT at the onset of a migraine attack would induce the endothelial production and

release of nitric oxide (NO). Nitric oxide can dilate cranial blood vessels and activate trigeminovascular afferents, thus invoking two aspects of the neurogenic inflammation response thought to be involved in pain generation and transmission. This mechanism reinforces the view that central dysfunctions in migraine will lead to perturbations of the cranial circulation. Indeed, activation of 5-HT_{1B/1D} receptors causing cranial vasoconstriction and inhibition of trigeminovascular activity leads to alleviation of migraine symptoms (Kalkman, 1994; Lance 1993).

Arguments in favor of the biochemical triggering event being an increase in 5-HT availability include the observations that several drugs that release 5-HT from neurons and blood platelets (fenfluramine and reserpine) and some 5-HT reuptake inhibitors (zimeldine and femoxatine) are all able to provoke migraine attacks and more frequently so in migraine subjects than in controls (Humphrey, 1991). The same may be the case with red wines, which also release 5-HT from blood platelets, and possibly from neuronal stores. However, fenfluramine and reserpine used for extended periods can confer resistance to migraine headaches, and 5-HT given during an attack will induce a headache relief. It seems therefore that the mobilization of 5-HT from intracellular stores at an early stage will trigger migraine attacks. However the receptors inducing the migraine attack (possibly the 5-HT_{2B}) are different from those (5-HT₁ family) that relieve migraine headaches (Humphrey, 1991; Olesen et al., 2000, Srikiatkachorn et al., 2002).

It has been claimed that changes in circulating 5-HT alone cannot explain all the facets of a migraine attack (Humphrey, 1991). Despite the fact that a low brain serotonergic activity has been evidenced between attacks on the basis of an increase amplitude of auditory action potentials, an increase in central 5-HT neurotransmission at the onset and during an attack has not yet been demonstrated. Thus, whether the pharmacologic manipulations with 5-HT agonists and 5-HT releasing agents bear any relevance to a spontaneous migraine attack is still largely speculative. However, a positron emission tomography study performed in migraine patients during their spontaneous migraine attacks showed an increased cerebral blood flow in the brain stem, including in an area corresponding closely in location to the serotonergic dorsal raphe nucleus (Olesen et al., 2000). This fascinating observation may suggest that serotonergic dorsal raphe neurons become active and release 5-HT during a migraine attack, and as such they have been considered as part of the migraine generating center. These neurons project to many areas of the central nervous system, including

the cerebral cortex and the area postrema, where abnormal information processing has been documented during migraine. They are also intricately related to the cranial vasculature, which constitutes the primary focus of pain generation in migraine. These characteristics, together with the known interactions between serotonergic, dopaminergic, and noradrenergic systems in the brain, suggest that dysfunctions of the 5-HT system are likely to have functional repercussions much larger than those expected on the basis of 5-HT neurotransmission alone. This may explain some of the complexity of the neurochemical changes associated with migraine, most specifically those related to other amines (Olesen et al., 2000).

VANILLOID RECEPTOR SUBTYPE 1 (VR1) AND TRANSDUCTION OF NOXIOUS STIMULATION

VR1 is a non selective cation channel expressed by primary sensory neurons of the “pain” pathway. It can be activated by vanilloid compound (e.g. capsaicin), protons, or heat (>43 degrees C). After being activated, this receptor allows sodium, calcium, and possibly potassium ions to flow down their concentration gradients, causing initial depolarization and neurotransmitter release.

Accumulating evidences show that expression of VR1 receptor in dorsal root ganglion (DRG) cells is subjected to change. For example, Amaya et al., (2003) demonstrated that inflammation can increase in VR1 positive neuronal profile in rat DRG neurons using histochemical methods. In their experimental, peripheral inflammation was generated by intraplantar injection of Freund’s complete adjuvant (CFA) into the left hind paws. They found that the inflammation induced a 1.5 fold increase in percentage of VR1-like immunoreactivity positive profiles. Area frequency histogram showed that VR1 expression was increase exclusively in small and medium-sized neurons after inflammation.

Beside inflammation, injury in nervous system can also alter VR1 expression. In 2002, Fukuoka, Tokunaga and Tachibabana investigated the expression of VR1 receptor in rat DRG neurons after spinal nerve ligation. They found that VR1 mRNA expression was increased in the small and medium-sized DRG neurons. This change could be observed at the first day after injury and persisted to 28th day. The increase in VR1 expression was confirmed by immunoreactive at the third day after surgery.

The above data provide evidence that both noxious stimulation and injury in nervous system can increase VR1 expression in DRG. Such change may relate to functional alteration of pain perception and may underlie the development of chronic pain syndrome

STRUCTURE OF VR1

The rat VR1 cDNA contains an open reading frame of 2514 nucleotides. This cDNA encodes a protein of 838 amino acids with 6 transmembrane domains. The cytoplasmic, N-terminal hydrophilic segment (423 amino acids) contains a relatively proline rich region followed by three ankyrin-repeat domains (Fig 2.9). The C-terminus (154 amino acids) has no identifiable proteins motifs (Table 2.1).

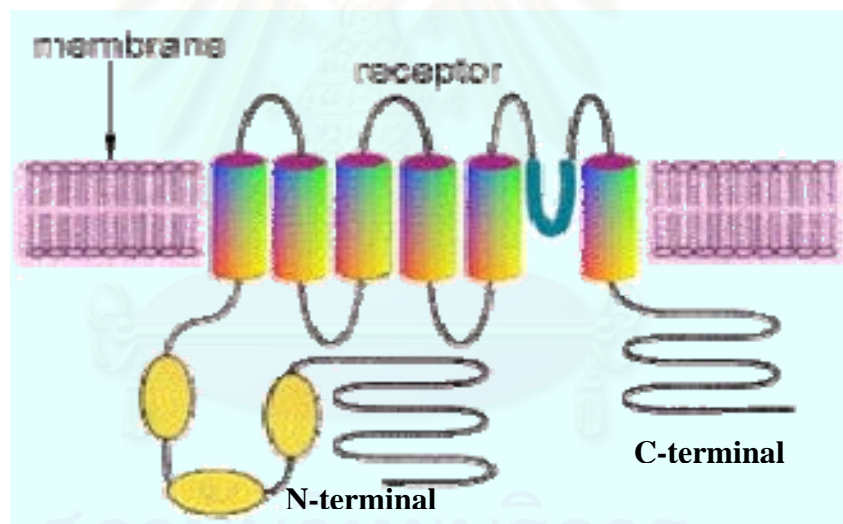


Figure 2.9 Structure of vanilloid receptor subtype 1 (Caterina et al., 1997)

ANATOMICAL LOCALIZATION AND TISSUE SPECIFICITY OF VR1

VR1 IN PRIMARY SENSORY NEURONS

As first shown by resiniferatoxin (RTX) autoradiography (Szallasi, 1995), VRs are expressed along the entire length of vanilloid-sensitive sensory neurons, from the peripheral terminal to the axons to the somata to the central ending. In corresponding areas the presence of VR1-like immunoreactivity has also been demonstrated (Guo et al., 1999; Tominaga et al., 1998). Northern blot analysis confirmed the presence of VR1 transcripts in dorsal root and trigeminal ganglia (Caterina et al., 1997; Helliwell et al., 1998a). VR1-like immunoreactivity was detected in more than 50% of DRG neurons, with the expression being most prevalent in small to medium sized neurons (Guo et al., 1999). VR1-like immunoreactivity was also observed in both the central (e.g. dorsal horn of the spinal cord) and peripheral (e.g. skin and cornea) processes of primary afferent neurons (Guo et al., 1999). In DRG neurons, VR1-like immunoreactivity was associated with the Golgi complex and plasma membrane (Guo et al., 1999). In the dorsal horn of the spinal cord, the VR1 protein was associated with “small clear vesicles” in preterminal axons and with the plasma membrane of nerve terminal (Guo et al., 1999). The latter finding is in line with an earlier observation of Szolcsanyi (Szolcsanyi and Jancso-Gabor, 1975), according to which capsaicin depletes “small clear vesicles” from nerve ending.

The distribution of VR1-like immunoreactivity in the spinal dorsal horn deserves particular attention. The labeling is strongest in the Lissauer zone (lamina I). VR1 protein is also abundant in the inner, but not in the outer, layer of lamina II (Guo et al., 1999). It should be noted that several important proteins involved in pain transmission are also enriched in the inner layer of lamina II (i.e. in close proximity to VR1).

VR1 IN VAGAL (NODOSE GANGLION) NEURONS

An unexpected result in the VR1 cloning article by Julius and colleagues (Caterina et al., 1997) is the failure of Northern blot hybridization to detect mRNAs encoding VR1 in nodose ganglia. However, using a probe corresponding to nucleotides 1513-2482 of the rat VR1 sequence, a strong in situ hybridization signal was detected in nodose ganglia neurons (Helliwell et al., 1998)

VR1 IN BRAIN

The presence of VR1 mRNA in the hypothalamus has recently been confirmed by reverse transcription-polymerase chain reaction (Sasamura, 1998). These vanilloid-sensitive terminals in the hypothalamus are probably glutaminergic because capsaicin evokes glutamate release from slices of hypothalamus (Sasamura, 1998). In 1988, capsaicin microinjected into the substantia nigra or caudatus putamen was reported to induce peripheral vasodilatation and a subsequent hypothermic response (Hajor, 1988). These biological actions suggested the existence of intrinsic vanilloid-sensitive cells in the basal ganglia. VR1 mRNA seems to be widely present in the brain. Relative levels are as follows: hypothalamus and cerebellum > cortex, striatum, and midbrain > olfactory bulb, pons, hippocampus, and thalamus (Sasamura, 1998).

VR1 IN NONNEURONAL TISSUES

It has been long noted that capsaicin exerts a variety of effects on nonneuronal tissues (Buck and Burks, 1986; Holzer, 1991). These actions were considered nonspecific because they were at variance with prevailing concept of capsaicin being selective for sensory neurons. In 1998, they showed that vanilloids induce calcium uptake by mast cells (Biro et al., 1998a) and in a glioma cell line (Biro et al., 1998b)

VR1 AND PAIN

VR1 are predominantly expressed on C and A δ fibers projecting to the dorsal horn of the spinal cord and in trigeminal ganglion neurons projecting to the spinal nucleus of the trigeminal tract. Of the many stimuli that activate cation currents in primary sensory neurons, low extracellular pH and noxious heat have been proposed as physiological activators of vanilloid receptors (Table 2.2).

VR1 AS A RECEPTOR FOR NOXIOUS THERMAL STIMULI

Many proteins, including receptors and channels, show alterations in their structure or activity as a function of temperature, but VR1 has thermal response characteristics that make it especially interesting in the context of nociception. Most notably, VR1 is gated by heat, but only when ambient temperatures exceed 43°C (Tominaga et al., 1998), a threshold matching that of heat-evoked pain responses in humans and animals or heat-evoked electrophysiological responses in primary afferent nerve fibers or cultured sensory neurons (Cesare and McNaughton 1996,

LaMotte and Campbell 1978, Raja et al., 1999). Evidence for a direct relationship between VR1 expression and heat sensitivity is supported by several observations (Tominaga et al., 1998), the most basic of which is that sensitivity to capsaicin and heat sensitivity are significantly correlated (in both frequency and magnitude) among VR1-transfected HEK239 cells. Responses to these stimuli also show cross-desensitization, and both capsaicin- and heat-evoked currents are attenuated by the vanilloid receptor antagonists capsazepine and ruthenium red. In addition, both responses are characterized by outwardly rectifying current-voltage relations and relatively high permeability to calcium ions. Some distinctions do exist, such as quantitative differences in cation permeability ratios or requirements for extracellular calcium in desensitization, suggesting that vanilloid and heat activate VR1 through overlapping but distinct mechanisms. In VR1-transfected HEK293 cells (as in sensory neurons), capsaicin or heat evokes single-channel currents in excised membrane patches, demonstrating that channel activation occurs via a membrane-delimited mechanism that does not require the action of diffusible cytoplasmic second messengers (Tominaga et al., 1998). Site-specific mutations in VR1 can significantly alter capsaicin potency or thermal activation thresholds (Jordt, Tominaga and Julius, 2000), providing further evidence that VR1 itself transduces responses to these stimuli when expressed in heterologous cells.

These observations of heterologous nonneuronal systems have led us to propose that VR1 functions as a molecular transducer of noxious thermal stimuli *in vivo*. Consistent with this hypothesis, sensitivity to capsaicin and sensitivity to noxious heat are also well correlated among small-diameter sensory neurons in culture (Kirschstein, Busselberg and Treede, 1997; Nagy and Rang 1999a,b). Moreover, VR1 and native heat-evoked currents have a number of properties in common, including similar current-voltage relationships (Cesare and McNaughton, 1996, Nagy and Rang, 1999b, Reichling and Levine, 1997), selective permeability to cations (Cesare and McNaughton, 1996, Nagy and Rang, 1999b, Reichling and Levine, 1997), and in some studies, sensitivity to vanilloid receptor antagonists (Kirschstein et al., 1999). At the same time, numerous discrepancies between native heat- and vanilloid-evoked responses have been reported, including differences in relative permeability to calcium and sodium ions (Cesare and McNaughton, 1996, Nagy and Rang, 1999b) and sensitivity to vanilloid receptor antagonists (Nagy and Rang, 1999b, Reichling and Levine, 1997). Moreover, Nagy and Rang have recently

shown that amplitudes of the capsaicin-and heat-evoked responses among individual sensory neurons are not tightly correlated, contrary to the scenario expected if the same channel responds to both stimuli. Most significantly, capsaicin and heat-evoked responses showed poor co segregation at the single-channel level in membrane patches excised from cultured rat sensory neurons (Nagy and Rang, 1999b). That is, most patches were sensitive to capsaicin or heat, but only a few patches responded to both stimuli. From these findings, Nagy and Rang (1999a) proposed that distinct ion channels respond to capsaicin and heat. These channels could consist of entirely different molecules or different functional isoforms of VR1 generated through alternative RNA splicing, post-translational modification, or association with other cellular proteins. Unfortunately, similar patch clamp analyses have not been carried out with VR1-expressing HEK293 cells; such experiments might help to address these issues.

VR1 AS A RECEPTOR FOR PROTONS

Tissue damage, such as that associated with infection, inflammation, or ischemia, produces an array of chemical mediators that activate or sensitize nociceptor terminals to elicit pain and promote tenderness at the site of injury (Handwerker and Reeh, 1991, Levine and Taiwo, 1994). Protons constitute one important component of this pro-algesic response, reducing the extracellular pH to levels below the physiological norm of 7.6. Extracellular protons elicit both transient and sustained excitatory responses in cultured sensory neurons, the latter of which is believed to account for persistent pain associated with local tissue acidosis (Bevan and Geppetti, 1994). Protons are capable of modulating the activity of a number of receptors and ion channels expressed by primary afferent nociceptors, including acid-sensitive channels of the degenerin family (Chen et al., 1998; Lingueglia et al., 1997; Waldmann et al., 1997a, b), ATP-gated channels (Li et al., 1997, stoop et al., 1997), and vanilloid receptors (Caterina et al., 1997, Jordt et al., 2000, Kress et al., 1996, Martenson et al., 1994, Petersen and LaMotte 1993, Tominaga et al., 1998). Which, if any, of these entities contributes to acid-evoked pain is presently unclear, but electrophysiological and genetic studies of native and cloned vanilloid receptors suggest that they play a significant role in mediating sustained proton responses in vivo.

Because protons have been proposed to act as modulators of native vanilloid receptors, there is significant interest in understanding the relationship between sensitivity to capsaicin and protons sensitivity at the cellular and molecular levels. Temperature response curves generated in VR1-expressing oocytes or HEK239 cells show that a reduction in extracellular pH produces markedly larger responses at temperatures that are noxious to mammals ($>43^{\circ}\text{C}$). Moreover, a reduction in pH dramatically lower the threshold for channel activation, such that at pH 6.3, substantial currents can be seen at temperatures as low as 35°C , conditions under which the channel is normally closed (at pH 7.6). This augmentation of VR1 thermal responsiveness by protons closely resembles the increase in nociceptor thermal sensitivity associated with inflammation (Handwerker and Reeh, 1991). In both cases, there is a significant decrease in the threshold for heat-evoked responses and an increase in responses magnitudes at temperatures above the initial pain threshold. Importantly, VR1 shows especially dynamic modulation of heat-evoked currents between pH 8 and 6 (Jordt, Tominaga and Julius, 2000), sensitivity rang that matches the extent of local acidosis attained during most forms of tissue injury. Below pH 6, sustained membrane currents can be observed in VR1-expressing HEK239 cells at room temperature (22°C), with a half-maximal effective pH of 5.4 (Tominaga et al., 1998). Whether these proton-evoked responses result simply from a decrease in the channel's thermal response threshold or involve additional steps is not entirely clear, but recent structure function studies suggest that proton-evoked channel activation and proton-mediated potentiation can be functionally uncoupled (Jordt, Tominaga and Julius, 2000).

PLASTICITY OF VR1

VR1 is responsive to multiple stimuli, including heat, protons. Injury brings on many changes that affect the activity of the nociceptor, including local tissue acidosis and the production of pro-algesic agents, such as bradykinin, ATP, monoamines, and arachidonic acid metabolites. The result is one in which response thresholds to noxious stimuli are decreased, thereby contributing to the development of thermal and mechanical hypersensitivity. The capacity of VR1 to detect and integrate information from diverse physical and chemical inputs makes this channel potentially well suited for assessing the physiological environment of the primary

afferent nerve terminal and for altering nociceptor excitability in the setting of tissue injury.

This prediction is clearly borne out by the analyses of VR1-deficient mice. In these studies, tissue injury was elicited by treatment of the hindpaw with an inflammatory agent or nerve injury was produced by partial ligation of the sciatic nerve. Wild-type mice exhibit increased sensitivity to both thermal and mechanical stimuli after such treatments. In contrast, VR1-null mice show hypersensitivity to mechanical stimuli, as well as normal thermal hypersensitivity following nerve injury, but they do not show increased sensitivity to thermal stimuli following tissue injury. Thus, VR1 appears to be essential for the development of thermal hypersensitivity associated with tissue inflammation, but not that associated with nerve injury.

Clearly, inflammation-induced thermal hypersensitivity may result from the convergent action on VR1 of heat, low pH, and other inflammatory mediators. However, other mechanisms, such as up-regulation of VR1 expression or sensitization of VR1 by post-translation modification may also come into play.

PERIPHERAL STIMULATION AND FOS EXPRESSION

The proto-oncogene *c-fos* is one of several immediated-early genes that can be rapidly induced in many kinds of cells following various from stimulation. There are two possible, but not incompatible, views of result of mobilizing the Fos transcription factor complex. First, some evidence suggests that reducing *c-fos* levels with antisense treatments decreases nociceptive thresholds (i.e., animals become more sensitive to painful stimuli) (Hunter et al., 1995). This observation implies that Fos is leading a reactive response against excessive stimulation by mobilizing inhibitory mechanisms, such as an increase in the production of dynorphin (Noranjo et al., 1991; Noguchi et al., 1991; Dubner and Ruda 1992; Lucas et al., 1993). The second view, for which there is no evidence as yet, is that the activation of *c-fos* is the first step in establishing long-term changes in excitability that may be reflected in the development of behavioral states, for example, hyperalgesia.

The acute expression of Fos in the spinal cord depends upon the nature and site of noxious stimulation and on the time after stimulation. At two hours following noxious thermal, chemical, or mechanical stimulation, Fos expression is seen mainly in neurons within the superficial laminae (I-II) and lamina V. This acute expression of Fos is largely transient, especially in the superficial layers of the cord where it is rarely seen three to four hours after stimulation. Extensive non-noxious stimulation of the hind paw by brushing will induce Fos within neurons of laminae III-IV, where the non-nociceptive large-diameter A β fibers terminate (Hunt et al., 1987; Herdegen et al., 1991a,b).

With extended survival times (greater than 12-24 hours after noxious thermal stimulation of the skin), the distribution of Fos becomes bilateral, and positive neurons are found predominantly within the deeper laminae of the dorsal horn (V-VI) and the intermediated gray matter (lamina VII). The unfolding of this pattern following acute heat stimulation cannot be blocked by the application of local anesthetic to the peripheral nerve, which suggests independence from ongoing nociceptor activity (Williams et al., 1990).

Table 2.1 Characteristics of vanilloid-sensitive primary sensory neurons (Szallasi and Blumberg, 1999)

Main division	<p>1. Dorsal root ganglion neurons projecting to spinal dorsal horn</p> <p>2. Trigeminal ganglion neurons projecting to spinal nucleus of trigeminal tract</p> <p>Small neurons with unmyelinated fibers (C-fiber neurons)</p> <p>Large neurons with thin-myelinated fibers (Aδ-neurons)</p> <p>Peptidergic neurons expressing neurotrophin receptors trkA and p75</p> <p>Nonpeptidergic neurons that bind the lectin B4 and express P2X3 receptors</p>
Sensory modalities evoked by capsaicin	<p>Pain and itch</p> <p>C-afferents: polymodal nociceptors; heat nociceptors and warm receptors; mechano-heat insensitive chemonociceptors (mechano-cold receptors?)</p> <p>Aδ-afferents: polymodal receptors</p>
Selected neuropeptides	<p>Arginine vasopressin</p> <p>Bombesin/gastric-releasing peptide</p> <p>CGRP, CCK, Dynorphin, Eledoisin, Galanin, NKA, Somatostatin, SP, VIP</p>
Selected receptors	<p>ASICs, α2-Adrenoreceptors, Bradykinin receptors, CCK receptors,</p> <p>γ-Aminobutyric acid receptors, Histamine receptors, NK-1R, NMDA receptors, Opiate receptors, Prostaglandin receptors, VRs</p>
Selected activators	<p>a. Endogenous: inflammatory mediators (e.g. bradykinin and histamine) protons (low pH)</p> <p>b. Exogenous: noxious heat, protons (low pH), toluene diisocyanated vanilloids</p>

Table 2.2 Biochemical Pharmacology of Vanilloid receptors (Szallasi and Blumberg, 1996)

Signal transduction mechanism	Ligand-gated non-selective cation channel
Anatomical location	Primary sensory neurons in dorsal root as well as trigeminal ganglia (peripheral and central fibers and their endings; perikary): predominantly small neurons with unmyelinated (C)-fibers, but also some large neurons with thin myelinated (A δ)-fibers Sensory neurons of the vagus with somata in nodose ganglia Intrinsic neurons in the CNS (e.g. preptic area, locus ceruleus, reticular formation, etc.)
Naturally occurring agonists (Vanilloids)	Capsaicinoid (e.g. capsaicin in red peppers or piperine in black pepper) Resiniferanoid (e.g. resiniferatoxin in the cactus-like plant <i>Euphorbia resinifera</i>) Unsaturated dialdehydes (e.g. isovelleral in the mushroom <i>Lactarius vellereus</i>)
Endogenous agonist	Unknown (protons or proton-generated substances?)
Notable synthetic agonists	Olvanyl and nuvanyl (apparently more active on central than on peripheral receptors) Phorbol 12-phenylacetate 13-acetate 20-homovanillate (abolishes positive cooperativity of binding by the receptors)
Antagonists	Competitive: capsazepine Functional: ruthenium red (believed to block the channel without interfering with ligand binding)
Modulators of ligand binding or channel function	pH Temperature Calcium concentration in the extracellular fluid
Receptors structure	Thiol-protein; most likely oligomeric with at least two interacting binding sites (positive cooperativity)

Based on this review, 5-HT depletion and inflammation are accepted to be involved in the pathogenesis of migraine. Here, we performed study the effects of inflammation and 5-HT depletion on development of cortical activity and activation of neural cell in trigeminal nociceptive pathway. The cortical activity was studies using cortical electrode, the neural activity in trigeminal nociceptive pathway were evaluated by VR1 and Fos immunoreactivity.

THE OBJECTIVES OF THIS STUDY

1. To study the effects of facial inflammation on cortical activity and trigeminal nociceptive system in CSD model.
2. To study the effects of 5-HT depletion on cortical activity and trigeminal nociceptive system in CSD model.
3. To study the effects of facial inflammation with 5-HT depletion on cortical activity and trigeminal nociceptive system in CSD model.

สถาบันวิทยบริการ
จุฬาลงกรณ์มหาวิทยาลัย

CHAPTER III

MATERIALS AND METHODS

EXPERIMENTAL ANIMALS

Adult male Wistar rats weighing 200-300 grams were purchased from the National Laboratory Animal Center of Salaya Campus, Mahidol University. The animals were housed five animals per cage in stainless-steel bottom cages and were kept in a well-ventilated room in which the temperature was 25-30°C with an automatic lighting schedule. All animals were allowed to access food and tap water *ad libitum*. To limit the effect of nonspecific stress, all animals were accustomed to daily handling for at least 5 days before experimentation. All the protocols in this study were approved by the local ethics committee in Chulalongkorn University.



สถาบันวิทยบริการ
จุฬาลงกรณ์มหาวิทยาลัย

CHEMICALS

- Chemical agents

Pentobarbiturate sodium (Nembutal[®]) was purchased from Sanofi (Thailand) Ltd. Normal saline was purchased from Hospital Products Public Co, Ltd. DL-P-chlorophenylalanine (PCPA) and Complete Freund's Adjuvant (CFA) were purchased from Sigma, USA. Potassium chloride (KCl), calcium chloride (CaCl₂), hydrogenperoxide (H₂O₂) and magnesium sulphate (MgSO₄) were purchased from Riedel-de Hach, Germany. Sodium chloride (NaCl), sodium carbonate (NaHCO₃) and methanol were purchased from Merck, USA. ABC streptavidin-horseradish peroxidase complex was purchased from Vector, USA. 3,3'-Diaminobenzidine (DAB) were purchased from Dako, Denmark. Paraformaldehyde and Triton-X100 were purchased from Sigma, USA.

- Antibodies

Goat anti-VR1 and Rabbit anti c-fos were purchased from Santa Cruz, USA. Polyclonal Rabbit anti goat immunoglobulin/Biotinylated, Normal horse serum and Streptavidin-HRP were purchased from Dako, Denmark.

สถาบันวิทยบริการ
จุฬาลงกรณ์มหาวิทยาลัย

EXPERIMENTAL DESIGN

The experiments in this study were divided into three major parts as follows:

Part I: Study of the effect of facial inflammation on CSD-evoked changes in cortical activity and trigeminal nociceptive system.

Part II: Study of the effect of 5-HT depletion on CSD-evoked changes in cortical activity and trigeminal nociceptive system.

Part III: Study of the effect of facial inflammation with 5-HT depletion on CSD-evoked changes in cortical activity and trigeminal nociceptive system.



สถาบันวิทยบริการ
จุฬาลงกรณ์มหาวิทยาลัย

Part I: The effect of facial inflammation on CSD-evoked changes in cortical activity and trigeminal nociceptive system.

This study was conducted to determine the effect of peripheral tissue inflammation on CSD and trigeminal nociceptive. Inflammation of facial was induced by injection of CFA. Activity of cerebral cortex was measured by cortical electrode. Trigeminal nociceptive was determined by expression of Fos positive.

In order to evaluate the effect of the s.c. administration of CFA in the study of depolarization shift, VR1 and c-fos expression, the rats in this group were subdivided into two subgroups (Figure 3.1).

A. Facial inflammation group.

In the facial inflammation group, rats were injected subcutaneously with 0.1 ml of CFA (Sigma) (Amaya et al., 2003) into their forehead.

B. Control group.

In the control group, rats were injected subcutaneously with 0.1 ml of PBS into their forehead.

Three days after administration of CFA or PBS. CSD was introduced in both groups by topical application of solid KCl (3 mg). Cortical activity in response to KCl application (so called depolarization shift) was monitored using cortical electrode. One hour after monitoring, DC shift was measured area under the curve from Acqknowledge 3.2.4 software program version 3.4. After DC shift measurement, the rats were deeply anesthetized and perfused transcardially with 250 ml PBS, followed by 250 ml of 4% paraformaldehyde. After perfusion the brain and the spinal cord were removed and were processed for VR1 and c-fos immunoreactivity. (see page 41, 46 for detail of straight method)

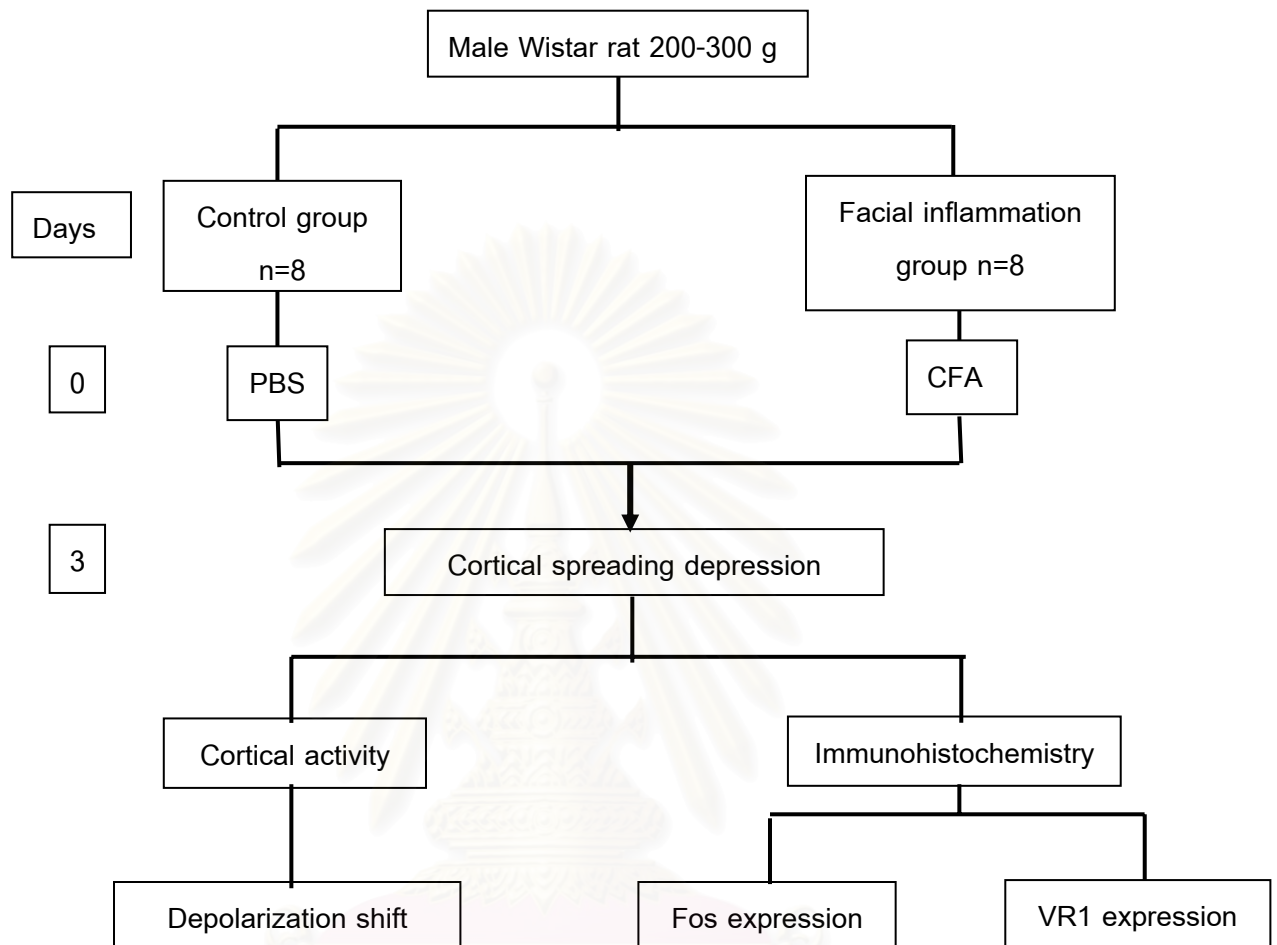


Figure 3.1 Diagram of experimental I design

สภามหาวิทยาลัย
จุฬาลงกรณ์มหาวิทยาลัย

Part II: The effect of 5-HT depletion on CSD-evoked changes in cortical activity and trigeminal nociceptive system.

This study was conducted to determine the effect of 5-HT depletion on CSD and trigeminal nociceptive. 5-HT depletion was induced by injection of PCPA. Activity of cerebral cortex was measured by cortical electrode. Trigeminal nociceptive was determined by expression of Fos positive.

In order to assess the effect of the i.p. administration of PCPA in the study of depolarization shift, VR1 and c-fos expression, the rats in this group were subdivided into two subgroups (Figure 3.2).

A. 5-HT depletion group.

In the 5-HT depleted group, the rats were intraperitoneally injection with PCPA at the dosage of 100 mg/kg BW (Curzon and Green, 1970).

B. Control group

In the control group, the rats were intraperitoneally injection with PBS at the dosage of 0.1 ml.

Six days after administration of PCPA or PBS. CSD was introduced in both groups by CSD. The depolarization shift, VR1 and c-fos expression were detected. (see page 41, 46 for detail of straight method)

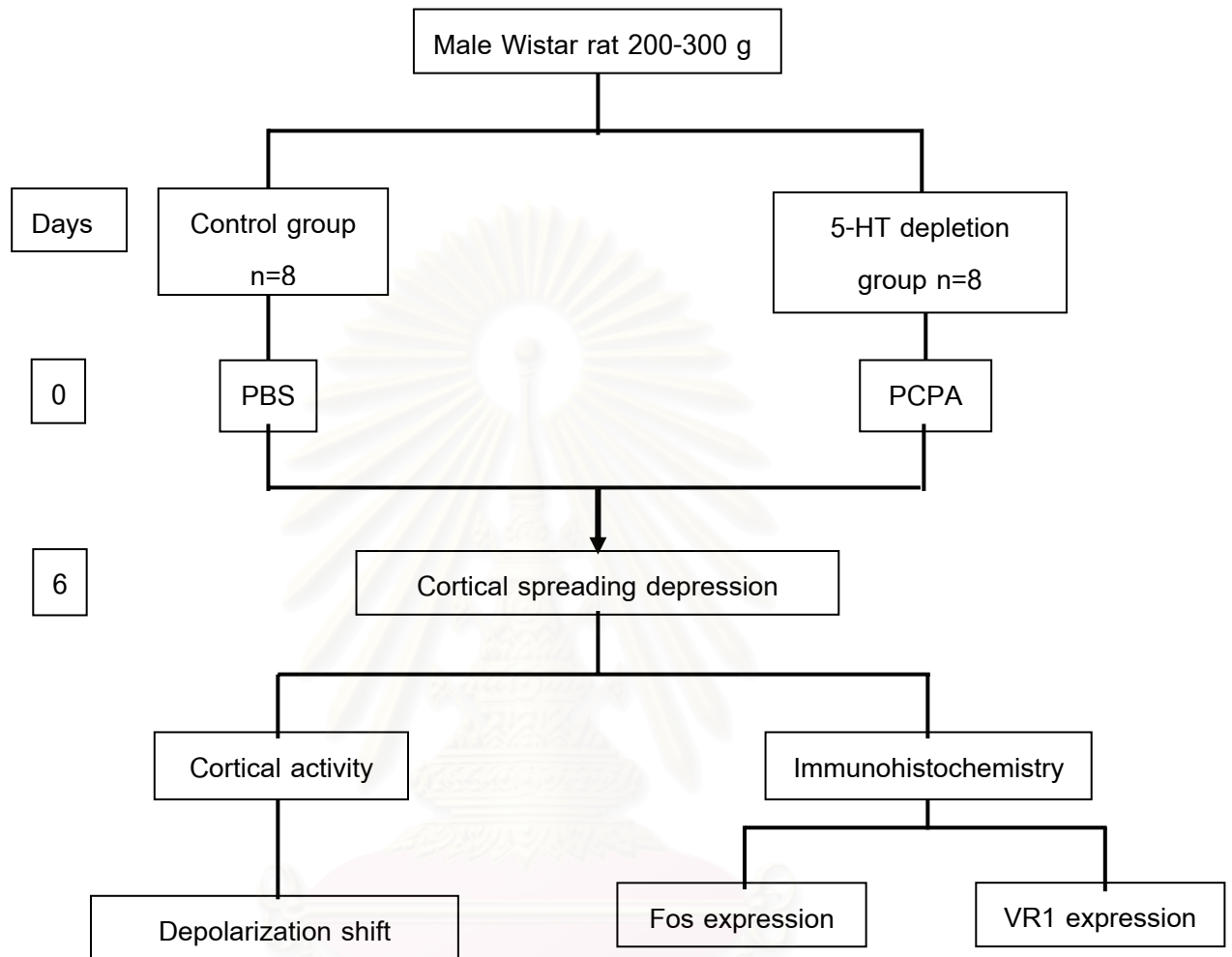


Figure 3.2 Diagram of experimental II design

Part III: The effect of facial inflammation with 5-HT depletion on CSD-evoked changes in cortical activity and trigeminal nociceptive system.

This study was conducted to determine the effect of peripheral tissue inflammation and 5-HT depletion on CSD and trigeminal nociceptive. Inflammation of facial tissue was induced by injected of CFA and 5-HT depletion was induced by injection of PCPA. Activity of cerebral cortex was measured by cortical electrode. Trigeminal nociceptive was determined by expression of Fos positive.

In order to evaluate the effect of the i.p. administration of PCPA and s.c. administration of CFA in the study of depolarization shift, VR1 and c-fos expression, the rats in this group were subdivided into two subgroups (Figure 3.3).

A. Facial inflammation with 5-HT depletion group.

In the facial inflammation with serotonin depletion group, the rats were intraperitoneally injection with PCPA at the dosage of 100 mg/kg BW. Three days after PCPA injection, rats were injected subcutaneously with 0.1 ml of CFA into their forehead.

B. Facial inflammation group.

The rats in the facial inflammation group, rats were injected subcutaneously with 0.1 ml of CFA into their forehead.

Six days after administration of PCPA with CFA or CFA. CSD was introduced in all groups of animals by CSD. The depolarization shift, VR1 and c-fos expression were detected. (see page 41, 46 for detail of straight method)

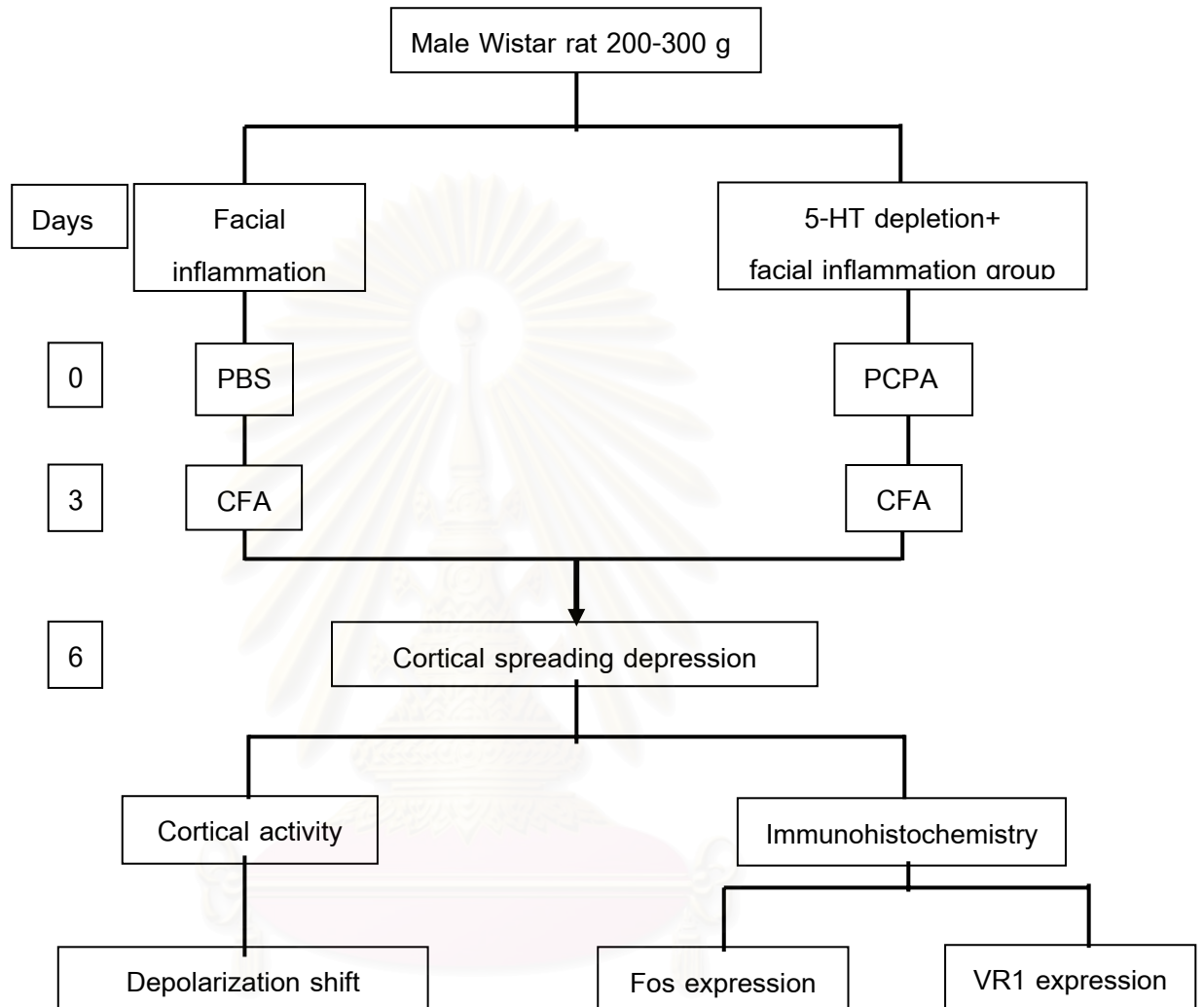


Figure 3.3 Diagram of experimental III design

METHODS

ANIMAL PREPARATION

The rats were anesthetized for the duration of the experiments by intraperitoneal administration of 60 mg/kg of sodium pentobarbital. Additional doses of anesthetics were given as required to maintain surgical anesthesia based on testing of corneal reflex and response to tail pinch. After tracheostomy, the ventilation was assured by using positive pressure ventilation (rodent ventilator model 683, Harvard Apparatus, USA). Blood pressure was monitored throughout the experiments with pressure transducer (Nikon model TP-300T) which was recorded on the Acqknowledge 3.2.4 software program. The femoral vein was cannulated for intravenously infusion of anesthetics drug.

THE CORTICAL SPREADING DEPRESSION MODEL

After tracheostomy and cannulation, the rat was placed on surgical frame and its head was fixed on a stereotaxic frame. The right parietal bone was exposed by mobilization of skin either side of the midline incision. The anterior craniotomy (diameter about 7 mm.) was performed using saline-cool drill in the frontal bone at 1mm anteriorly and laterally from bregma. The posterior craniotomy (diameter about 2 mm.) was performed in the parietal bone at 7mm posteriorly and 1mm laterally from bregma. The anterior and posterior craniotomy openings were used for placing of the electrode and for initiation of CSD, respectively. The dura was opened by using microneedle. An artificial cerebrospinal fluid was infused in the intracranial space. Solid KCl 3 mg was applied to the parietal craniotomy opening to induce CSD. Application of KCl induced a repeated pattern of cortical depolarization characterizing the CSD. However, NaCl application had no effect on cortical activity (Figure 3.4).

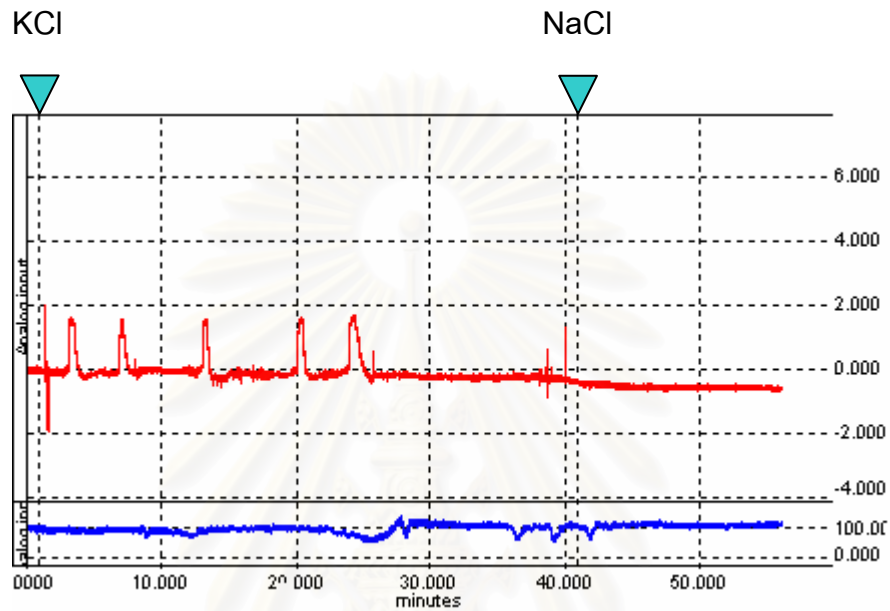


Figure 3.4 The tracing showing KCl application induced a repeated pattern of cortical depolarization characterizing the CSD, NaCl application had no effect on cortical activity.

สถาบันวิทยบริการ
จุฬาลงกรณ์มหาวิทยาลัย

DEPOLARIZATION SHIFT

Depolarization shift was measured by cortical electrode. Glass microelectrode (internal diameter 5 μm) was prepared from bromosilicate, pulled with microelectrode puller (Narishige PP-88, Scientific Instrument Lab, Tokyo, Japan). Microelectrode was filled with NaCl 4 M and then an Ag/AgCl wire was inserted.

Rats were fixed to stereotaxic frame. Completely filled glass microelectrode was inserted perpendicular to cortex to depth 500 μm from cortical surface using hydraulic micromanipulator (Narishige, Scientific Instrument Lab, Tokyo, Japan). Another Ag/AgCl electrode was fixed to the back which was served as a reference point. The obtained electrical signal was amplified using microelectrode amplifier (Nihon Koden, MEZ-8301, Japan). Analog data was converted to digital from using data acquisition system (BioPac Physiograph MP 100A Santa Barbara, CA). All tracing were analyzed using computer software AcqKnowledge version 3.4 (Biopac Physiograph System, Santa Barbara, CA) (Figure 3.5). Such waveform was continuously monitored for one hour.

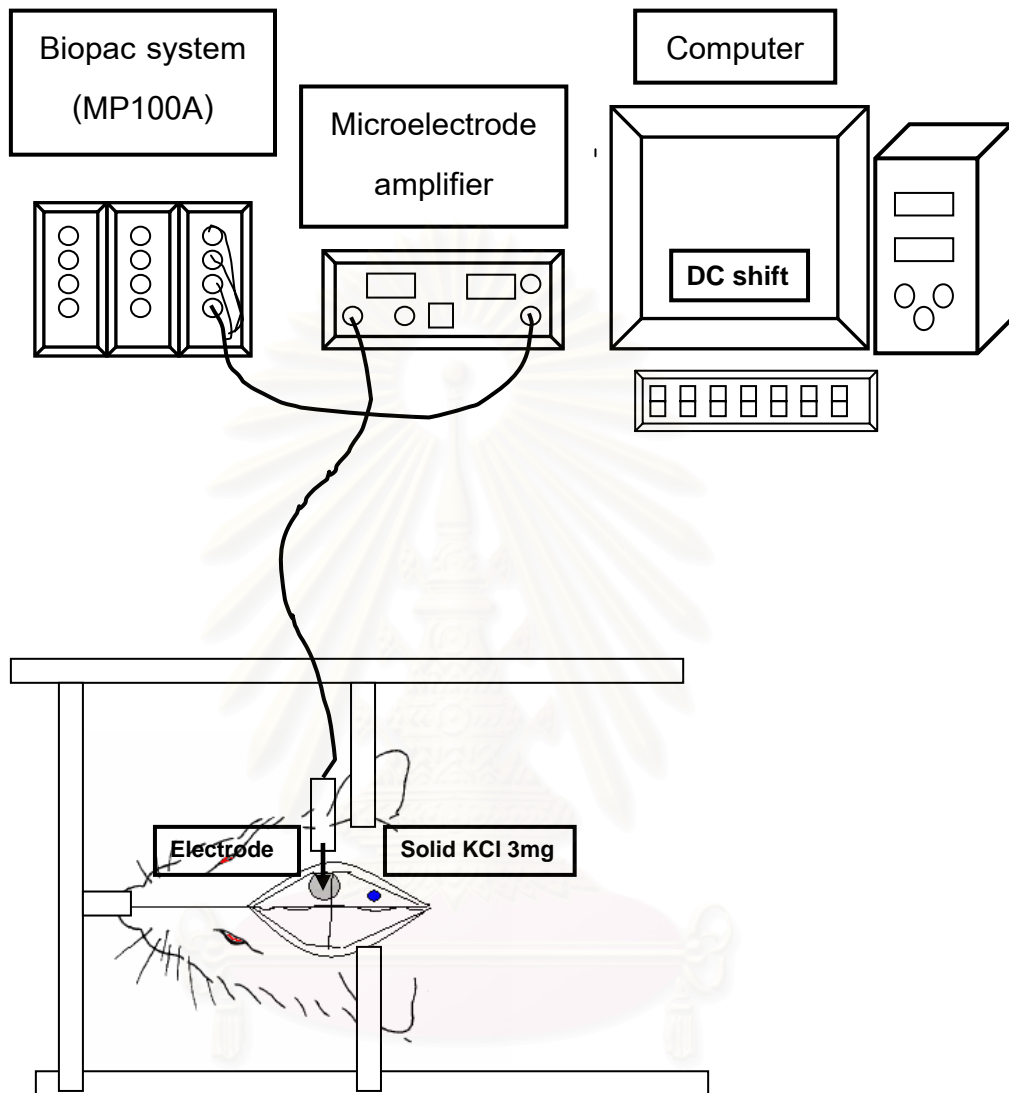


Figure 3.5 Diagram of experimental animal groups: measurement of depolarization shift.

MEASUREMENT OF DEPOLARIZATION SHIFT

Tracings of DC shift were recorded with Biopac system for 60 minute after CSD induction. Variables regarding CSD waves induced AUC, amplitude, duration, number of peak, interpeak interval and summed AUC with one hour were measured.

AREA UNDER THE CURVE OF DEPOLARIZATION SHIFT

To calculate the area under the curve (AUC) of each CSD wave, a line was draw between the endpoint of the selection area as the baseline (Figure 3.6). This calculation returns a positive result, and the measurement can be considered the total area between the waveform and the baseline. The area is expressed in terms of mV sec (amplitude units*horizontal units).

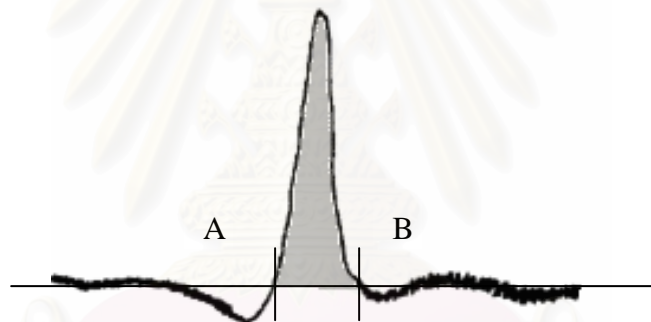


Figure 3.6 Schematic of DC shift showed the ascending point (A) and descending point (B). Area under the curve of DC shift was measured as the area above of A-B.

AMPLITUDE OF DEPOLARIZATION SHIFT

The amplitude of each selected DC shift was assessed by Acknowledge 3.2.4 computer program. The peak amplitude of the propagated wave was determined by the height of the peak above the baseline (Figure 3.7).

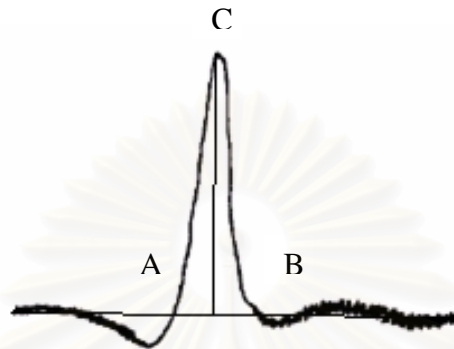


Figure 3.7 Schematic of DC shift showed the reference point A and defined point B and C. The amplitude of DC shift was measured as the distance between C-AB.

DURATION OF DEPOLARIZATION SHIFT

The duration of DC shift was measured as a time difference between the start and endpoints of the selected DC shift (Figure 3.8).

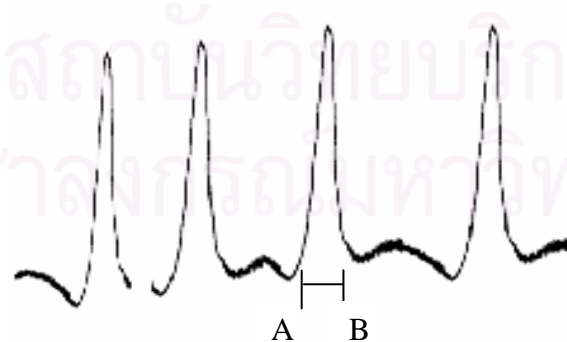


Figure 3.8 Schematic of DC shift showed the start time point (A) and finish time point (B). Duration of DC shift was measured as the time of A-B

THE TOTAL NUMBER OF THE PEAK OF DEPOLARIZATION SHIFT

The total number of peaks of the DC shift was counted during the time frame of 60 minutes (Figure 3.9).

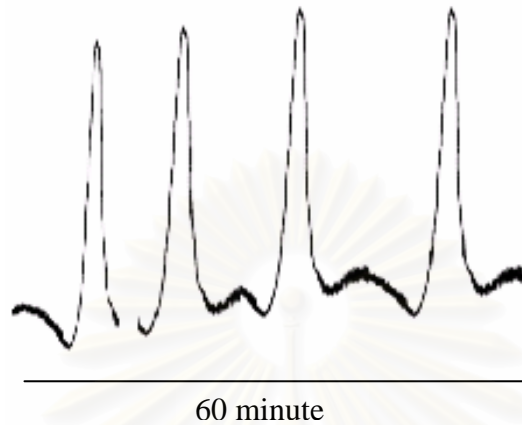


Figure 3.9 Schematic of DC shift showed the total number of the peak of DC shift was measured as the length of 60 minute.

THE INTERPEAK INTERVAL OF DEPOLARIZATION SHIFT

The interpeak interval of DC shift was measured by a time difference between two peaks (Figure 3.10).

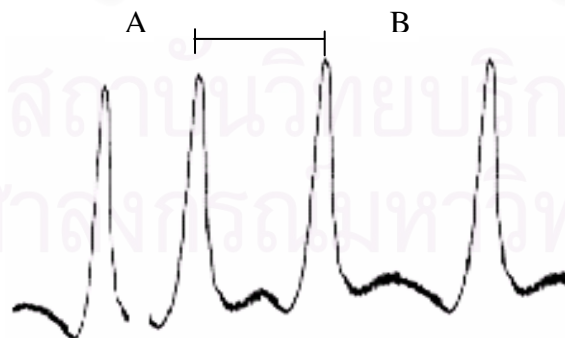


Figure 3.10 Schematic of DC shift showed the reference point A and point B. The interpeak interval of DC shift was measured as the length of A-B.

SUMMED AREA UNDER THE CURVE OF DEPOLARIZATION SHIFT

The AUC of all DC shift was summed during the time frame of 60 minute (Figure 3.11).

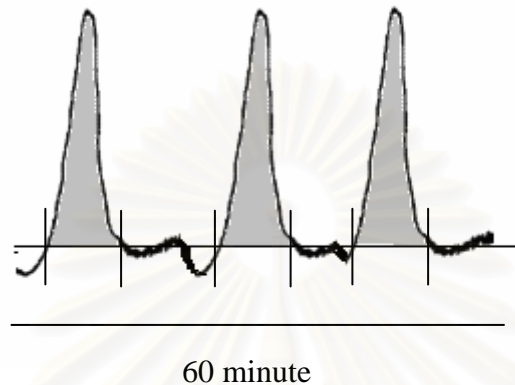


Figure 3.11 Schematic of DC shift showed the total AUC of the peak of DC shift was measured as the length of 60 minute.

IMMUNOHISTOCHEMISTRY

PERFUSION AND TISSUE PREPARATION

After completion of CSD monitory, animals were further proceeding for immunohistochemical study. The experimental rats were deeply anesthetized with sodium pentobarbital. Laparotomy and thoracotomy were done. A cannula was inserted into the apex of the heart and was advanced just distally to the aortic arch. Then, the vasculature was flushed transcardially with 250 ml PBS, followed by 250 ml of 4% paraformaldehyde in a 0.1 M phosphate buffer, pH 7.4. Brain and the cervical spinal cord were removed and were immediately immersed in 4% paraformaldehyde in 0.1 M PBS for 60 minutes. Then the tissue was stored in a 30% sucrose solution in a phosphate buffer overnight for cryoprotection. The cervical spinal cord (C1-C2) was cut in a horizontal plane by a cryostat microtome (Microm HM 50N) at 30 μ m thickness and collected in a series of two in four sections.

IMMUNOHISTOCHEMICAL STUDY FOR THE VR1

The sections were rinsed in three changes of PBS and, incubated with 50% ethanol for 30 minutes. To block endogenous peroxidase, the sections were incubated with 3% hydrogen peroxide in 50% ethanol for 30 minutes. After repeated rinses in PBS, the non-specific binding of the antibody was blocked by incubating the tissues with a 3% normal horse serum (NHS), 1% bovine serum albumin (BSA) in PBS for 60 minutes at room temperature. After three rinses in PBS, the sections were incubated in the Goat anti VR1 antiserum at a dilution of 1:1000 in PBS at 4 °C for 3 day. After incubation, the sections were rinsed 3×10 min with PBS and were then incubated with biotinylated Rabbit anti-Goat immunoglobulin at a dilution of 1:400 in PBS at 4 °C for 24 hours. After overnight incubation, the sections were rinsed 3×10 min with PBS, and incubated for 30 minute with ABC-horseradish peroxidase complex. After incubation, the sections were then again rinsed 3×10 min in PBS. Finally, they were reacted for peroxidatic activity in a solution containing diaminobenzidine (DAB) and 0.01% hydrogen peroxide for 10 minutes. Then, tissue sections were washed 2×5 min with PBS, mounted onto gelatinized glass slides, and coverslipped the slides with permount.

IMMUNOHISTOCHEMICAL STUDY FOR THE c-FOS

The sections were rinsed in three changes of PBS. To block endogenous peroxidase, the sections were incubated with 50% ethanol for 30 minute and 3% hydrogen peroxide in 50% ethanol for 30 minutes. After repeated rinses in PBS, the non-specific binding of the antibody was blocked by incubating the tissues with a 3% normal horse serum (NHS), 1% bovine serum albumin (BSA) in PBS for 60 minutes at room temperature. After three rinses in PBS, the sections were incubated in the specific antibody solution (Rabbit anti c-fos antiserum) at a dilution of 1:1000 in the same solution at 4 °C for 24 hours. After overnight incubation, the sections were then rinsed in PBS, incubated for 90 minutes with biotinylated mouse anti rabbit IgGs at a 1:200 dilution in PBS containing 2% NHS and 1% BSA, rinsed again in PBS, and incubated for 90 minutes in an avidin-biotin-peroxidase solution (Vectastain ABC kit, vector, Burlingham). This was followed by rinses in PBS and bound peroxidase was revealed by incubation of all sections in a solution containing DAB, 0.01% hydrogen peroxide for 10 minutes. The reaction was stopped by repeated rinses in PBS.

Following this reaction the tissue sections were washed and mounted onto gelatinized glass slides.

MEASUREMENT OF THE NUMBER OF THE VR1 IMMUNOREACTIVE CELLS

VR1 immunoreactive (VR1-IR) neurons were distinguished by their darkly stained cell bodies and processes. Expression of VR1 in trigeminal ganglion in each rat was determined by counting the VR1-IR cells from 10 randomized selected sections per animal. Total 100 cells were counted per section. Data was expressed as percent of VR1-IR cells per rat. ($100/\text{slide} \times 10 \text{ slide}$)

The VR1-IR cells were counted and reported as the number of immunoreactive cells in the TG ipsilateral to the KCl (CSD group) application and contralateral side. VR1 positive cells in TG ipsilateral / contralateral TG neurons counted separately.

MEASUREMENT OF THE NUMBER OF THE c-FOS IMMUNOREACTIVE CELLS

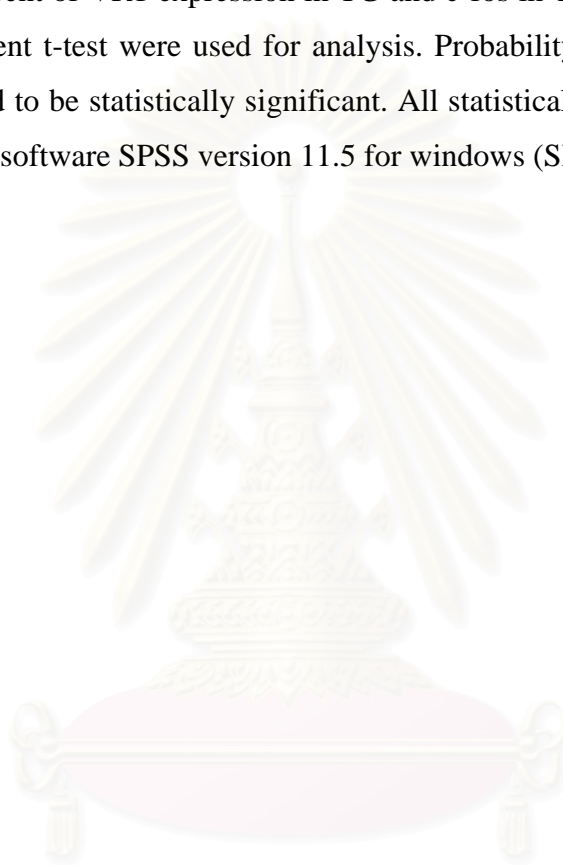
Cell counts were carried out in sections processed for the c-fos immunohistochemistry. A total of 10 sections per animal were used. Only cell profiles with a visible nucleus on the focal plane were analysed. The c-fos immunoreactive cells (Fos-IR cells) were defined as those with a dark brown stain in their nucleus. The Fos-IR neurons in the lamina I and the lamina II area of each section were counted. Fos-IR cells in ipsilateral and contralateral side to CSD induction were counted separately.

For all experimental rats, the Fos-IR cells were counted and reported as the number of immunoreactive cells in the dorsal horn ipsilateral to the KCl (CSD group) application and contralateral side.

DATA ANALYSIS

All values were presented as mean \pm standard deviation (SD). The results of DC shift were presented in sum area under the curve, amplitude of DC shift, the total number of the peak and duration of DC shift. The differences among groups were tested using Student t-test. Probability values of less than 0.05 were considered to be statistically significant.

The percent of VR1 expression in TG and c-fos in TNC were present in mean \pm SD and Student t-test were used for analysis. Probability values of less than 0.01 were considered to be statistically significant. All statistical analyses were performed using computer software SPSS version 11.5 for windows (SPSS, Chicago, IL, USA).



สถาบันวิทยบริการ
จุฬาลงกรณ์มหาวิทยาลัย

CHAPTER IV

RESULTS

The results of this study were organized into three parts as follows.

Part I: Results from all experiments performed for studying the effect of facial inflammation on cortical activity and trigeminal nociceptive system in CSD model.

Part II: Results from all experiments performed for studying the effect of 5-HT depletion on cortical activity and trigeminal nociceptive system in CSD model.

Part III: Results from all experiments performed for studying the effect of facial inflammation with 5-HT depletion on cortical activity and trigeminal nociceptive system in CSD model.

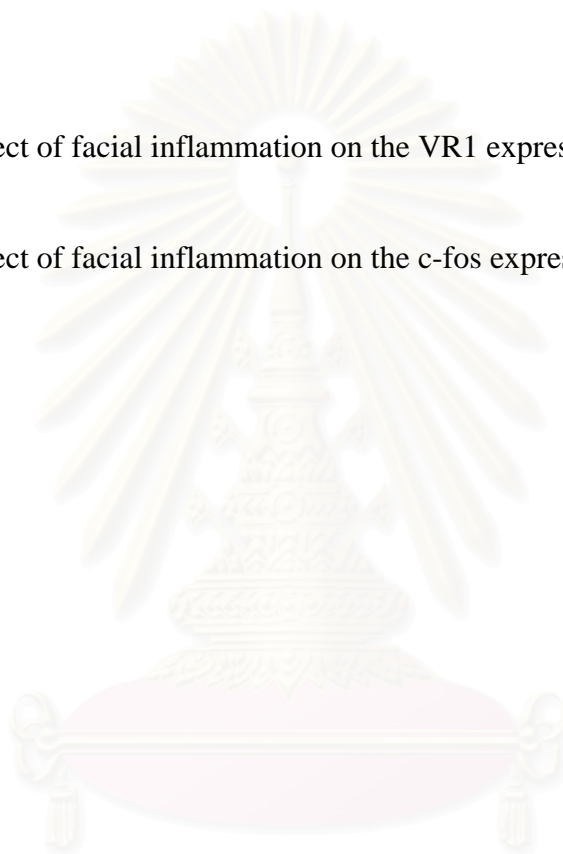


สถาบันวิทยบริการ
จุฬาลงกรณ์มหาวิทยาลัย

I: THE EFFECT OF FACIAL INFLAMMATION ON CORTICAL ACTIVITY AND TRIGEMINAL NOCICEPTIVE SYSTEM IN THE CSD MODEL

The results of this part are subdivided into three parts as follows:

1. The effect of facial inflammation on the depolarization shift changes induced by CSD.
2. The effect of facial inflammation on the VR1 expression induced by CSD.
3. The effect of facial inflammation on the c-fos expression induced by CSD.



สถาบันวิทยบริการ
จุฬาลงกรณ์มหาวิทยาลัย

1. The effect of facial inflammation on the depolarization shift changes induced by CSD.

The DC shift changes was studied in the all group in order to evaluate the effect of CSD on duration, peak amplitude, number of peak, interpeak latency, averaged and summed AUC of depolarization shift changes in one hour.

Application of KCl induced a repeated pattern of cortical depolarization characterizing the CSD (Figure 4.1). In control group, the averaged amplitude and duration of these CSD waves was 24.65 ± 1.59 mV and 43.13 ± 7.67 seconds, respectively (Table 4.1) (Table 4.2). The mean number of CSD wave occurring within one hour was 11.13 ± 1.25 waves (Table 4.3) and interpeak latency was 4.72 ± 1.53 minutes (Table 4.4). The averaged AUC and sum was 58.99 ± 10.01 mV-seconds, 648.32 ± 73.57 mV-seconds, respectively (Table 4.5) (Table 4.6). Comparing with the CFA-treated group, we found that the averaged and sum AUC of CSD wave were increased significantly (77.22 ± 12.56 mV-seconds and 1054.43 ± 175.86 mV-seconds, respectively) (Figure 4.7) (Figure 4.8). Pretreatment with CFA shortened the interpeak latency and increase total number of wave (Figure 4.2). The averaged number of CSD wave occurring with one hour was 14 ± 1.51 waves (Table 4.3) and the interpeak latency in this group was 3.20 ± 0.35 minutes (Table 4.4) and In the contrary, no significant difference was observed when the peak amplitude and duration of CSD waves were compared with the control group (Figure 4.3) (Figure 4.4). The peak amplitude and duration of CSD waves in the CFA-treated group were 26.2 ± 3.94 mV and 57.58 ± 19.50 seconds, respectively (Table 4.1) (Table 4.2).

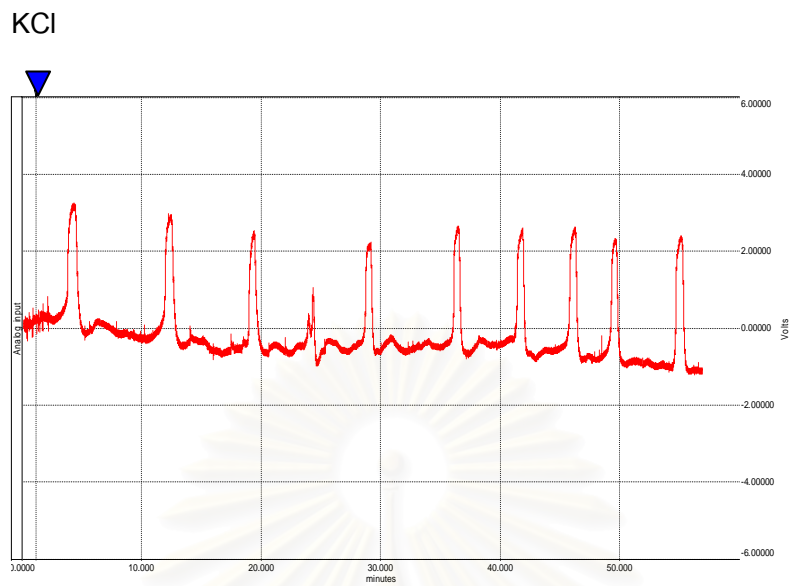


Figure 4.1 The tracing showing the depolarization shift changes after KCl 3 mg application in control group. Arrow shows the start of KCl application.

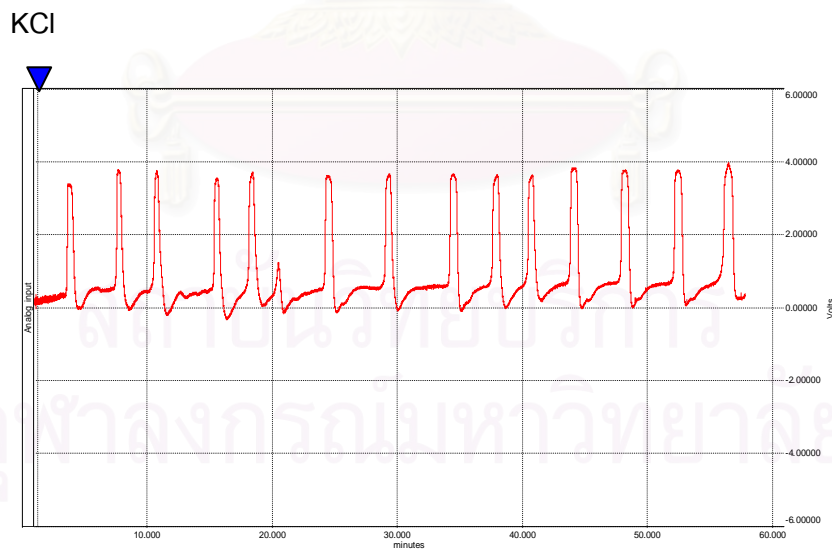


Figure 4.2 The tracing showing the depolarization shift changes after KCl 3 mg application in CFA-treated group. Arrow shows the start of KCl application.

Table 4.1 The mean value \pm SD of amplitude of DC shift obtained from control group and CFA-treated group.

Group	Mean \pm SD of amplitude (-mV)
Control	24.65 \pm 1.59
Inflammation	26.20 \pm 3.94

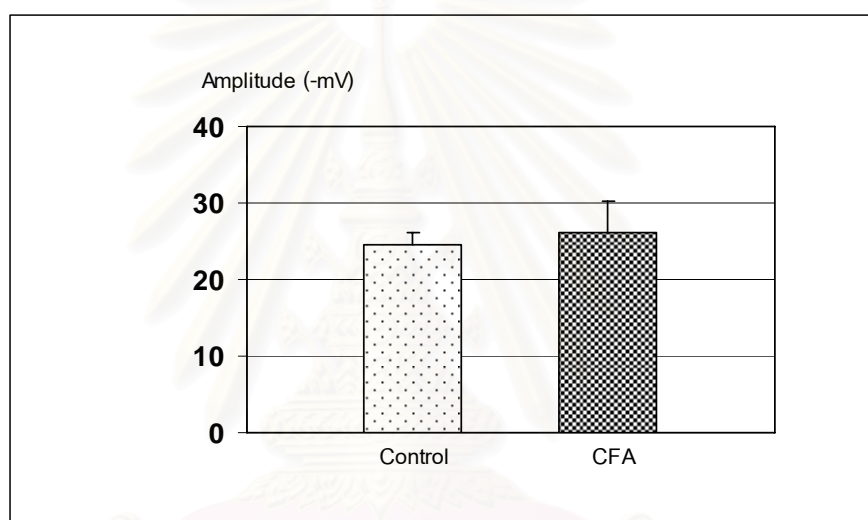


Figure 4.3 Bar graphs showing the mean value \pm SD of amplitude of DC shift obtained from control group and CFA-treated group.

จุฬาลงกรณ์มหาวิทยาลัย

Table 4.2 The mean value \pm SD of duration of DC shift obtained from control group and CFA-treated group.

Group	Mean \pm SD of duration (seconds)
Control	43.13 \pm 7.68
Inflammation	57.58 \pm 19.5

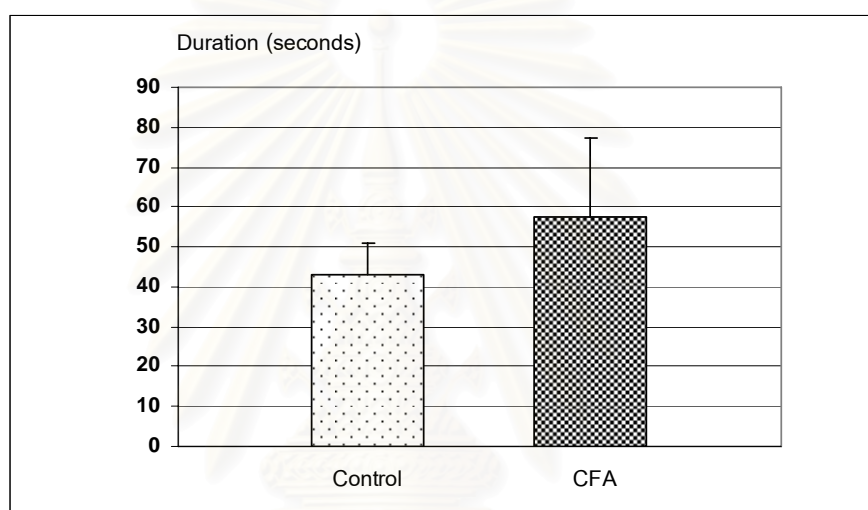


Figure 4.4 Bar graphs showing the mean value \pm SD of duration of DC shift obtained from control group and CFA-treated group.

สถาบันวิทยบริการ
จุฬาลงกรณ์มหาวิทยาลัย

Table 4.3 The mean value \pm SD of number of peak of DC shift obtained from control group and CFA-treated group.

Group	Mean\pm SD of number of peaks (waves)
Control	11.13\pm 1.25
Inflammation	14.00\pm 1.51*

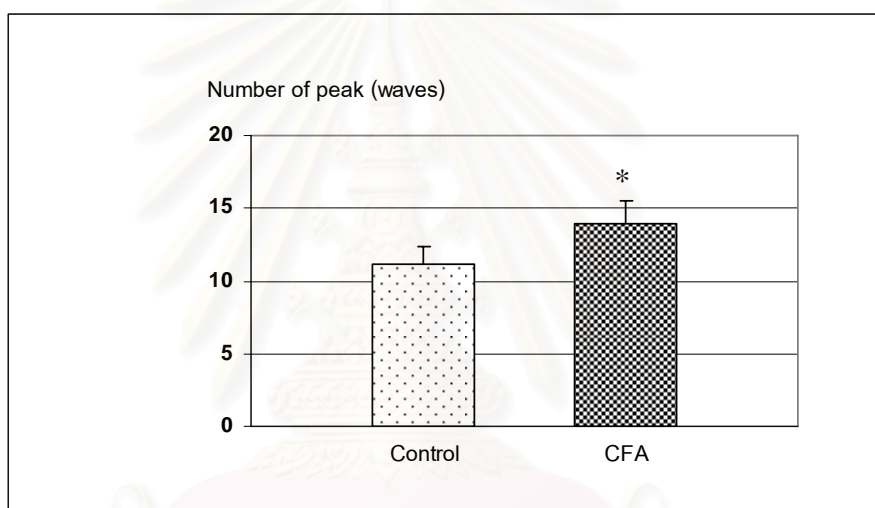


Figure 4.5 Bar graphs showing the mean value \pm SD of number of peaks of DC shift obtained from control group and CFA-treated group. Significant difference was assessed with Student t-test.* $p < 0.05$ compared with control group.

Table 4.4 The mean value \pm SD of interpeak latency of DC shift obtained from control group and CFA-treated group.

Group	Mean \pm SD of interpeak latency (minutes)
Control	4.73 \pm 1.54
Inflammation	3.20 \pm 0.35*

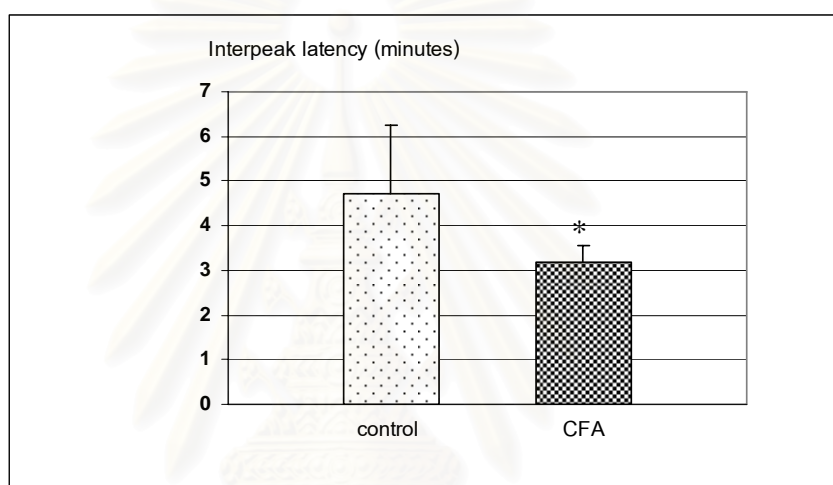


Figure 4.6 Bar graphs showing the mean value \pm SD of interpeak latency of DC shift obtained from control group and CFA-treated group. Significant difference was assessed with Student t-test.*p<0.05 compared with control group.

Table 4.5 The mean value \pm SD of average AUC of DC shift in one hour obtained from control group and CFA-treated group.

Group	Mean \pm SD of average AUC (mV-second)
Control	58.99 \pm 10.01
Inflammation	77.22 \pm 12.56*

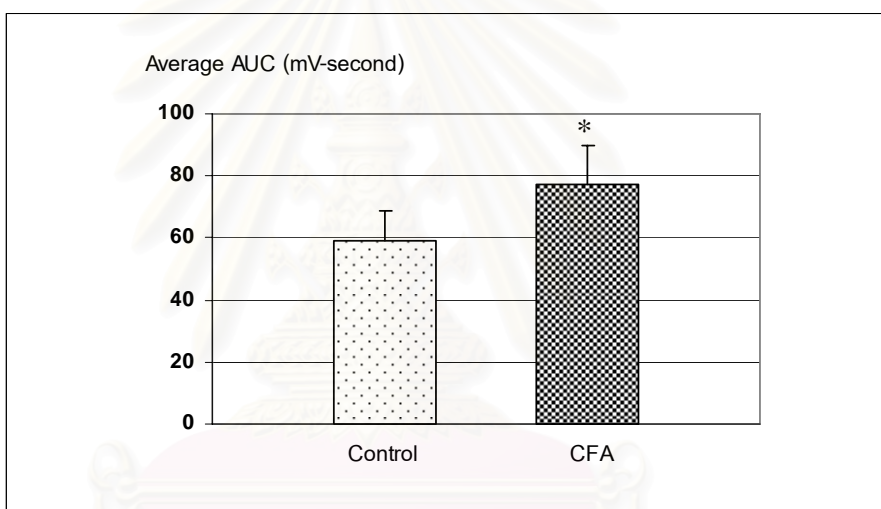


Figure 4.7 Bar graphs showing the mean value \pm SD of average AUC of DC shift in one hour obtained from control group and CFA-treated group. Significant difference was assessed with Student t-test.* $p < 0.05$ compared with control group.

Table 4.6 The mean value \pm SD of sum AUC of DC shift in one hour obtained from control group and CFA-treated group.

Group	Mean\pm SD of sum AUC (mV-second)
Control	648.32\pm 73.57
Inflammation	1054.43\pm 175.68*

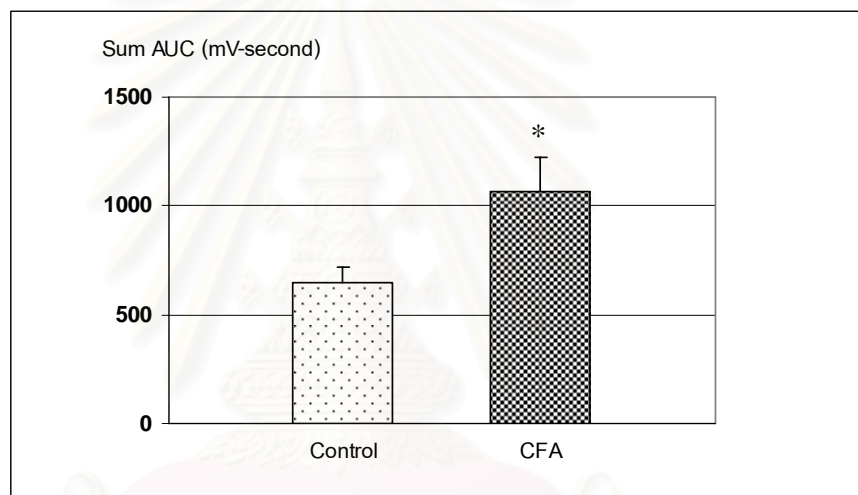


Figure 4.8 Bar graphs showing the mean value \pm SD of sum AUC of DC shift in one hour obtained from control group and CFA-treated group. Significant difference was assessed with Student t-test.* $p < 0.05$ compared with control group.

Table 4.7 Comparing the electrophysiological variables related to CSD between the inflammation group and control group.

	Inflammation	Control	Mean difference (95% CI)	p-value
Amplitude (mV)	26.20± 3.94	24.65± 1.59	1.55 (-0.04 to 5.59)	0.319
Duration (seconds)	57.58± 19.50	43.13± 7.68	14.45 (-6.67 to 5.05)	0.072
Number of peaks (waves)	14.00± 1.51	11.13± 1.25	3.00 (-4.51 to -1.49)	0.001
Interpeak latency (minutes)	3.20± 0.35	4.73± 1.54	1.53 (-1.88 to -0.01)	0.016
Average AUC (mV-second)	77.22± 12.56	58.99± 10.01	18.23 (5.67 to 30.79)	0.006
Summed AUC (mV-second)	1054.43± 175.68	648.32± 73.57	406.11 (156.86 to 655.36)	<0.001

2. The effect of facial inflammation on the VR1 expression induced by CSD.

In this experiment, 10 sections of TG were collected from each group. The slides of the sections were studied under the light microscope and neurons were classified as immunoreactive or non-reactive based on the immunostaining feature. The VR1-IR neurons were defined as those with dark-brown stained in their cytoplasm. It was shown that the VR1-IR neurons comprised small to medium sized neurons. The large-diameter neurons were usually VR1-negative. The total of 100 cells was counted from each slide. Data were expressed as mean and standard deviation of percent of VR1-IR neurons.

The effect of CFA on the VR1 expression induced by CSD was tested by evaluating the number of VR1-IR cells in the CFA pretreated group and in the control group (Figure 4.10).

CSD induced expression of VR1 in the TG. VR1-IR cells were confined in TG and were more prevalent on the side ipsilateral to the operation. In control group, the numbers of VR1-IR cells in the ipsilateral and contralateral sides were 28.88 ± 0.60 cells and 21.66 ± 1.32 cells per section respectively. Pretreatment with CFA enhanced the response of trigeminal nociceptive to CSD. The numbers of VR1-IR cells in CFA-treated group were 41.66 ± 3.51 cells and 41.72 ± 3.55 cells per section for ipsilateral and contralateral sides, respectively. The data are shown in Table 4.8. The difference in the number of VR1-IR cells between CFA and control groups were statistically significant (Figure 4.9).

Table 4.8 The mean value \pm SD of the number of VR1-IR cells in the TG sections obtained from control and CFA-treated groups.

Group	Contralateral side	Ipsilateral side
Control	21.66 \pm 1.32	28.88 \pm 0.60
Inflammation	41.72 \pm 3.55 *	41.66 \pm 3.51 *

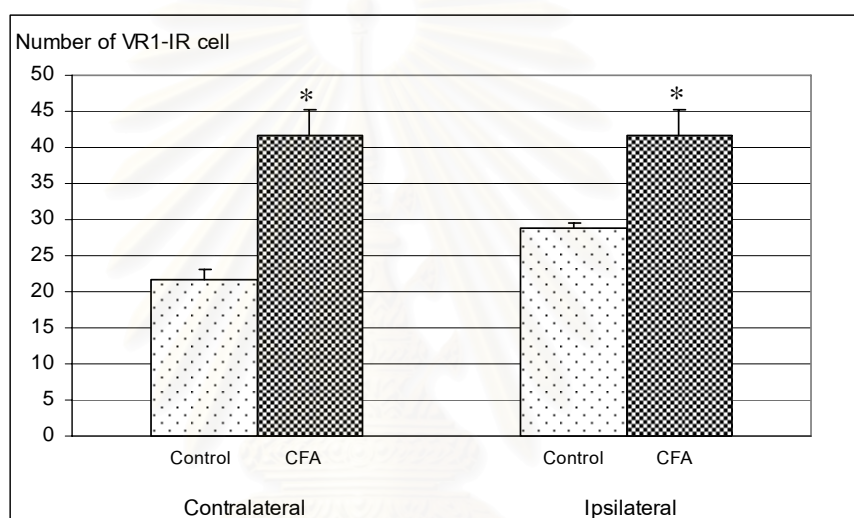
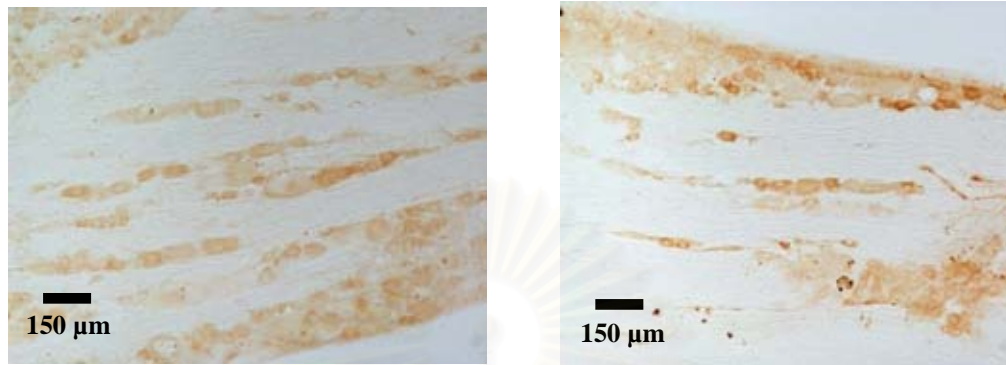


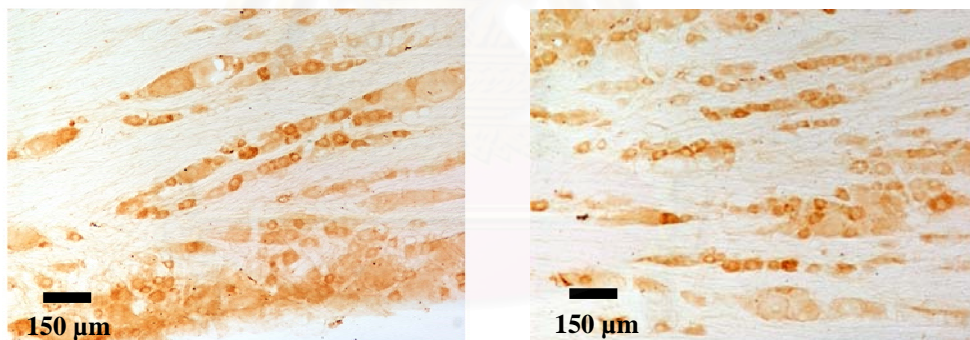
Figure 4.9 Bar graphs showing the mean value \pm SD of the number of VR1-IR cells in the TG sections obtained from control group and CFA-treated group. Significant difference was assessed with Student t-test. * p <0.05 compared with control group.



A. Control group

Ipsilateral side

Contralateral side



B. Inflammation group

Ipsilateral side

Contralateral side

Figure 4.10 The photomicrograph showing the VR1-IR cells in the TG sections (ipsilateral side to KCl application) obtained from the A) Control group ($\times 10$) and B) Inflammation group ($\times 10$). Bar = 150 μm .

3. The effect of facial inflammation on the c-fos expression induced by CSD

To test whether the second order neuron in trigeminal nociceptive system is activated by CSD the expression of Fos, a surrogate marker for neuronal activation, was examined. Ten sections were randomly selected from each rat and the Fos-IR cells were counted and reported as the number of immunoreactive cells in the dorsal horn contralateral side and ipsilateral to the KCl application (in the CSD group). The data are reported as the mean value and the standard deviation.

The Fos expression after CSD induction for 1 hour was mainly distributed in the lamina I and II of the cervical spinal cord sections on the side ipsilateral to the KCl application (Figure 4.12). The numbers of Fos-IR cells in ipsilateral and contralateral sides were 7.28 ± 0.57 and 1.95 ± 0.49 cells /slides respectively. Pretreatment with CFA enhanced the response of trigeminal nociception to CSD. The numbers of Fos-IR cells in CFA-treated group were 13.71 ± 2.35 cells and 6.50 ± 2.00 cells per slide for ipsilateral and contralateral sides, respectively. The data are shown in Table 4.9. The difference in the number of Fos-IR cells between CFA and control groups were statistically significant (Figure 4.11).

Table 4.9 The mean value \pm SD of number of Fos-IR cells in the C1 and C2 cervical spinal cord sections obtained from control and CFA-treated groups.

Group	Contralateral side	Ipsilateral side
Control	1.95 \pm 0.49	7.28 \pm 0.57 #
Inflammation	6.50 \pm 2.00 *	13.71 \pm 2.35 * #

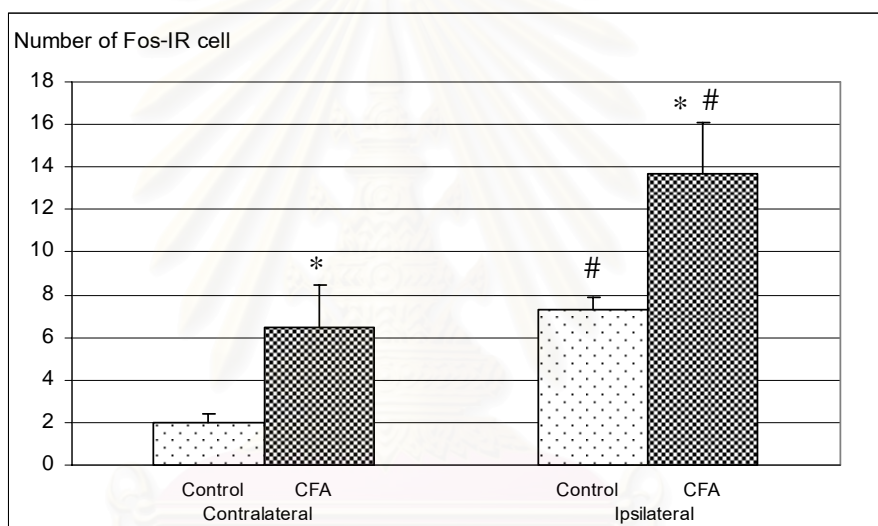


Figure 4.11 Bar graph showing the mean value \pm SD of the number of Fos-IR cells in the C1 and C2 cervical spinal cord sections obtained from control group and CFA-treated group. Significant difference was assessed with Student t-test. *p<0.05 compared with control group. # p<0.05 compared with contralateral side.

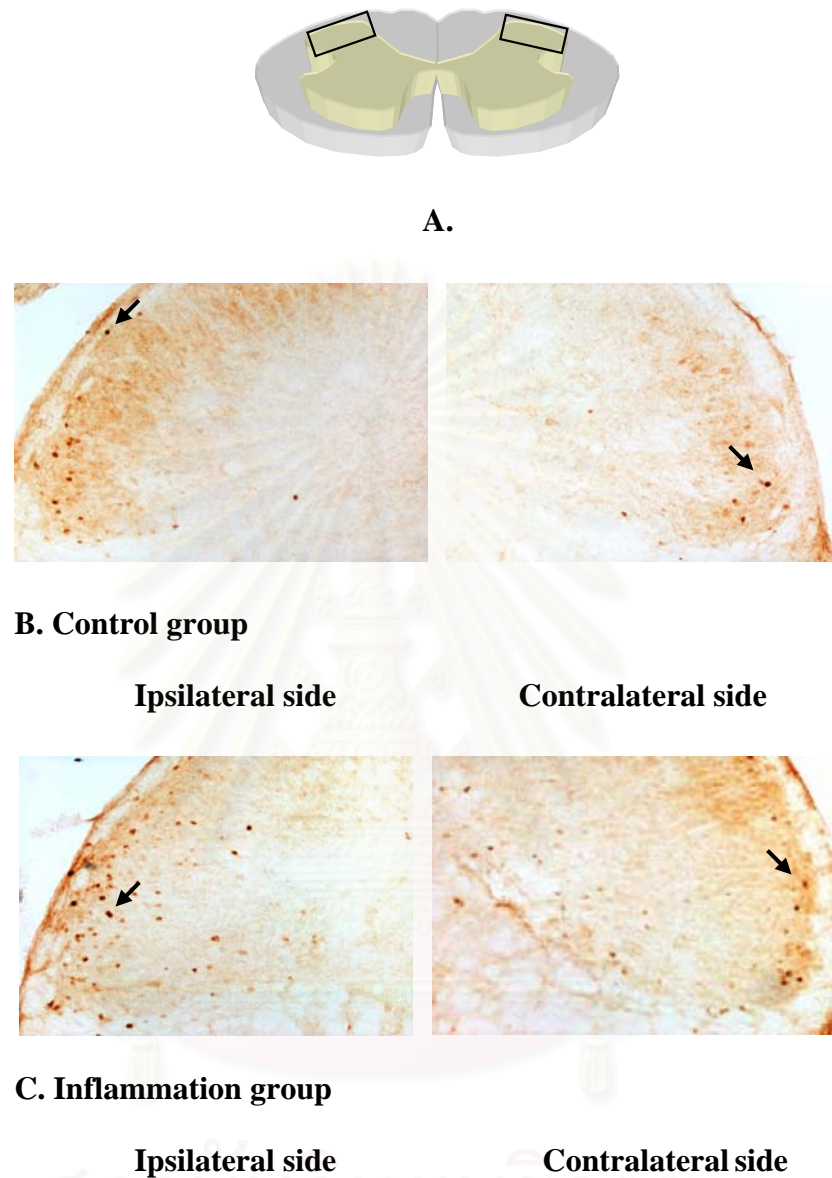
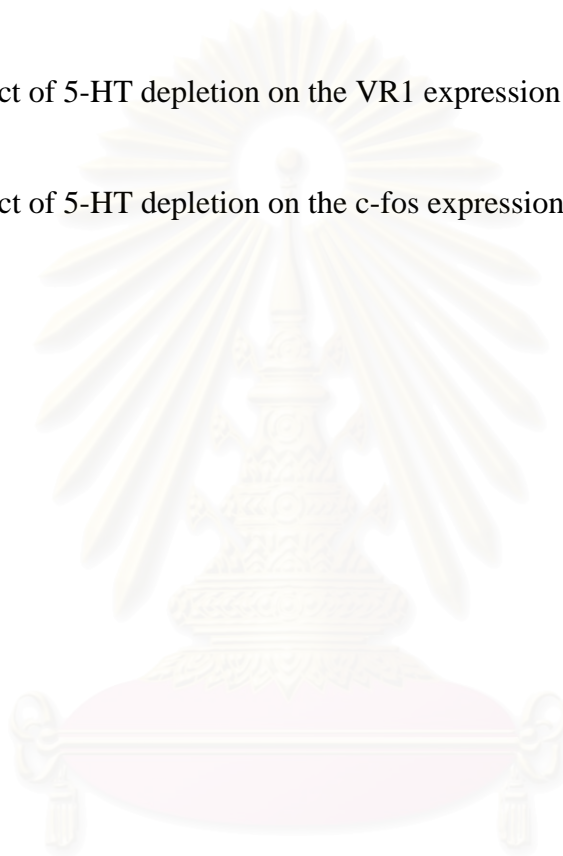


Figure 4.12 The photomicrograph showing the Fos-IR cells in the C1 and C2 cervical spinal cord sections (ipsilateral side to KCl application). Fos positive cells (arrow) are easily visible and well differentiated from the background. Box in the schematic drawings indicate the area the respective photographs were taken from. A) Spinal cord, B) Control group ($\times 10$) and B) Inflammation group ($\times 10$).

II: THE EFFECT OF 5-HT DEPLETION ON CORTICAL ACTIVITY AND TRIGEMINAL NOCICEPTIVE SYSTEM IN THE CSD MODEL

The results of this part are subdivided into three parts as follows:

1. The effect of 5-HT depletion on the depolarization shift changes induced by CSD.
2. The effect of 5-HT depletion on the VR1 expression induced by CSD.
3. The effect of 5-HT depletion on the c-fos expression induced by CSD.



สถาบันวิทยบริการ
จุฬาลงกรณ์มหาวิทยาลัย

1. The effect of 5-HT depletion on the depolarization shift changes induced by CSD

The DC shift changes was studied in all groups in order to evaluate the effect of CSD on peak amplitude, duration, number of peak, interpeak latency, averaged and sum AUC of depolarization shift changes in one hour.

Pretreatment with PCPA induced CSD generation (Figure 4.13). The peak amplitude and duration of CSD waves in the PCPA-treated group were 26.92 ± 3.26 mV and 43.67 ± 8.83 seconds, respectively (Table 4.10) (Table 4.11). Pretreatment with PCPA increase total number of wave and shortened the interpeak latency. The averaged number of CSD wave occurring with one hour was 14.88 ± 2.17 waves (Table 4.12) and interpeak latency in this group was 3.18 ± 0.64 minutes (Table 4.13). The averaged and sum AUC of CSD wave were increased significantly (73.12 ± 11.43 mV-seconds and 1065.82 ± 160.93 mV-seconds, respectively) (Table 4.14) (Table 4.15). In the contrary, no significant difference was observed when the peak amplitude and duration of CSD waves were compared with the control group (Figure 4.14) (Figure 4.15).

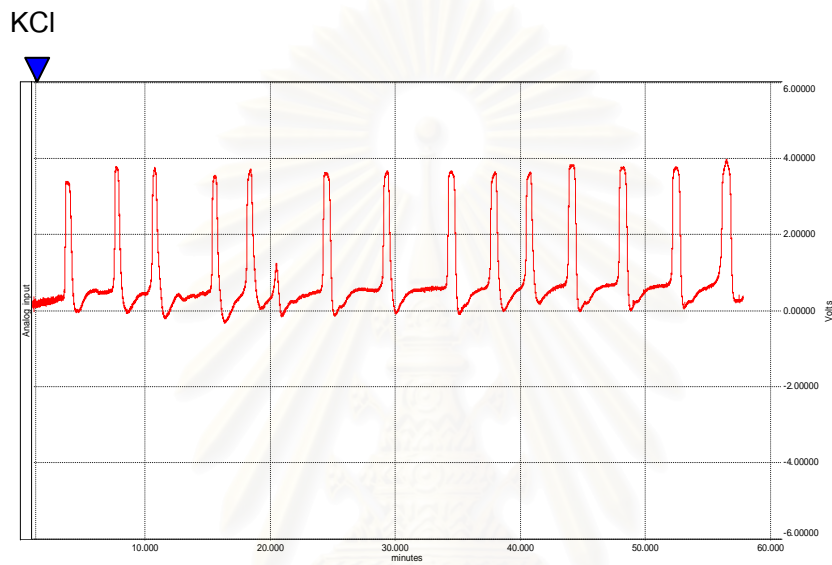


Figure 4.13 The tracing showing the depolarization shift changes after KCl 3 mg application in PCPA-treated group. Arrow shows the start of KCl application.

จุฬาลงกรณ์มหาวิทยาลัย

Table 4.10 The mean value \pm SD of amplitude of DC shift obtained from control group and PCPA-treated group.

Group	Mean \pm SD of amplitude (mV)
Control	24.65 \pm 1.59
5-HT depletion	26.92 \pm 3.26

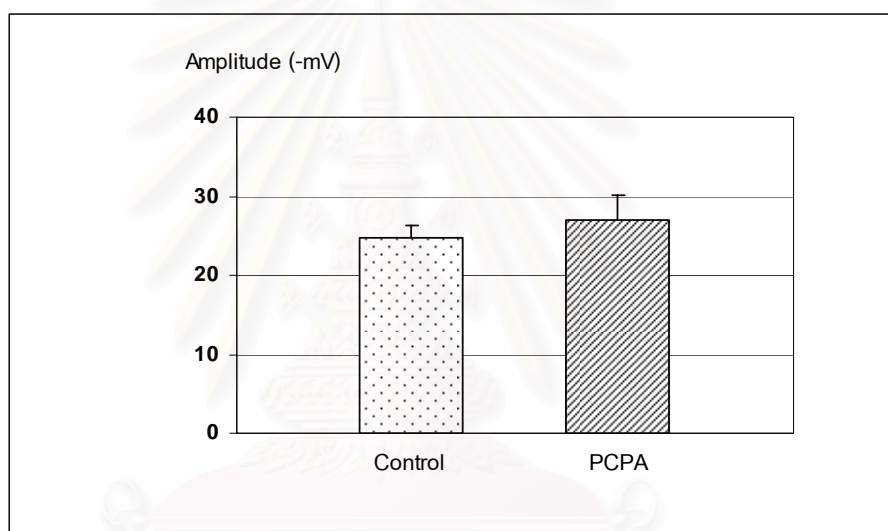


Figure 4.14 Bar graphs showing the mean value \pm SD of amplitude of DC shift obtained from control group and PCPA-treated group.

จุฬาลงกรณ์มหาวิทยาลัย

Table 4.11 The mean value \pm SD of duration of DC shift obtained from control group and PCPA-treated group.

Group	Mean \pm SD of duration (seconds)
Control	43.13 \pm 7.68
5-HT depletion	43.67 \pm 8.83

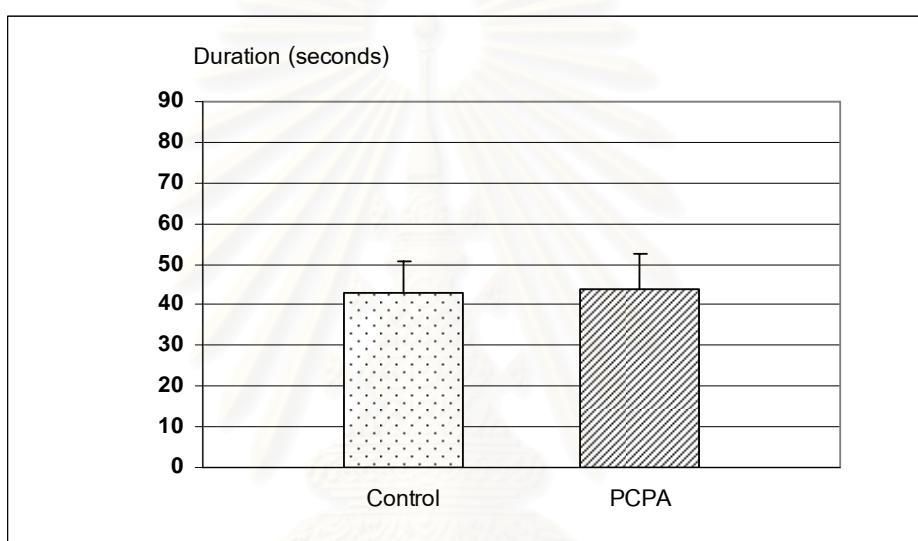


Figure 4.15 Bar graphs showing the mean value \pm SD of duration of DC shift obtained from control group and PCPA-treated group.

Table 4.12 The mean value \pm SD of number of peak of DC shift obtained from control group and PCPA-treated group.

Group	Mean\pm SD of number of peaks (waves)
Control	11.13\pm 1.25
5-HT depletion	14.88\pm 2.17 *

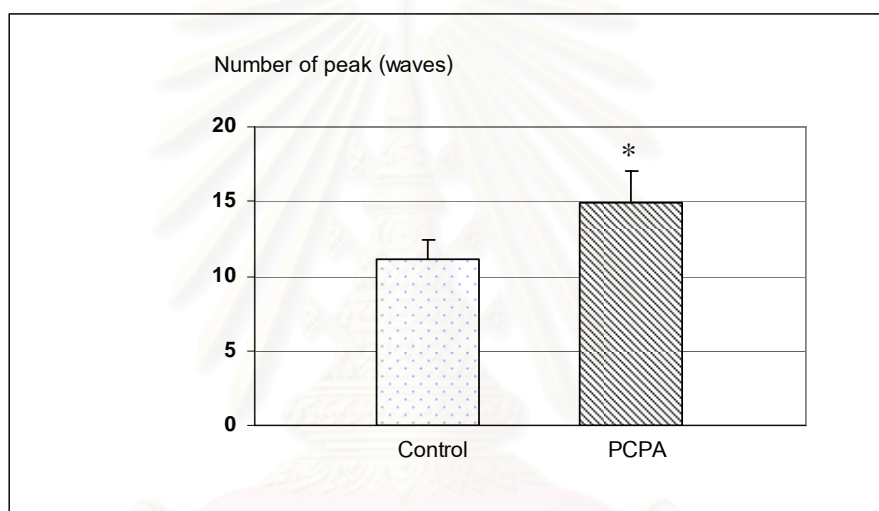


Figure 4.16 Bar graphs showing the mean value \pm SD of number of peaks of DC shift obtained from control group and PCPA-treated group. Significant difference was assessed with Student t-test. * $p < 0.05$ compared with control group.

Table 4.13 The mean value \pm SD of interpeak latency of DC shift obtained from control group and PCPA-treated group.

Group	Mean \pm SD of interpeak latency (minutes)
Control	4.73 \pm 1.54
5-HT depletion	3.18 \pm 0.64*

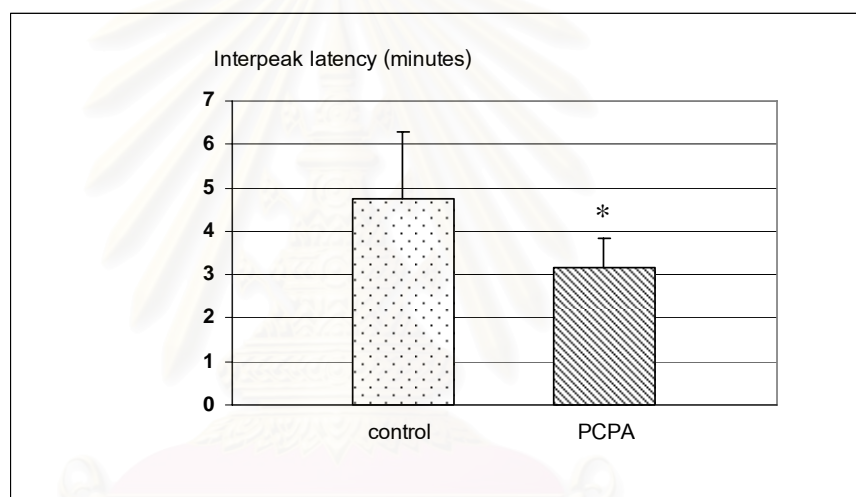


Figure 4.17 Bar graphs showing the mean value \pm SD of interpeak latency of DC shift obtained from control group and PCPA-treated group. Significant difference was assessed with Student t-test. * $p < 0.05$ compared with control group.

Table 4.14 The mean value \pm SD of average AUC of DC shift in one hour obtained from control group and PCPA-treated group.

Group	Mean \pm SD of average AUC (mV-second)
Control	58.99 \pm 10.01
5-HT depletion	73.12 \pm 11.43*

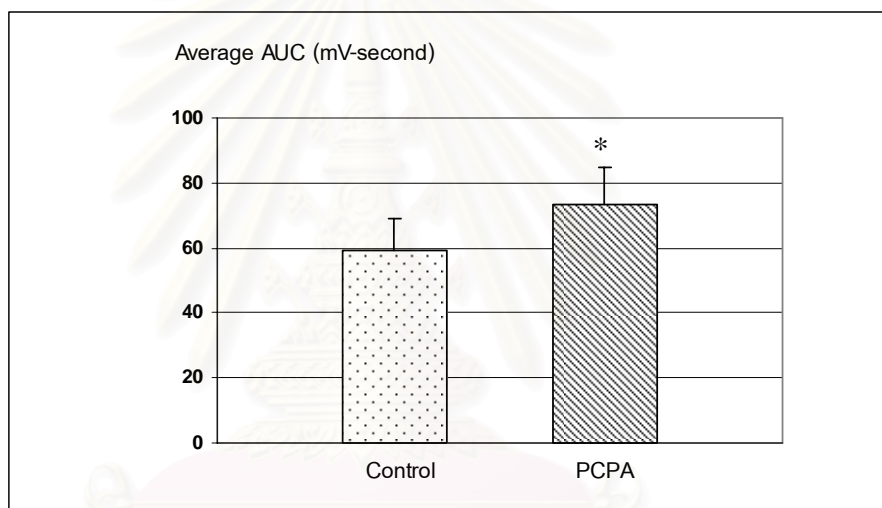


Figure 4.18 Bar graphs showing the mean value \pm SD of average AUC of DC shift in one hour obtained from control group and PCPA-treated group. Significant difference was assessed with Student t-test. *p<0.05 compared with control group.

Table 4.15 The mean value \pm SD of sum AUC of DC shift in one hour obtained from control group and PCPA-treated group.

Group	Mean \pm SD of sum AUC (mV-second)
Control	648.32 \pm 73.57
5-HT depletion	1065.82 \pm 160.93*

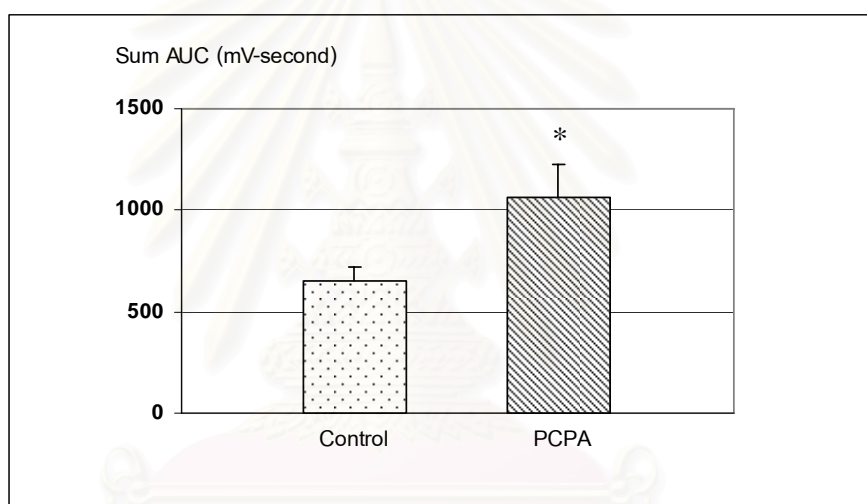


Figure 4.19 Bar graphs showing the mean value \pm SD of sum AUC of DC shift in one hour obtained from control group and PCPA-treated group. Significant difference was assessed with student t-test. * $p < 0.05$ compared with control group

Table 4.16 Comparing the electrophysiological variables related to CSD between the 5-HT depletion group and control group.

	5-HT depletion	Control	Mean difference (95% CI)	p-value
Amplitude (mV)	26.92± 3.94	24.65± 1.59	2.27 (-0.49 to 5.03)	0.098
Duration (seconds)	43.67± 8.83	43.13± 7.68	0.53 (-9.41 to 8.33)	0.899
Number of peaks (waves)	14.88± 2.17	11.13± 1.25	3.00 (-5.65 to -1.85)	0.001
Interpeak latency (minutes)	3.18± 0.64	4.73± 1.54	-1.55 (-2.81 to -0.28)	0.020
Average AUC (mV-second)	73.12± 11.43	58.99± 10.01	14.13 (2.61 to 25.65)	0.020
Summed AUC (mV-second)	1065.82± 160.93	648.32± 73.57	417.50 (-5.65 to -1.85)	<0.001

2. The effect of 5-HT depletion on the VR1 expression induced by CSD

The effect of PCPA on the VR1 expression induced by CSD was tested by evaluating the number of VR1-IR cells in the PCPA pretreated group and in the CSD group.

CSD induced expression of VR1 in the TG. VR1-IR cells were confined in TG and were more prevalent on the side ipsilateral to the operation. In control group, the numbers of VR1-IR cells in the ipsilateral and contralateral sides were 28.88 ± 0.60 cells and 21.66 ± 1.32 cells per section respectively. Pretreatment with PCPA enhanced the response of trigeminal nociceptive to CSD. The numbers of VR1-IR cells in PCPA-treated group were 39.22 ± 1.64 cells and 38.44 ± 3.04 cells per section for ipsilateral and contralateral sides, respectively. The data are shown in Table 4.17. The difference in the number of VR1-IR cells between PCPA-treated group and control group were statistically significant (Figure 4.20).

Table 4.17 The mean value \pm SD of the number of VR1-IR cells in the TG sections obtained from control group and PCPA-treated group.

Group	Contralateral side	Ipsilateral side
Control	21.66 \pm 1.32	28.88 \pm 0.60
5-HT depletion	38.44 \pm 3.04 *	39.22 \pm 1.64 *

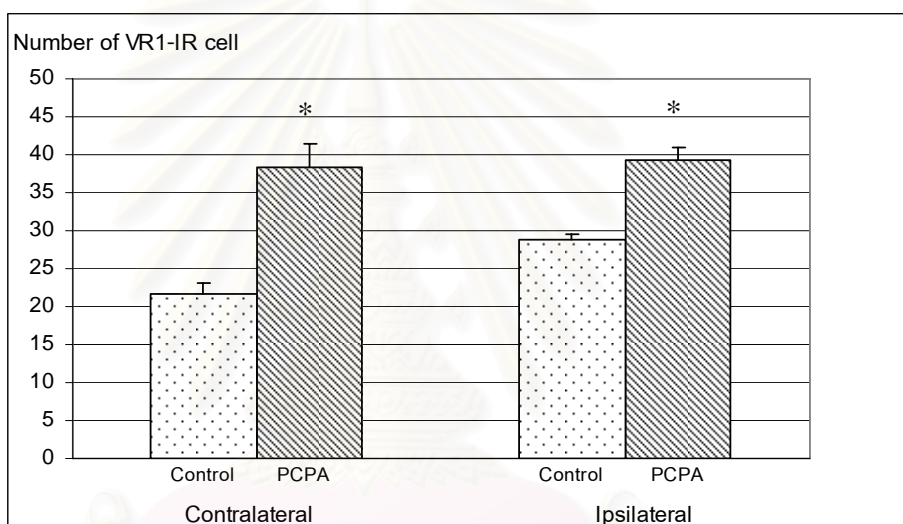
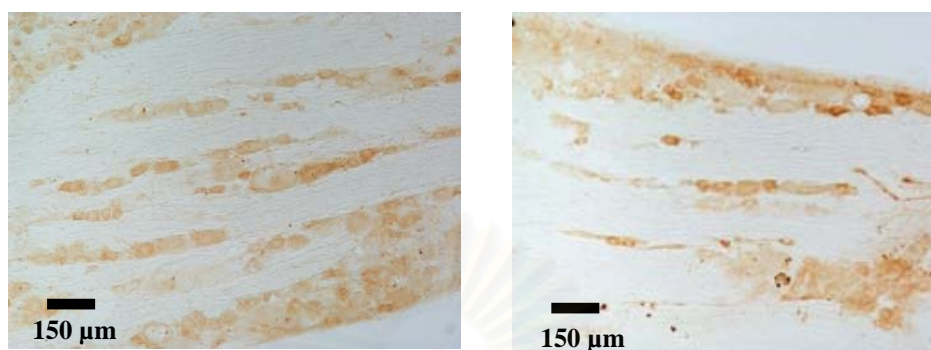


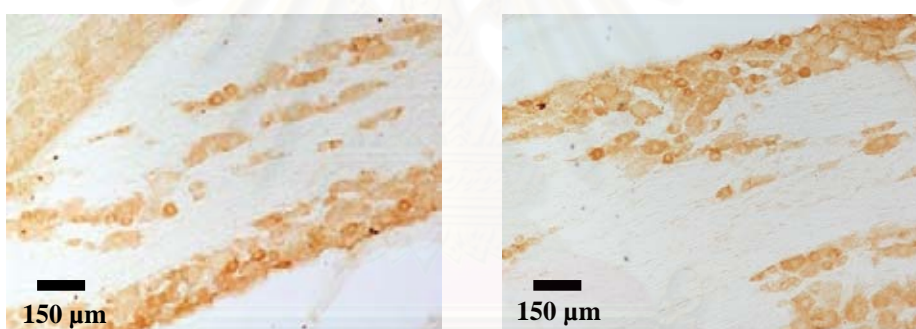
Figure 4.20 Bar graphs showing the mean value \pm SD of the number of VR1-IR cells in the TG sections obtained from control group and PCPA-treated group. Significant difference was assessed with student t-test. * p <0.05 compared with control group.



A. Control group

Ipsilateral side

Contralateral side



B. 5-HT depletion group

Ipsilateral side

Contralateral side

Figure 4.21 The photomicrograph showing the VR1-IR cells in the TG sections (ipsilateral side to KCl application) obtained from the A) Control group ($\times 10$) and B) PCPA-treated group ($\times 10$). Bar = 150 μm

3. The effect of 5-HT depletion on the c-fos expression induced by CSD

The Fos expression after CSD induction for 1 hour was mainly distributed in the lamina I and II of the cervical spinal cord sections on the side ipsilateral to the KCl application (Figure 4.23). The numbers of Fos-IR cells in ipsilateral and contralateral sides were 7.28 ± 0.57 and 1.95 ± 0.49 cells /slides respectively. Pretreatment with PCPA enhanced the response of trigeminal nociception to CSD. The numbers of Fos-IR cells in PCPA-treated group were 11.63 ± 3.07 cells and 6.64 ± 2.21 cells per slide for ipsilateral and contralateral sides, respectively. The data are shown in Table 4.18. The difference in the number of Fos-IR cells between PCPA-treated group and control group were statistically significant (Figure 4.22).



Table 4.18 The mean value \pm SD of number of Fos-IR cells in the C1 and C2 cervical spinal cord sections obtained from control group and PCPA-treated group.

Group	Contralateral side	Ipsilateral side
Control	1.95 \pm 0.49	7.28 \pm 0.57 #
5-HT depletion	6.64 \pm 2.21 *	11.63 \pm 3.07 * #

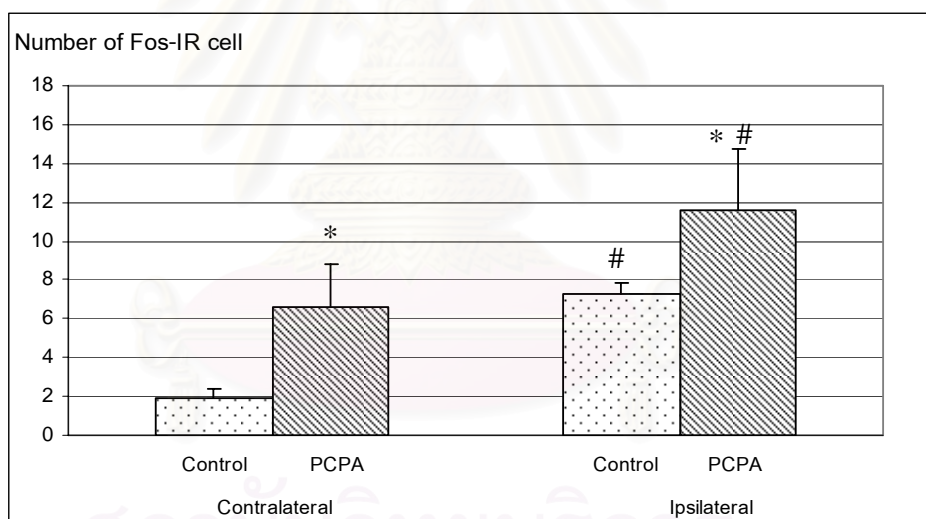


Figure 4.22 Bar graph showing the mean value \pm SD of the number of Fos-IR cells in the C1 and C2 cervical spinal cord sections obtained from the control group and PCPA-treated group. Significant difference was assessed with Student t-test. * $p < 0.05$ compared with control group. # $p < 0.05$ compared with contralateral side.

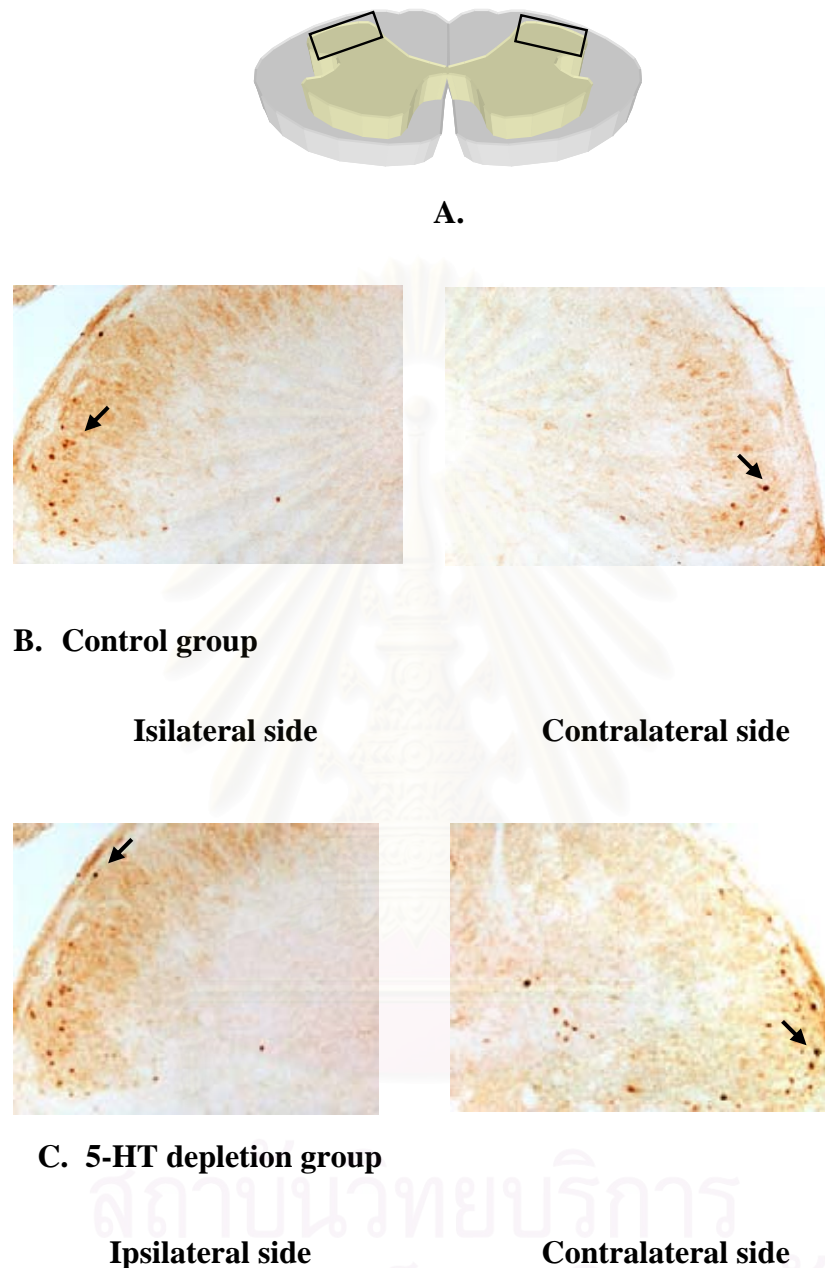


Figure 4.23 The photomicrograph showing the Fos-IR cells in the C1 and C2 cervical spinal cord sections (ipsilateral side to KCl application). Fos positive cells (arrow) are easily visible and well differentiated from the background. Box in the schematic drawings indicate the area the respective photographs were taken from. **A)** Spinal cord, **B)** Control group ($\times 10$) and **C)** 5-HT depletion group ($\times 10$).

III: THE EFFECT OF 5-HT DEPLETION AND FACIAL INFLAMMATION ON CORTICAL ACTIVITY AND TRIGEMINAL NOCICEPTIVE SYSTEM IN THE CSD MODEL

The results of this part are subdivided into three parts as follows:

1. The effect of 5-HT depletion and facial inflammation on the depolarization shift changes induced by CSD.
2. The effect of 5-HT depletion and facial inflammation on the VR1 expression induced by CSD.
3. The effect of 5-HT depletion and facial inflammation on the c-fos expression induced by CSD.



สถาบันวิทยบริการ
จุฬาลงกรณ์มหาวิทยาลัย

1. The effect of 5-HT depletion with facial inflammation on depolarization shift induced by CSD

The DC shift changes was studied in the all group in order to evaluate the effect of CSD on peak amplitude, duration, number of peak, interpeak latency , averaged and sum AUC of depolarization shift changes in one hour.

Pretreatment with PCPA and CFA induced CSD generation (Figure 4.24). The peak amplitude and duration of CSD waves in the PCPA with CFA-treated group were 27.51 ± 2.15 mV and 43.57 ± 2.66 seconds, respectively (Table 4.19) (Table 4.20). The averaged and sum AUC of CSD wave were 66.80 ± 10.04 mV-seconds and 1164.95 ± 248.73 mV-seconds, respectively) (Table 4.23) (Table 4.24). Statistical analysis showed no significant compared with CFA-treated group. The averaged number of CSD wave occurring with one hour and interpeak latency were increased significantly (17.38 ± 2.26 waves and 2.63 ± 0.41 minutes, respectively) (Table 4.21) (Table 4.22).

KCl

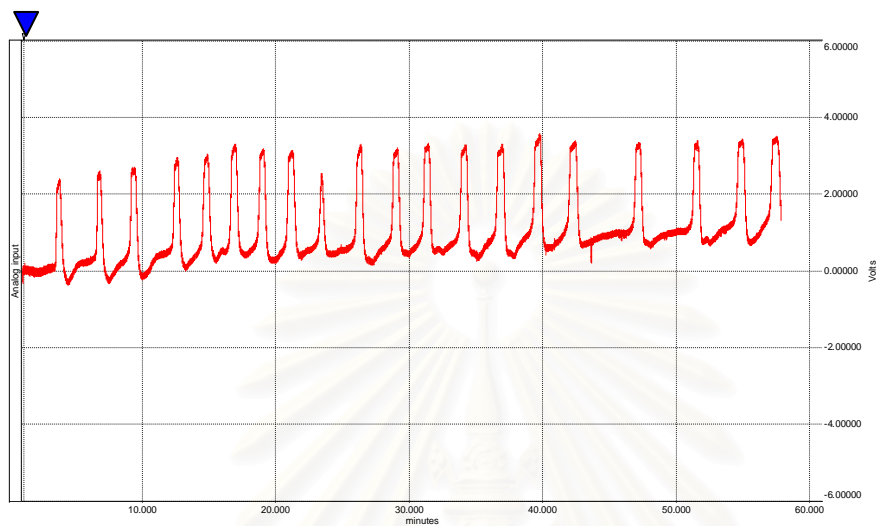


Figure 4.24 The tracing showing the depolarization shift changes after KCl 3 mg application in PCPA with CFA-treated group. Arrow shows the start of KCl application

สถาบันวิทยบริการ
จุฬาลงกรณ์มหาวิทยาลัย

Table 4.19 The mean value \pm SD of amplitude of DC shift obtained from CFA-treated group and PCPA with CFA treated group.

Group	Mean \pm SD of amplitude (-mV)
inflammation	26.20 \pm 3.94
5-HT depletion +inflammation	27.51 \pm 2.15

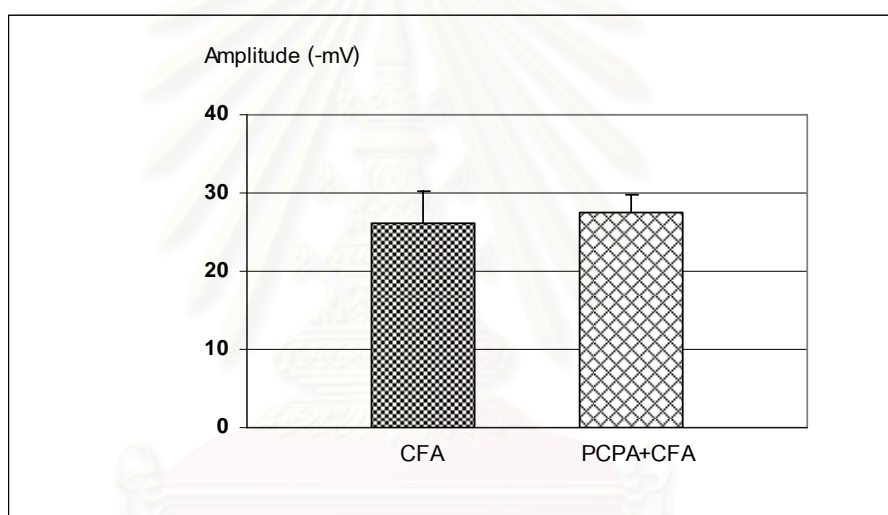


Figure 4.25 Bar graphs showing the mean value \pm SD of amplitude of DC shift obtained from CFA-treated group and PCPA with CFA-treated group.

Table 4.20 The mean value \pm SD of duration of DC shift obtained from CFA-treated group and PCPA with CFA-treated group.

Group	Mean \pm SD of duration (Seconds)
Inflammation	57.58 \pm 19.50
5-HT depletion +inflammation	43.57 \pm 2.66

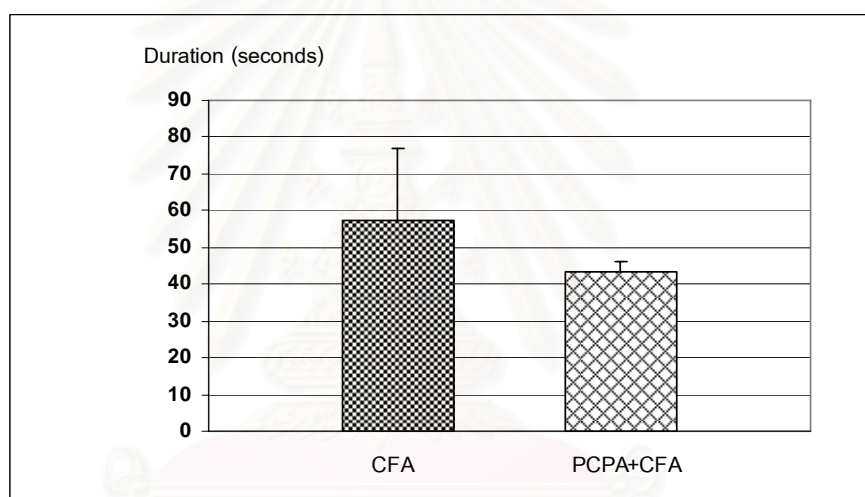


Figure 4.26 Bar graphs showing the mean value \pm SD of duration of DC shift obtained from CFA-treated group and PCPA with CFA-treated group.

Table 4.21 The mean value \pm SD of number of peak of DC shift obtained from CFA-treated group and PCPA with CFA-treated group.

Group	Mean\pm SD of number of peaks (waves)
Inflammation	14.00\pm 1.51
5-HT depletion + inflammation	17.38\pm 2.26 *

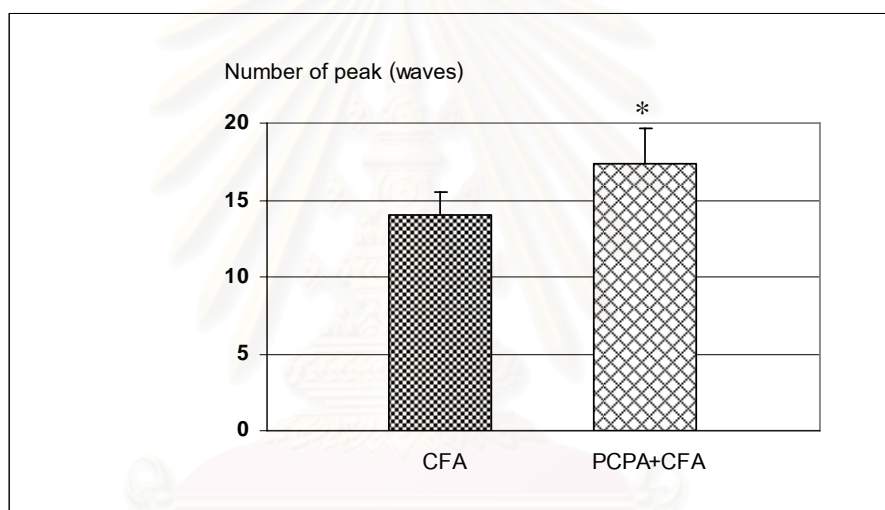


Figure 4.27 Bar graphs showing the mean value \pm SD of number of peaks of DC shift obtained from CFA-treated group and PCPA with CFA-treated group. Significant difference was assessed with student t-test. * $p < 0.05$ compared with CFA-treated group.

Table 4.22 The mean value \pm SD of interpeak latency of DC shift obtained from CFA-treated group and PCPA with CFA-treated group

Group	Mean \pm SD of interpeak latency (minutes)
Inflammation	3.20 \pm 0.35
5-HT depletion +inflammation	2.63 \pm 0.41 *

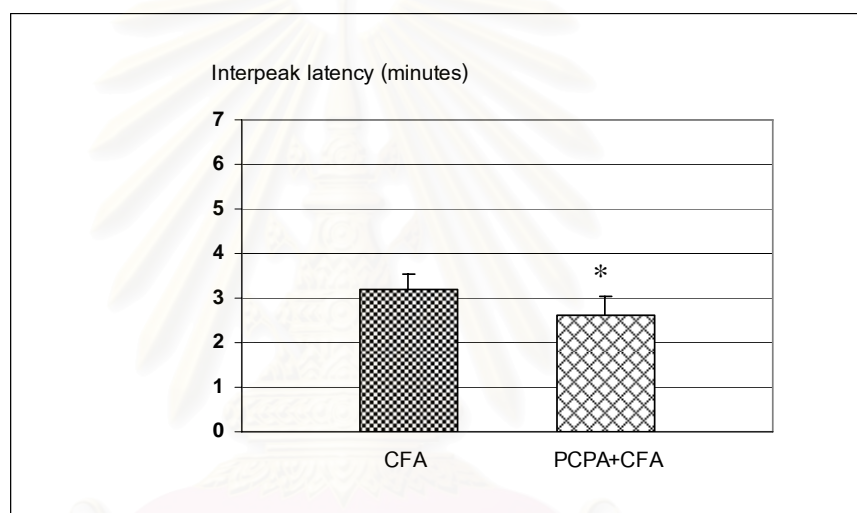


Figure 4.28 Bar graphs showing the mean value \pm SD of interpeak latency of DC shift obtained from CFA-treated group and PCPA with CFA-treated group. Significant difference was assessed with student t-test. * $p < 0.05$ compared with CFA-treated group.

Table 4.23 The mean value \pm SD of average AUC of DC shift in one hour obtained from CFA-treated group and PCPA with CFA-treated group.

Group	Mean\pm SD of average AUC (mV-second)
inflammation	77.22\pm 12.56
5-HT depletion +inflammation	66.80\pm 10.04

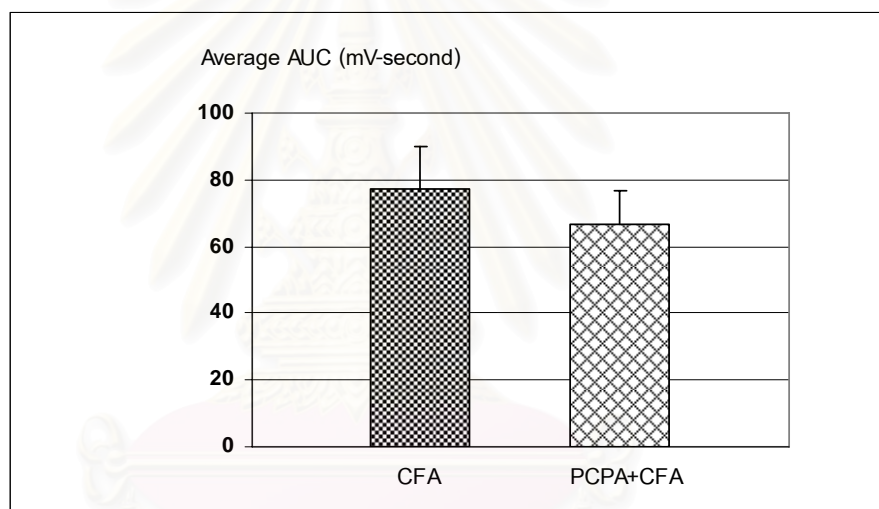


Figure 4.29 Bar graphs showing the mean value \pm SD of average AUC of DC shift in one hour obtained from CFA-treated group and PCPA with CFA-treated group.

Table 4.24 The mean value \pm SD of sum AUC of DC shift in one hour obtained from CFA-treated group and PCPA with CFA-treated group.

Group	Mean\pm SD of sum AUC (mV-second)
inflammation	1054.43\pm 175.68
5-HT depletion +inflammation	1164.95\pm 248.73

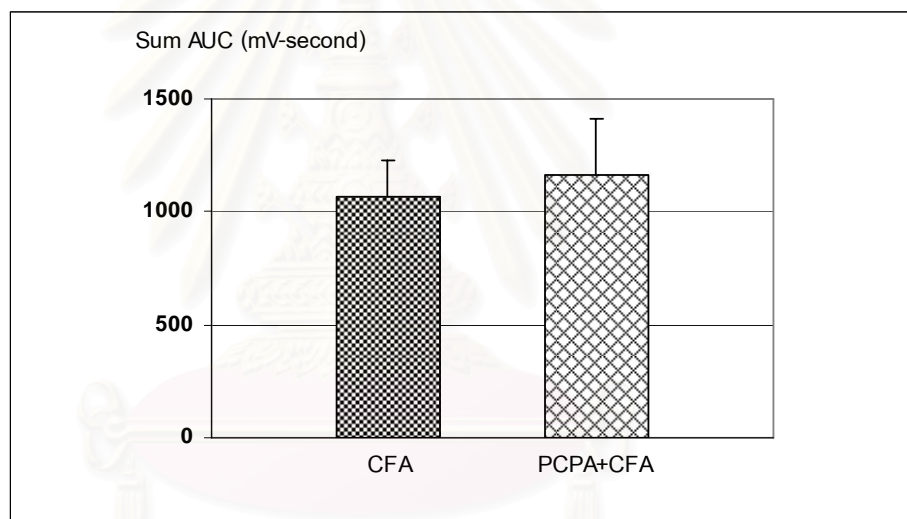


Figure 4.30 Bar graphs showing the mean value \pm SD of sum AUC of DC shift in one hour obtained from CFA-treated group and PCPA with CFA-treated group.

Table 2.5 Comparing the electrophysiological variables related to CSD between the inflammation and inflammation with serotonin depletion groups.

	Inflammation	Inflammation +5-HT depletion	Mean difference (95% CI)	p-value
Amplitude (mV)	26.20± 3.94	27.51± 2.15	1.31 (-2.56 to 5.25)	0.421
Duration (seconds)	57.58± 19.50	43.57± 2.66	14.01 (-33.51 to 5.49)	0.064
Number of peaks (waves)	14.00± 1.51	17.38± 2.26	3.00 (-4 to -1)	0.003
Interpeak latency (minutes)	3.20± 0.35	2.63± 0.41	0.57 (-0.92 to -0.16)	0.008
Average AUC (mV-second)	77.22± 12.56	66.80± 10.04	10.42 (-2.14 to 22.98)	0.088
Summed AUC (mV-second)	1054.43± 175.68	1164.95± 248.73	110.52 (313.89 to 534.93)	0.456

2. The effect of 5-HT depletion and facial inflammation on the VR1 expression induced by CSD.

The effect of PCPA with CFA on the VR1 expression induced by CSD was tested by evaluating the number of VR1-IR cells in the PCPA with CFA pretreated group and in the CSD group.

CSD induced expression of VR1 in the TG. VR1-IR cells were confined in TG and were more prevalent on the side ipsilateral to the operation. In CFA-treated group, the numbers of VR1-IR cells in the ipsilateral and contralateral sides were 41.66 ± 3.51 cells and 41.72 ± 3.55 cells per section respectively. Pretreatment with PCPA and CFA enhanced the response of trigeminal nociceptive to CSD. The numbers of VR1-IR cells in PCPA with CFA-treated group were 42.52 ± 3.59 cells and 37.30 ± 2.36 cells per section for ipsilateral and contralateral sides, respectively. The data are shown in Table 4.26. The difference in the number of VR1-IR cells between CFA-treated group and PCPA with CFA-treated group was statistically no significant (Figure 4.31).

Table 4.26 The mean value \pm SD of the number of VR1-IR cells in the TG sections obtained from CFA-treated group and PCPA with CFA-treated group.

Group	Contralateral side	Ipsilateral side
inflammation	41.72\pm 3.55	41.66\pm 3.51
5-HT depletion +inflammation	37.30\pm 2.36	42.52\pm 3.59

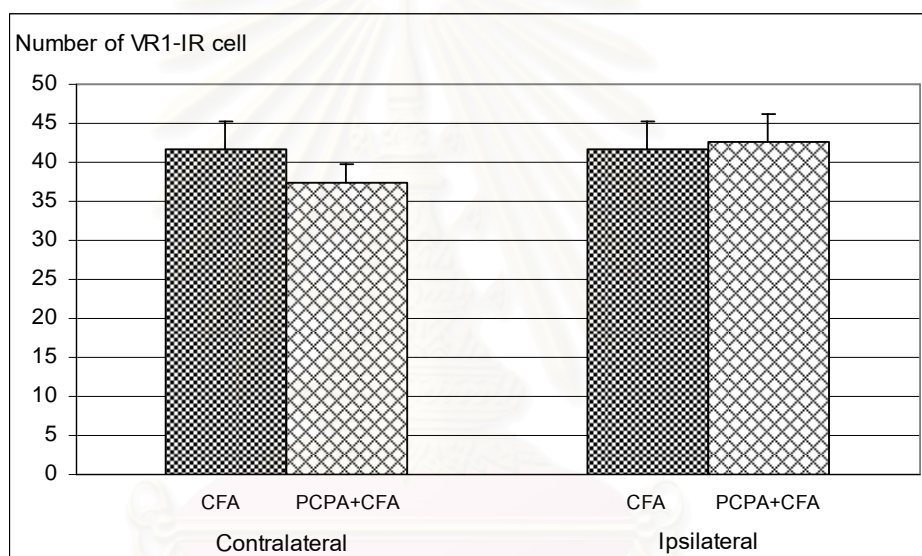
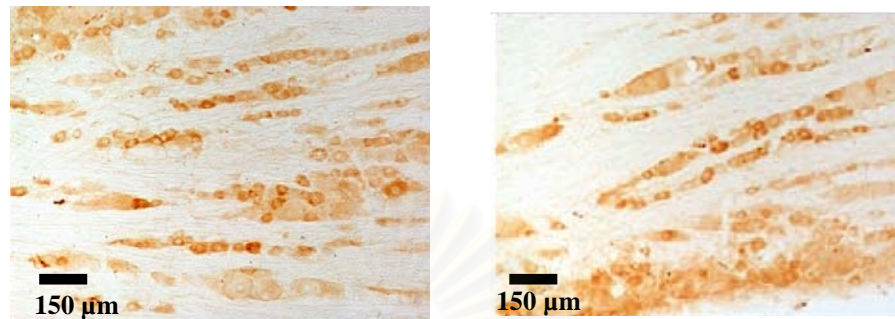


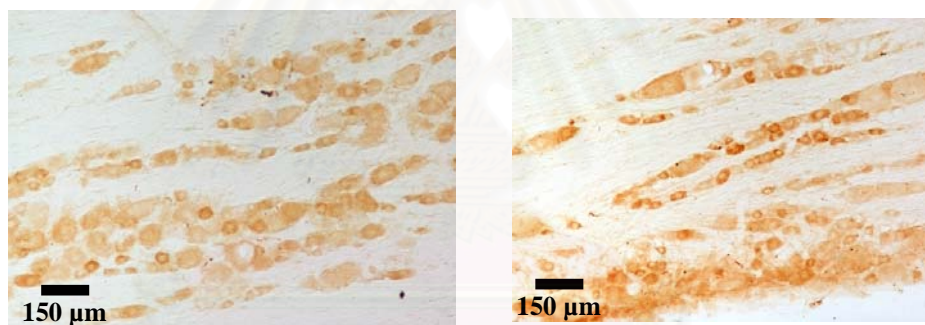
Figure 4.31 Bar graphs showing the mean value \pm SD of the number of VR1-IR cells in the TG sections obtained from the CFA-treated group and PCPA with CFA-treated group.



A. Inflammation group

Ipsilateral side

Contralateral side



B. 5-HT depletion with inflammation group

Ipsilateral side

Contralateral side

Figure 4.32 The photomicrograph showing the VR1-IR cells in the TG sections (ipsilateral side to KCl application) obtained from the A) inflammation group ($\times 10$) and B) 5-HT depletion with inflammation group ($\times 10$). Bar = 150 μm

3. The effect of 5-HT depletion and facial inflammation on the c-fos expression induced by CSD

The Fos expression after CSD induction for 1 hour was mainly distributed in the lamina I and II of the cervical spinal cord sections on the side ipsilateral to the PCPA with CFA application (Figure 4.34). In CFA-treated group, the numbers of Fos-IR cells in ipsilateral and contralateral sides were 13.71 ± 2.35 and 6.50 ± 2.00 cells /slides respectively. Pretreatment with PCPA and CFA enhanced the response of trigeminal nociception to CSD. The numbers of Fos-IR cells in PCPA with CFA-treated group were 12.28 ± 1.92 cells and 6.75 ± 2.85 cells per slide for ipsilateral and contralateral sides, respectively. The data are shown in Table 4.27. The difference in the number of Fos-IR cells between CFA-treated and PCPA with CFA-treated groups was statistically no significant (Figure 4.33).

Table 4.27 The mean value \pm SD of number of Fos-IR cells in the C1 and C2 cervical spinal cord sections obtained from CFA-treated group and PCPA with CFA-treated group.

Group	Contralateral side	Ipsilateral side
Inflammation	6.50\pm 2.00	13.71\pm 2.35 *
5-HT depletion +inflammation	6.75\pm 2.85	12.28\pm 1.92 #

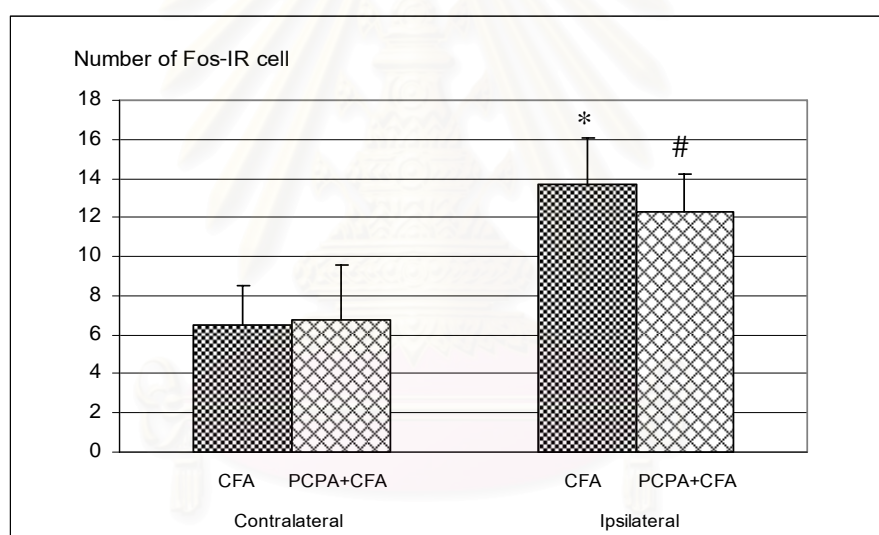
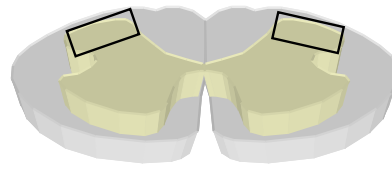


Figure 4.33 Bar graph showing the mean value \pm SD of the number of Fos-IR cells in the C1 and C2 cervical spinal cord sections obtained from CFA-treated group and PCPA with CFA-treated group. Significant difference was assessed with Student t-test. * p <0.05 compared with CFA-treated group. # p <0.05 compared with contralateral side.



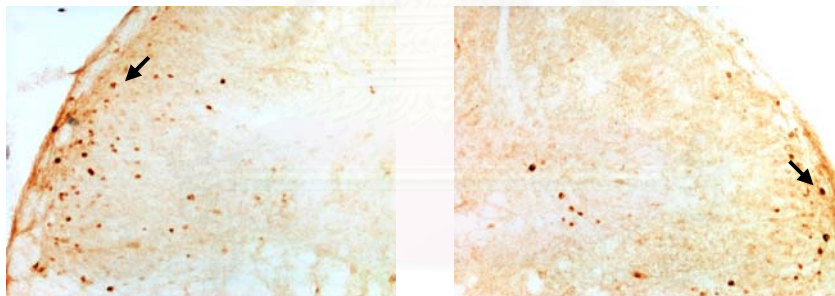
A.



B. Inflammation group

Ipsilateral side

Contralateral side



C. 5-HT depletion with inflammation group

Ipsilateral side

Contralateral side

Figure 4.34 The photomicrograph showing the Fos-IR cells in the C1 and C2 cervical spinal cord sections (ipsilateral side to KCl application). Fos positive cells (arrow) are easily visible and well differentiated from the background. Box in the schematic drawings indicate the area the respective photographs were taken from. A) Spinal cord, B) Control group ($\times 10$) and C) 5-HT depletion with inflammation group ($\times 10$).

CHAPTER V

DISCUSSION

This study was conducted to investigate the effect of inflammation and serotonin depletion on the development of CSD-evoked cortical activity and trigeminal nociceptive system. The first part of this research was conducted to investigate the effects of inflammation on CSD-evoked cortical activity and trigeminal nociceptive system. The second part was conducted to investigate the effect of serotonin depletion on CSD-evoked cortical activity and trigeminal nociceptive system. The third part was conducted to investigate the effect of serotonin depletion combine inflammation on CSD-evoked cortical activity and trigeminal nociceptive system.

CSD is an electrical phenomenon, considered to play an important role in the mechanism generating aura of migraine whereas inflammation and serotonin are recognized to play significant roles in the process of headache phase.

CSD cause extensive changes in neurophysiological condition during its propagation across the brain surface (Hansen, Quisstorff and Gjedde, 1980; Lauritzen, 1987a, b; Sugaya, Yakato and Nada, 1975). Cortical cell are depolarized, extracellular K^+ concentration rises, vasoactive metabolites and neurotransmitter released (Krivanek, 1961). In these circumstances, various factors could promote cortical changes during CSD.

1. The effect of facial inflammation on CSD-evoked depolarization shift, VR1 and c-fos expression

Peripheral inflammation can often result in enhanced transmission of sensory input through the spinal cord dorsal horn, this is termed central sensitization. The process of central sensitization also enlarges the receptive fields of these neurons, thus expanding the pain area. Most of the previous evidences demonstrated that sensitized trigeminal caudalis neurons initiated by chemical stimulation of the intracranial dura showed an increased response to facial stimulation (Burstein et al., 1998). The induction of peripheral and central sensitization has been proposed to be significant steps in the development of headache and allodynia in migraine patients. Here, we demonstrated that induction of inflammation may cause instability of neuronal function which enhances the excitability of the brain to develop a migraine attack. The present study showed that development of CSD and CSD-evoked trigeminal nociceptive were enhanced in the inflammatory state.

The results from the first study show that the injection of CFA induced VR1-IR expression in TG. In inflammation group, the numbers of VR1-IR cells in ipsilateral and contralateral sides to the CSD were significantly greater than those of the control group. This finding agrees with process studies which showed that levels of VR1 increase within nerve fibers at the site of inflammation in human and rodents (Carlton and Coggeshall, 2001; Yiangou et al., 2001). These and our results indicate that increase expression of VR1 in the DRG enhances the transport of this receptor. VR1 participates in inflammatory hyperalgesia because mice lacking this receptor do not develop thermal hyperalgesia after local inflammation (Caterina et al., 2000; Davis et al., 2000). Induction of hyperalgesia immediately after inflammation seems to be, therefore, mainly due to activation of VR1 channel activity.

In addition to the change in VR1 expression on cortical activity of depolarization shift obtained from the CFA treated group was also enhanced. In the inflammation group, the AUC of CSD waves was increase, the interpeak latency was decreased and the number of CSD waves was increased. On the other hand, no significant difference in peak amplitude or duration of CSD wave was detected. This pattern implied that inflammation may interfere with the process of repolarization hence increasing the cortical excitability. Increasing in cortical excitability may result in a more intense nociceptor activation and increase trigeminal nociception. This

hypothesis can be confirmed by our observation of an increase in Fos-IR cell in TNC. In 2003, Weissman-Fogel et al showed that noxious stimulation of the skin enhances cutaneous pain perception of migraine patients. These changes probably reflect sensitization of trigeminal nociceptive pathways. In the present study an increase in Fos-IR cells was observed in both ipsilateral and contralateral to the side of CSD activation. The increased Fos-IR cell in contralateral side may indicate an increase in nociceptive susceptibility in both TNC.

2. The effect of 5-HT depletion on CSD-evoked depolarization shift, VR1 and c-fos expression

Alteration of 5-HT system is the most important hypothesis for explaining the pathogenesis of migraine. Clinically, the concentration of 5-HT in platelets were found to be fluctuated depending on the phases of migraine. Most of the previous evidences showed that attack of migraine was associated with the period of low 5-HT (Anthony, Hinterberger and Lance, 1969; Ferrari et al., 1989). This observation is also true regarding the syndrome of frequent headache especially those associated with analgesic overuse. Therefore it is likely that, by unknown mechanism, depletion of this transmitter may predispose the patients to have migraine attack. Here, we demonstrated that depletion of 5-HT may set the brain to be more vulnerable to migraine attacks by increasing its excitability. The present study showed that development of CSD-evoked trigeminal nociception was enhanced in the low 5-HT state.

The pattern of CSD change associated with low 5-HT observed in this study was similar to these observed in CFA-treated group. In the low 5-HT group, the AUC of CSD waves was increased, the interpeak latency was decreased and the number of CSD waves was increased. On the other hand, no significant difference in peak amplitude or duration of CSD wave was detected. This pattern implied that the 5-HT depletion may interfere with the process of repolarization hence increasing the cortical excitability. It is widely recognized that 5-HT has diverse modulatory effects on cortical neurons depending on the receptor subtypes. Generally, activation of 5-HT₁ receptor exerts inhibitory effect whilst activation of 5-HT₂ receptor leads to cortical activation (Araneda and Andrade, 1991). Therefore, the increased cortical excitability observed in the low 5-HT group may result either from a decrease in 5-HT₁ receptor activation or an increase in 5-HT₂ receptor activation. We have

previously reported that 5-HT_{2A} receptor was up-regulated in the conditions with low 5-HT such as migraine patients with analgesic overuse and rats chronically treated with acetaminophen (Srikiatkachorn and Anthony, 1996; Srikiatkachorn, Tarasub and Govitropony, 2000). However, we cannot conclude that increased CSD response observed in this study is caused by up-regulation of this receptor subtype. More studies regarding the plasticity of 5-HT receptors in response to 5-HT depletion may help clarifying the role of receptor subtypes involving in the development of cortical hyperexcitability.

Several clinical evidences showed that depletion of 5-HT or its precursor affects the cortical activity in many aspects. Recent reviews confirmed that tryptophan depletion has mood-lowering effect. This effect was more prominent in recovered depressed persons and vulnerable healthy subjects (Moore et al., 2000; Willem, 2001). Depression is a common symptom observed in the prodromal period of migraine as well as in persons with chronic daily headache. Whether or not the prodromal depression is associated with a decrease level of 5-HT is still unknown.

Previously, we have proposed that 5-HT depletion may increase headache frequency by interfering with the endogenous pain control system (Srikiatkachachorn, 2002). Results of the present study revealed that, in addition to the facilitating the nociceptive process at brainstem or spinal level, low 5-HT may alter threshold for cortical activation.

Another change observed in PCPA-treated group is an increase in VR1-IR. Since this dram of receptor plays a pivotal role in nociceptive response. An increase in its number may enhance the response to noxious stimuli. Such change can lead to the facilitated of noxious perception as indicated by an increase in Fos-IR in TNC. Activation of nociceptors causes these sensory fibers to release neuropeptides, including substance P and calcitonin gene related peptide (CGRP). In 1995, Ichikawa and coworker reported that the co-expression of VR1 and CGRP in the TG. Although CGRP is mainly localized to small primary neurons with unmyelinated axons, substantial subpopulations of the CGRP-IR cells emit myelinated axons (Ishida-Yamamoto et al., 1989). While, low 5-HT activated c-fos expression in trigeminal nociceptor showed significant increase as compare with the control group. In 2000 Sharma et al., demonstrated that PCPA attenuated the c-fos upregulation along with the edematous expansion of the cord. However, the mechanism underlying the increase in VR1 in low 5-HT state is unclear.

3. The effect of 5-HT depletion and facial inflammation on CSD-evoked depolarization shift, VR1 and c-fos expression

In the final part, we demonstrated an enhancing effect of PCPA combine CFA induced depolarization shift, VR1-IR and Fos-IR changes as compare with facial inflammation group. The result showed no additional two synergistic effect when both interventions were combined. It could be possible that either the inflammation or the depletion of serotonin can already activate the neurons to the maximal response.



สถาบันวิทยบริการ
จุฬาลงกรณ์มหาวิทยาลัย

CHAPTER VI

CONCLUSION

The objectives of the present study were to determine the effect of 5-HT depletion and/or facial inflammation on the development of CSD and trigeminal nociception. The results of this study demonstrated that 5-HT depletion and facial inflammation could enhance the generation of CSD and facilitated trigeminal nociception. In CSD model, CFA could increase AUC and number of peak depolarization shift. These findings reflected the cortical hyperexcitability. Furthermore CFA could enhance trigeminal pathway which then led to increase of the activation in synaptic area and second order neurons. The similar results were observed the effect of low 5-HT using PCPA injection. The combination of CFA and PCPA did not show the synergistic effects response of the neurons-evoked by CSD.

The present study demonstrated the plasticity of trigeminal nociceptive system. Several factors, including facial tissue inflammation and 5-HT depletion as shown in the present study, can enhance this system by increasing the cortical response as well as facilitate the trigeminal nociception in general. Modification of trigeminal nociceptive system is a prime target for development of headache aborting agents.



สถาบันวิทยบริการ
จุฬาลงกรณ์มหาวิทยาลัย

REFERENCES

- Amaya, F., Oh-hashi, K., Naruse, Y., and Iilima, N. Local inflammation increases vanilloid receptor 1 expression within distinct subgroups of DRG neurons. Brain Res. 963(2003) : 190-196.
- Andres, K.H., Von, D.M., Muszynski, K., and Schmidt, R.F. Nerve fibers and their terminals of the duramater encephali of the rat. Anat Embryol. 175(1987) : 289-301.
- Anthony, M., Hinterberger, H., and Lance, J.W. The possible relationship of serotonin to the migraine syndrome. In: Friendman AP, editor. Research and Clinical Studies in Headache. New York: S. Karger, (1969) : 29-59.
- Araneda, R., and Andrade, R. 5-Hydroxytryptamine₂ and 5-hydroxytryptamine_{1A} receptors mediate opposing responses on membrane excitability in rat association cortex. Neuroscience 40(1991) : 399-412.
- Arban, M.D., Wiklund, L., and Svendgaard, N.A. Origin and distribution of cerebral vascular innervation from superior cervical, trigeminal and spinal ganglia investigated with retrograde and anterograd WGA-HRP tracing in the rat. Neuroscience 19(1986) : 695-708.
- Avoli, M., Drapeau, C., and Louvel, J. Epileptiform activity induced by low extracellular magnesium in the human cortex maintained in vitro. Ann. Neurol. 30(1991) : 589-596.
- Basbaum, A.I., and Jessel, T.M. The perception of pain. In Kendel ER, Schwartz JH, Jessel TM, editors. Principles of neuroscience. New York: McGraw Hill, 2000 : 472-490.
- Berger, R.J., Zuccarello, M., and Keller, J.T. Nitric oxide synthase immunoreactivity in the rat dura mater. Neuro Report. 5(1994) : 519-521.
- Bevan, S., and Geppetti, P. Proton: small stimulants of capsaicin-sensitive sensory nerves. Trend Neurosci. 17(1994) : 509-512.
- Bhattachary, S.K., and Das, N., Central serotonergic modulation of carageenan-induced pedal inflammation in rats. Pharm Res. 85(1985) : 315-318.
- Biro, T., Maurer, M., Modarres, S., Lewin, N.E., Brodie, C., and Acs, G. Characterization of function vanilloid receptors expressed by mast cells. Blood. 91(1998a) : 1332-1340.

- Biro, T., Brodie, C., Modarres, S., Lewin, N.E., Acs, G., and Blumberg, P.M. Specific vanilloid responses in C6 rat glioma cells. Mol. Brain Res. 56(1998b) : 89-98.
- Blau, J.N. Migraine: theories of pathogenesis. Lacet. 339(1992) : 1202-1207
- Bonvento, G., MacKenzie, ER., and Edvinsson, L. Serotonergic innervation of the cerebral vasculature: relevance to migraine and ischaemia. Brain Res Rev. 16(1991) : 257-263.
- Bruinvels, A.T., Landwehrmeyer, B., Gustafson, E.L., and Durkin, M.M. Localization of the 5-HT_{1B}, 5-HT_{1Da}, 5-HT_{1E} and 5-HT_{1F} receptor messenger RNA in rodent and primate brain. Neuropharmacology 33(1994) : 367-386.
- Bures, J., Buresova, O., and Krivanek, J. The mechanism and applications of Leao's spreading depression of electroencephalographic activity. Prague : Academia,1974.
- Burnet, P.W.J., Eastwod, S.L., Lacey, K., and Harrison, P.J. The distribution of 5-HT_{1A} and 5-HT₂ receptor mRNA in human brain. Brain Res. 676(1995) : 157-168.
- Burstein, R., Yamamura, H., Malick, A., and Strassman, A.M. Chemical stimulation of the intracranial dura induces enhanced responses to facial stimulation in brain stem trigeminal neurons. J. Neurophysiol. 79(1998) : 964-968.
- Buck, S.H., and Burks, T.F. The neuropharmacology of capsaicin: a review of some recent observations. Pharmacol. Rev. 38(1986) : 179-226.
- Buzzi, M.G., and Moskowitz, M.A. The antimigraine drug sumatriptan (GR43175), selectivity blocks neurogenic plasma extravasation in the rat dura mater. Br. J. Pharmacol. 99(1990) : 202-206.
- Cameron, A.A., Leah, J.D., and Snow, P.J. The coexistence of neuropeptides in feline sensory neurons. Neuroscience 27(1988) : 969-979.
- Carlton, S.M., and Coggeshall, R.E. Peripheral capsaicin receptors increase in the inflamed rat hindpaw: a possible mechanism for peripheral sensitization. Neurosci. Lett. 310(2001) : 53-56.
- Caterina, M.J., Schumacher, M.A., Tominaga, M., Rosen, T.A., Levine, J.D., and Julius, D. The capsaicin receptor: a heat-activated ion channel in the pain pathway. Nature 398(1997) : 816-824.

- Caterina, M.J., Leffler, A., Malmberg, W.J., and Trafton, K.R. Impaired nociception and pain sensation in mice lacking the capsaicin receptor. Science 288(2000) : 306-313.
- Cesare, P., and McNaughton, P. A novel heat-activated current in nociceptive neurons and its sensitization by bradykinin. Proc. Natl. Acad. Sci. 93(1996) : 15435-15439.
- Chen, C.C., England, S., Akopian, A.N., and Wood, J.N. A sensory neuron-specific, proton gated ion channel. Proc. Natl. Acad. Sci. 95(1998) : 10240-10245.
- Cohen, Z., Bonvento, G., Lacombe, P., MacKenzie, E.T., Seylaz, J., and Hamel, E. Cerebrovascular nerve fibers immunoreactive for tryptophan-5-hydroxylase in the rat: distribution, putative origin and comparison with sympathetic noradrenergic nerve. Brain Res. 598(1992) : 203-214.
- Colonna, D.M., Meng, W., and Deal, D. Neuronal NO promotes cerebral cortical hyperemia during cortical spreading depression in rabbit. Am. J. Physiol. 272(1997) : H1315-H1322.
- Curzon, G., and Green, A. The effect of D- and L-p-chlorophenylalanine on the metabolism of 5-hydroxytryptamine in brain. Br. J. Pharmacol. 39(1970) : 653-655.
- Cutrer, F.M., Moussaoui, S., Garret, C., and Moskowitz, M.A. The non-peptide neurokinin-1 antagonist, RPR 100893, decrease c-fos expression in trigeminal nucleus caudalis following noxious chemical meningeal stimulation. Neuroscience 64(1995) : 741-750.
- Davies, F.M., Diesz, R.A., Prince, D.A., and Peroutka, S.J. Two distinct effects of 5-hydroxytryptamine on single cortical neurons. Brain Res. 423(1987) : 347-352.
- Davis, J.B., Gray, M.J., Gunthorpe, J.P., Hatcher, P.T., Davey, P., Overend, M.H., and Harries, J. Vanilloid receptor-1 is essential for inflammatory thermal hyperalgesia. Nature 405(2000) : 183-187.
- De Vries, P., Villalon, C.M., Heiligers, J.P., and Saxena, P.R. Characterization of 5-HT receptors mediating constriction of porcine carotid arteriovenous anastomoses; involvement of 5-HT_{1B/1D} and novel receptors. Br. J. Pharmacol. 123(1998) : 1561-1570.

- Douen, A.G., Akiyama, K., and Matthew, J. Preconditioning with cortical spreading depression decreases intraschemic cerebral glutamate levels and dose-regulates excitatory amino acid transporters EAAT1 and EAAT2 from rat cerebral cortex plasma membranes. *J. Neurochem.* 75(2000) : 812-817.
- Ebersberger, A., Schaible, H.G., and Averbeck, B. IS there a correlation between spreading depression, neurogenic inflammation and nociception that might cause migraine headache. *Ann. Neurol.* 49(2001) : 7-13.
- Ferrari, M.D., Odink, J., Tapparelli, C., and Van Kempen, G.M. Serotonin metabolism in migraine. *Neurology* 39(1989) :1239-1242.
- Fields, H.L., and Basbaum, A.I. Brainstem control of spinal pain-transmission neurons. *Annu. Rev. Physiol.* 40(1978) : 217-248.
- Fukuoka, T., Tokunaga, A., and Tachibana, T. VR1, but not P₂X₃, increases in the spared L₄ DRG in rats with L₅ spinal nerve ligation. *Pain* 99(2002) : 111-120.
- Gardner-Medwin, A.R. Possible roles of vertebrate neuroglia in potassium dynamics, spreading depression and migraine. *J. Exp. Biol.* 95(1981) : 1111-1127.
- Gill, R., Andine, P., and Hillered, L. The effect of MK-801 on cortical spreading depression in the penumbral zone following focal ischaemia in the rat. *J. Cerebral Blood Flow Metab.* 12(1992) : 371-379.
- Gloor, P. Regional cerebral blood flow in migraine. *Trends Neurosci.* 6(1986) : 21.
- Goadsby, P.J. Current concepts of the pathophysiology of migraine. In: editor. *Neurologic Clinics: Advances in Headache*. Philadelphia, pa: WB Saunders Co, 15(1997) : 27-42.
- Goadsby, P.J., and Edvinsson, L. The trigeminovascular system and migraine: studies characterizing cerebrovascular and neuropeptide changes seen in man and cat. *Ann. Neurol.* 33(1993) : 48-56.
- Gorji, A., Zahn, P.K., Pogatzki, E.M., and Speckmann, E.J. Spinal and cortical spreading depression enhance spinal cord activity. *Neurobiol. Disease* 15(2004) : 70-79.
- Grafstein, B. Neuronal release of potassium during spreading depression. In M.A.B. Brazier (ed.). *Brain function, Vol. 1, Cortical excitability and steady potentials*, pp.87-124. Berkeley: University of California Press, 1963.

- Guo, A., Vulchanova, L., Wang, J., Li, X., and Elde, R. Immunocytochemical localization of the vanilloid receptor 1 (VR1): relationship to neuropeptides, the P₂X₃ purinoceptor and IB4 binding site. Eur. J. Neurosci. 11(1999) : 946-958.
- Hajor, M. Capsaicin- sensitive vasodilatory mechanisms in the rat substantia nigra and striatum. J Neural Transm. 74(1988) : 129-139.
- Handwerker, H.O., and Reeh, P.W. Pain and inflammation. Elsevier 1991 : 59-70.
- Hansen, A.J., Quisstorff, B., and Gjedde, A. Relationship between local changes in cortical blood flow and extracellular K⁺ during spreading depression. Acta Physiol Scand. 109(1980) : 1-6.
- Hardebo, J.E. Migraine-why and how a cortical excitatory wave may initiate the aura and headache. Headache 31(1991) : 213-221.
- Haring, J.H., Henderson, T.A., and Jacquin, M.F. Principalis or parabrachial-projecting spinal trigeminal neurons do not stain for GABA or GAD. Somato Motor . Res. 7(1990) : 391-397.
- Helliwell, R.J.A., McLantchie, L.M., Clarke, M., Winter, J., Bevan, S., and McIntyre, P. Capsaicin sensitivity is associated with the expression of the vanilloid (capsaicin) receptor (VR1) mRNA in adult rat sensory ganglia. Neurosci. Lett. 250(1998) : 177-180.
- Herrara, D.G., Maysinger, D., and Gadiant, R. Spreading depression induces c-fos-like immunoreactivity and NGF mRNA in the rat cerebral cortex. Brain Res. 602(1993) : 99-103.
- Holzer, P. Capsaicin: cellular targets, mechanisms of action, and selectivity for thin sensory neurons. Pharmacol. Rev. 43(1991) : 144-201.
- Hoyer, D., Clarke, D.E., Fozard, J.R., and Hartig, P.R. International union of pharmacology classification of receptors of 5-hydroxytryptamine (serotonin). Pharmacol. Rev. 46(1994) : 157-203.
- Humphrey, P.P. 5-Hydroxytryptamine and the pathophysiology of migraine. J. Neurol. 238(1991) : S38-S44.
- Ichikawa, H., and Helke, C.J. Distribution, origin and plasticity of galanin-immunoreactivity in the rat carotid body. Neuroscience 52(1993) : 757-767.

- Ichikawa, H., Deguchi, T., Nakago, T., Jacobowitz, D.M., and Sugimoto, T. Parvalbumin- and calretinin-immunoreactive trigeminal neurons innervating the rat molar tooth pulp. Brain Res. 679(1995) : 205-211.
- Ijima, T., Mies, G., and Hossmann, K.A. Repeated negative DC deflections in rat cortex following middle cerebral artery occlusion are abolished by MK-801; effect on volume of ischaemic injury. J. Cereb. blood Flow Metab. 12(1992) : 727-733.
- Ingvar, B.K., Laursen, H., Olesen, U.B., and Hansen, A.J. Possible mechanism of c-fos expression in trigeminal nucleus caudalis following cortical spreading depression. Pain 72(1997) : 407-415.
- International Headache Society Headache Classification Committee. Classification and diagnostic criteria for headache disorders, cranial neuralgia and facial pain. Cephalalgia 24(2004) :1-160.
- Jacobs, B.L., Wilkinson, L.O., and Fornal, C.A. The role of brain serotonin: a neurophysiologic perspective. Neuropsychopharmacology 3(1990) : 473-479.
- Jordan, L.M., Fredrickson, R.C.A., Phillis J.M., Lake, N., Microelectrophoresis of 5-hydroxytryptamine: a clarification of its action on cerebral cortical neurons. Brain Res. 40(1972) : 552-558.
- Jordt, S.E, Tominaga, M., and Julius, D. Acid potentiation of the capsaicin receptor determined by a key extracellular site. Proc. Natl. Acad. Sci. 97(2000) : 8134-8135.
- Kai-kai, M.A. Cytochemistry of the trigeminal and dorsal root ganglia and spinal cord of the rat. Comp. Biochem. Physiol. 93(1989) : 183-193.
- Kalkman, H.O. Is migraine prophylactic activity caused by 5-HT_{2B} or 5-HT_{2C} receptor blockade?. Life sci. 54(1994) : 641-644.
- Kallela, M., Farkia, M., Saijonmaa, O., Saijonmaa O, and Fyhrquist F. Endothelin in migraine patients. Cephalalgia 18(1998) : 329-332.
- Kimball, R.W., Friedman, A.P., and Vallejo, E. Effect of serotonin in migraine patients. Neurology 10(1960) : 107-111.
- Kirschstein, T., Busselberg, D., and Treede, R.D. Coexpression of heat-evoked and capsaicin-evoked inward currents in acutely dissociated rat dorsal root ganglion neurons. Neurosci. Lett. 231(1997) : 33-36.

- Kirschstein, T., Greffrath, W., Busselberg, D., and Treede, R.D. Inhibition of rapid heat responses in nociceptive primary sensory neurons of rats by vanilloid receptor antagonists. J. Neurophysiol. 82(1999) : 2853-2860.
- Koponen, S., Keinanen, R., and Roivanen, T. Spreading depression induces expression of calcium-independent protein kinase C subspecies in ischaemia-sensitive cortical layers. Neuroscience 93(Suppl 3) (1999) : 985-993.
- Kraig, R.P., Dong, L.M., Thisted, R., and Jaeger, C.B. Spreading depression increases immunohistochemical staining of glial fibrillary acidic protein. J. Neurosci. 11(1991) : 2187-2198.
- Kress, M., Fetzer, S., Reeh, P.W., and Vyklicky, L. Low pH facilitates capsaicin responses in isolated sensory neurons of the rat. Neurosci. 211(1996) : 5-8.
- Krivanek, J. Some metabolic changes accompanying Leao's spreading cortical depression in the rat. J. Neurochem. 6(1961) : 183-189.
- Krnjevic, K., Phillis, J.W., Ionophoretic studies of neurons in the mammalian cerebral cortex. J. physiol (Lond). 165(1963) : 274-304.
- Lakoski, J.M., Aghajanian, G.K., Effects of ketanserin on neuronal responses to serotonin in the prefrontal cortex, lateral geniculate, and dorsal raphe nucleus. Neuropharmacology 24(1985) : 265-273.
- LaMotte, R.H., and Campbell, J.N. Comparison of response of warm and nociceptive c-fiber afferents in monkey with human judgments of thermal pain. J. Neurophysiol. 41(1978) : 509-528.
- Lambert, G.A., and Michalicek, J. Effect of cortical spreading depression on activity of trigeminovascular sensory neurons. Cephalalgia 19(1999) : 631-638.
- Lambert, G.A., and Michalicek, J. Cortical spreading depression reduces dural blood flow: a possible mechanism for migraine pain. Cephalalgia 14(1994) : 430-436.
- Lance, J.W. Current concepts of migraine pathogenesis. Neurology 43(Suppl 3) (1993) : 11-15.
- Lauritzen, M., Olsen, T.S., Lassen, N.A., and Paulson, O.B. Regulation of regional cerebral blood flow during and between migraine attacks. Brain 14(1984) : 569-572.
- Lauritzen, M. Pathophysiology of the migraine aura: the spreading depression theory. Brain 117(1994) : 199-210.

- Lauritzen, M. Cerebral blood flow in migraine and cortical spreading depression (review). Acta. Neurol. scand. 76 (Suppl 13) (1987a) : 1-40.
- Lauritzen, M. Cortical spreading depression as a putative migraine mechanism. Trend. Neurosci. 10(1987b) : 8-13.
- Lauritzen, M., Hansen, A.J., Kronborg, D., and Wieloch, T. Cortical spreading depression is associated with arachidonic acid accumulation and preservation of energy change. J. Cereb blood Flow Metab. 10(1990) : 115-122.
- Leao, A.A.P. Spreading depression of activity in the cerebral cortex. J Neurophysiol. 7(1944) : 379-90.
- Leao, A.A.P., and Morison, R.S. Propagation of spreading cortical depression. J. Neurophysiol. 8(1945) : 33-45.
- Leibowitz, D.H. The glial spike theory on an active role of neuroglia in spreading depression and migraine. Proc. R. Soc. Lond. Biol. 250(1992) : 287-295.
- Levine, J., and Taiwo, Y. Inflammatory pain. In textbook of pain , ed. PD Wall, R Melzack, Edinburgh: Churchill Livingstone 1994 : 45-56.
- Lincoln, J. Innervation of cerebral arteries by nerves containing 5-hydroxytryptamine and noradrenaline. Pharmacol. Ther. 68(1995) : 473-501.
- Li, C., Peoples, R.W., and Weight, F.F. Enhancement of ATP-activated current by protons in dorsal root ganglion neurons. Eur. J. Physiol. 433(1997) : 446-454.
- Lingueglia, E., de Weille, J.R., Bassilana, F., Heurteaux, C., and Sakai, H. A modulatory subunit of acid sensing ion channels in brain and dorsal root ganglion cells. J. Biol.Chem. 272(1997) : 29778-29783.
- Lipton, R.B., and Stewart, W.F. Prevalence and impact of migraine. Neurol. Clin. 15(1997) : 1-13.
- Liu, L., Pugh, W., Ma, H., and Simon, S.A. Identification of acetylcholine receptors in adult rat trigeminal ganglion neurons. Brain Res. 617(1993) : 37-42.
- Magnusson, K.R., Larson, A.A, Madl, J.E., Altschuler, R.A., and Beitz, A.J. Co-localization of fixative-modified glutamate and glutaminase in neurons of the spinal trigeminal nucleus of the rat: An immunohistochemical and immunoradiochemical analysis. J. Comp. Neurol. 247(1986) : 477-490.

- Marek, G.J., Aghajanian, G.K., 5-hydroxytryptamine-induced excitatory postsynaptic currents in neocortical layer V pyramidal cells: suppression by μ -opioid receptor activation. Neuroscience 86(1998) : 485-497.
- Martenson, M.E., Ingram, S.L., and Baumann, T.K. Potentiation of rabbit trigeminal responses to capsaicin in a low pH environment. Brain Res. 651(1994) : 143-147.
- Martin, G.R. Vascular receptors for 5-hydroxytryptamine: distribution, function and classification. Pharmacol. Ther. 62(1994) : 283-324.
- Meng, W., Colonna, D.M., Tobin, J.R., and Busija, D.W. Nitric oxide and prostaglandins interact to mediate arterial dilation during cortical spreading depression. Am. J. Physiol. 269(1995) : 176-181.
- Milner, P.M. Note on a possible correspondence between the scotomas of migraine and spreading depression of Leao. Electroencephalogr. Clin. neurophysiol. 10(1958) : 705.
- Millan, M.J. The induction of pain: an integrative review. Prog. Neurobiol. 57(1999) : 1-164.
- Mies, G. Inhibition of reelin synthesis during repetitive cortical spreading depression. J. Neurochem. 60(1993) : 360-363.
- Moore, P., Landolt, H.P., Seifritz, E., Clark, C., Bhatti, T., and Kelsoe, J. Clinical and physiological consequences of rapid tryptophan depletion. Neuropsychopharmacology 23(2000) : 601-622.
- Morales, M., and Bloom, F.E. The 5-HT₃ receptor is present in different subpopulations of GABAergic neurons in the rat telencephalon. J. Neurosci. 17(1997) : 3157-3167.
- Moskowitz, M.A., and Cutrer, F.M. Sumatriptan: a receptor-targeted treatment for migraine. Ann. Rev. Med. 44(1993) : 145-154.
- Nagy, I., and Rang, H. Noxious heat activated all capsaicin-sensitive and also a subpopulation of capsaicin-insensitive dorsal root ganglion neurons. Neuroscience 88(1999a) : 995-997.
- Nagy, I., and Rang, H.P. Similarities and differences between the responses of rat sensory neurons heat and capsaicin. J. Neurosci. 19(1999b) : 10647-10655.

- Nedergaard, M., and Astrup, J. Infarct rim: effect of hyperglycemia on direct current potential and (14C) 2-deoxyglucose phosphorylation. J. Cereb. Blood Flow Metab. 6(1986) : 607-615.
- Nicholson, C. Volume transmission and the propagation of spreading depression. In: Lehmenkuhler A, Grottemeyer K-H, Tegtmeier F, edi. Migraine: basic mechanisms and treatment. Munich: Urban and Schwarzenberg, 1993 : 293-308.
- Nozaki, K., Moskowitz, M.A, Maynard, K.I, Koketsu, N., Dawson, T.M., and Bredt D.S. Possible origins and distribution of immunoreactive nitric oxide synthetase-containing nerve fibers in cerebral arteries. J. Cereb. Blood Flow Metab. 13(1993) : 70-79.
- Olesen, J., Friberg, L., and Olesen, T.S. Timing and topography of cerebral blood flow, aura, and headache during migraine attacks. Ann. Neurol. 28(1990) : 791-798.
- Olesen, J., and Jansen-Olesen, I. Nitric oxide mechanisms in migraine. Pathol. Biol. (Paris) 48(Suppl 7)(2000) : 648-657.
- Pentersen, M., and LaMotte, R.H. Effect of protons on the inward current evoked by capsaicin in isolated dorsal root ganglion cells. Pain 54(1993) : 37-42.
- Piper, R.D., Lambert, G.A., and Duckworth, J.W. Cortical blood flow changes during spreading depression in cat. Am. J. Physiol. 261(1991) : H96-H102.
- Pompeiano, M., Palacios, J.M., Mengod, G. Distribution of serotonin 5-HT₂ receptor family mRNAs: comparison between 5-HT_{2A} and 5-HT_{2C} receptors. Mol. Brain Res. 23(1994) : 163-178.
- Raja, S.N., Meyer, R.A., Ringkamp, M., and Campbell, J.N. Peripheral neural mechanisms of nociception. In textbook of pain, ed. PD Wall, R Melzack, Edinburgh:Churchill Livingstone 1999 : 11-57.
- Raskin, N.H. Serotonin receptors and headache. N. Engl. J. Med. 325(1991) : 353-354.
- Reader, T.A., Ferron, A., Descarries, L., and Jasper, H.H. Modulatory role for biogenic amines in the cerebral cortex. Microiontophoretic studies. Brain Res. 160(1979) : 217-229.
- Reichling, D.B., and Levine, J.D. Heat transduction in rat sensory neurons by calcium-dependent activation of a cation channel. Proc. Natl. Acad. Sci. 94(1997) : 7006-7011.

- Read, S.J., Smith, M.I., Hunter, A.J., and Parsons, A.A. SB-220453 a potential novel antimigraine agent, inhibits nitric oxide release following induction of cortical spreading depression in the anaesthetized cat. Cephalalgia 20(2000) : 92-99.
- Read, S.J., Smith, M.I., and Benham, C.D. Furosemide inhibits regenerative cortical spreading depression in anaesthetized cats. Cephalalgia 17(1997) : 826-832.
- Reuter, L.E., and Jacobs, B.L. A microdialysis examination of serotonin release in the rat forebrain induced by behavioral/environmental manipulations. Brain Res. 739(1996) : 57-69.
- Sasamura, T. Existence of capsaicin-sensitive glutamatergic terminals in rat hypothalamus. Neuro report 9(1998) : 2045-2048.
- Saxena, P.R. Serotonin receptors: subtypes, functional responses therapeutic relevance. Pharmacol. Ther. 66(1995) : 339-368.
- Schnider, P., Maly, J., and Grunberger, J. Improvement of decreased critical flicker frequency (CFF) in headache patients with drug abuse after successful withdrawal. Headache 35(1995) : 269-272.
- Shigenaga, Y., Chen, I.C., Suemune, S., Nishimori, T., and Nasution, I.D. Oral and facial representation within the medullary and upper cervical dorsal horns in the cat. J. Comp. Neurol. 243(1986) : 388-408.
- Siberstein, S.D. Advance in understanding the pathology of headache. Neurology 42(Suppl 2)(1992) : 6-10.
- Sicuteri, F., Testi, A., and Anselmi, B. Biochemical investigation in headache: increase in hydroxyindoleacetic acid excretion during migraine attack. Int. Arch. Allergy App. Immunol. 19(1961) : 55-58.
- Siniatchkin, M., Gerber, W.D., Kropp, P., Vein, A. Contingent negative variation in patients with chronic daily headache. Cephalalgia 18(1998) : 565-569.
- Smith, M.I., Read, S.J., and Chan, W.N. Repetitive cortical spreading depression in a gyrencephalic feline brain. Cephalalgia 20 (Suppl 6)(2000) : 546-553.
- Snell, R.S. The cranial nerve nuclei and their central connections. In: Snell RS, editor. Clinical neuroanatomy for medical students. Brown and company: Little 1992 : 430.
- Spain, W.J. Serotonin has different effects on two classes of Betz cells from the cat. J Neurophysiol. 72(1994) : 1925-1937.

- Sramka, M., Brozek, G., Bures, J., and Nadvornik, P. Functional ablation by spreading depression: possible use in human stereotactic neurosurgery. Neurophysiol. 40(1978) : 48-61.
- Srikiatkhachorn, A., and Anthony, M. Serotonin receptor adaptation in patients with analgesic induced headache. Cephalalgia 16(1996) : 419-422.
- Srikiatkhachorn, A., Tarasub, N., and Govitrapong, P., Effect of chronic analgesic exposure on the central serotonin system. A possible mechanism of analgesic abuse headache. Headache 40(2000) : 343-350.
- Srikiatkhachorn, A., Suwattanasophon, C., Ruangpattanatwee, U., and Phansuwan-Pujito, P. 5-HT_{2A} receptor activation and nitric oxide synthesis: a possible mechanism determining migraine attacks. Headache 42(2002) : 566-574.
- Srikiatkhachorn, A., Maneesri, S., Govitrapong, P., and Kasantikul, V. Derangement of serotonin system in migrainous patients with analgesic abuse headache: clues from platelets. Headache 38(1998) : 43-49.
- Srikiatkhachorn, A. Chronic daily headache: a scientist's perspective. Headache 42(2002) : 532-537.
- Statnick, M.A., Dailey, J.W., Jobe, P.C., and Browning, R.A. Abnormalities in 5-HT_{1A} and 5-HT_{1B} receptor binding in seizure genetically epilepsy-prone rats. Neuropharmacology 35(1996) : 111-118.
- Stoop, R., Surprent, A., and North, A. Different sensitivity to pH of ATP-induced currents at four cloned P_{2X} receptors. J. Neurophysiol. 78(1997) : 1837-1840.
- Sugaya, C., Yakato, M., and Noda, Y. Neuronal and glial activity during spreading depression in cerebral cortex of cat. J. Neurophysiol. 38(1975) : 822-841.
- Szallasi, A. Vanilloid (capsaicin) receptors in the rat: distribution in the brain, regional differences in the spinal cord, axonal transport to the periphery, and depletion by systemic vanilloid treatment. Brain Res. 703(1995) : 175-183.
- Szallasi, A., and Blumberg, P.M. Vanilloid receptors: new insights enhance potential as a therapeutic target. Pain 68(1996) : 195-208.
- Szallasi, A., and Blumberg, P.M. Vanilloid (Capsaicin) receptors and Mechanisms. Pharmacological Reviews 51(1999) : 160-202.

- Szolocsanyi, J., and Jancso-Gabor, A. Sensory effects of capsaicin congeners, I: relationship between chemical structure and pain-producing potency, Drug Res. 25(1975) : 1877-1881.
- Tanaka, E., and North, R.A. Actions of 5-hydroxytryptamine on neurons of the rat cingulate cortex. J. Neurophysiol. 69(1993) : 1749-1757.
- Thomsen, L.L. Investigations into the role of nitric oxide and the large intracranial arteries in migraine headache. Cephalalgia 17(1997) : 973-995.
- Tominaga, M. The cloned capsaicin receptor integrates multiple pain-producing stimuli. Neuron. 21(1998) : 531-543.
- Tominaga, M., Wada, M., and Masu, M. Potentiation of capsaicin receptor activity by metabolic ATP receptors as a possible mechanism for ATP-evoked pain and hyperalgesia. Proc. Natl. Acad. Sci. 98(2001) : 6951-6956.
- Tork, I. Anatomy of the serotonergic system. Ann N Y Acad Sci. 600(1990) : 9-34.
- Villalon, C.M., de Vries, P., and Saxena, P.R. Serotonin receptors as cardiovascular targets. Drug Dev Today. 2(1997) : 294-302.
- Vysokanov, A., Flores-Hernandez, J., and Surmeier, D.J. mRNAs for clozapine-sensitive receptors co-localize in rat prefrontal cortex neurons. Neurosci. Lett. 258(1998) : 179-182.
- Wahl, M., Schilling, L., Parsons, A.A., and Kaumann, A. Involvement of calcitonin-gene related peptide (CGRP) and nitric oxide (NO) in the pial artery dilatation elicited by cortical spreading depression. Brain Res. 637(1994) : 204-210.
- Waite, P.M.E., and David, T. Trigeminal sensory system. In: Paxinos G, editor. The rat nervous system New York: Academic Press. 1995 : 705-724.
- Waldmann, R., Bassilana, F., Weille, J., Champigny, G., Heurteaux, C., and Lazdunski, M. Molecular cloning of a non-inactivating proton-gated Na⁺ channel specific for sensory neurons. J. Biol Chem. 272(1997a) : 20975-20978.
- Wang, W., Timsit-Berthier, M., and Shoenen, J., Intensity dependent of excitatory evoked potentials is pronounced in migraine. Neurology 46(1996) : 1404-1409.
- Waldmann, R., Champigny, G., Bassilana, F., Heurteaux, C., and Lazdunski, M. A proton-gated channel involved in acid sensing. Nature 386(1997b) : 173-177.

- Waterhouse, B.D., Mahailoff, G.A., Baack, J.C., and Woodward, D.J. Topographical distribution of dorsal and median raphe neurons projecting to motor, sensorimotor, and visual cortical areas in the rat. J. Comp. Neurol. 249(1986a) : 460-476.
- Waterhouse, B.D., Moises, H.C., and Woodward, D.J. Interaction of serotonin with somatosensory cortical neuronal responses to afferent synaptic inputs and putative neurotransmitters. Brain Res. Bull. 17(1986b) : 507-518.
- Wiesenfeld-Hallin, Z., Hokfell, T., Lundberg, J.M., Firssmann, W.G., Revneche, M., Tschopp, F.A., and Fischer, J.A. Immunoreactive calcitonin gene-related peptide and substance P coexist in sensory neurons to the spinal cord and interact in spinal behavioral responses of the rat. Neurosci. Lett. 52(1984) : 199-204.
- Willem Van der Does, A.J. The effects of tryptophan depletion on mood and psychiatric symptoms. J. Affect Disord. 64(2001) : 107-119.
- Williams, G.V., Roa, S.G., and Goldman-Rakic, The physiological role of 5-HT_{2A} receptors in working memory. J. Neurosci. 22(2002) : 2843-2854.
- Willis, W.D., Westlund, K.N., and Carlton, S.M. Pain. In: Paxinos G, editor. The rat nervous system. New York: Academic Press 1995 : 705-724.
- Wright, D.E., Seroogy, K.B., Lundgren, K.H., Davis, B.M., and Jennes, L. Comparative localization of serotonin 1A,1C, and 2 receptor subtype mRNAs in rat brain. J. Comp. Neurol. 351(1995) : 356-373.
- Yamamura, H., Malick, A., Chamberlin, N.L., and Burstein, R. Cardio-vascular and neuronal responses to head stimulation reflect central sensitization and cutaneous allodynia in rat model of migraine. J. Neurophysiol. 81(1999) : 479-493.
- Yiangou, Y., Facer, P., Dyer, N.H., Chan, C.L., Knowles, C., Williams, N.S., and Anand, P. Vanilloid receptor 1 immunoreactivity in inflamed human bowel. Lancet. 357(2001) : 1338-1339.

BIOGRAPHY

Name	Mr. Weera Suprongsinchai
Date of birth	29 th July 1978
Place of birth	Suphanburi, Thailand
Instructions attended	Rangsit University (1998-2001) Bachelor of Science (Physical Therapy)



สถาบันวิทยบริการ
จุฬาลงกรณ์มหาวิทยาลัย